

GE Energy

Final Report on:

DOCKET	
12-IEP-1D	
DATE	JUN 11 2012
RECD	JUN 12 2012

Impact of Dynamic Schedules on Interfaces

Prepared by:

Kara Clark
Robert D'Aquila
Mark D. McDonald
Nicholas W. Miller
Miaolei Shao

January 6, 2011

Version 3



Table of Contents

EXECUTIVE SUMMARY	VII
1 INTRODUCTION	1.1
2 STUDY APPROACH	2.1
2.1 STEADY-STATE MODEL.....	2.1
2.2 STEADY-STATE ANALYSIS	2.3
2.2.1 COI Interface Study Area	2.5
2.2.2 WOR Interface Study Area.....	2.7
2.2.3 Performance Criteria and Monitoring.....	2.11
2.2.4 Contingency Lists.....	2.11
2.3 DYNAMIC ANALYSIS	2.11
2.3.1 Performance Criteria and Monitoring.....	2.13
2.3.2 Disturbance List.....	2.13
2.4 WIND AND PV SOLAR STATISTICAL ANALYSIS.....	2.14
2.4.1 Wind Data Development.....	2.15
2.4.2 Solar Data Development.....	2.16
3 COI INTERFACE	3.1
3.1 VOLTAGE PERFORMANCE.....	3.1
3.1.1 Steady-state $\Delta V/\Delta P$ Characteristic	3.1
3.1.2 Shunt Capacitor and LTC Switching	3.7
3.1.3 Sensitivity Analysis	3.8
3.1.4 Statistical Analysis of Wind Profiles.....	3.12
3.2 OSCILLATORY PERFORMANCE.....	3.16
3.2.1 Swing Mode Identification.....	3.16
3.2.2 Impact of Wind Variability on Small-Signal Stability.....	3.20
4 WOR INTERFACE	4.1
4.1 VOLTAGE PERFORMANCE.....	4.1
4.1.1 Steady-state $\Delta V/\Delta P$ Characteristic	4.1
4.1.2 Shunt Capacitor and LTC Switching	4.7
4.1.3 Sensitivity Analysis	4.8
4.1.4 Statistical Analysis of Solar Profiles.....	4.12
4.2 OSCILLATORY PERFORMANCE.....	4.16
4.2.1 Swing Mode Identification.....	4.16
4.2.2 Impact of Solar Variability on Small-Signal Stability.....	4.19
5 SUMMARY AND CONCLUSIONS	5.1
6 REFERENCES	6.1

Table of Figures

Figure 2-1. Tehachapi Renewable Transmission Project.....	2.2
Figure 3-1. ΔV of CAISO Monitored Buses For ΔP in Northwest, All Lines In.....	3.3
Figure 3-2. ΔV of CAISO Monitored Buses For ΔP in Northwest, Captain Jack-Olinda Out of Service Pre Generation Shift.....	3.3
Figure 3-3. $\Delta V/\Delta P_{gen}$ of CAISO Monitored Buses per 100 MW of ΔP in Northwest, All Lines In.....	3.4
Figure 3-4. $\Delta V/\Delta P_{gen}$ of CAISO Monitored Buses per 100 MW of ΔP in Northwest, Captain Jack-Olinda Out of Service Pre Generation Shift.....	3.4
Figure 3-5. ΔV of Round Mountain 500 kV Bus Voltage For ΔP in Northwest, All Lines In Service.....	3.5
Figure 3-6. ΔV of Round Mountain 500 kV Bus Voltage For ΔP in Northwest, All Lines In Service, Plotted Against COI Flow.....	3.5
Figure 3-7. ΔV of Round Mountain 500 kV Bus Voltage For ΔP in Northwest, Captain Jack-Olinda 500 kV Line Out of Service.....	3.6
Figure 3-8. ΔV of Round Mountain 500 kV Bus Voltage For ΔP in Northwest, Captain Jack-Olinda 500 kV Line Out of Service, Plotted Against COI Flow.....	3.6
Figure 3-9. ΔV of CAISO Monitored Buses For ΔP in Northwest, Base System and Five Worst-Case Outages.....	3.10
Figure 3-10. ΔV of CAISO Monitored Buses For ΔP in Northwest, Redispatch All CAISO Units (blue), Redispatch of Non-Baseload Units (pink), Redispatch Selected Units (green).....	3.10
Figure 3-11. ΔV of CAISO Monitored Buses For ΔP in Northwest, Spring (blue) vs. Summer (pink).....	3.11
Figure 3-12. $\Delta V/\Delta P_{gen}$ of CAISO Monitored Buses per 100 MW of ΔP in Northwest, Spring (blue) vs. Summer (pink).....	3.11
Figure 3-13. 10-Minute Deltas in 5,000 MW Wind Profile.....	3.13
Figure 3-14. 10-Minute Negative Deltas in 5,000 MW Wind Profile.....	3.14
Figure 3-15. COI Interface Flow in Response to Loss of Two Palo Verde Generators.....	3.17
Figure 3-16. COI Interface Flow in Response to Critical Fault Events: 2 Palo Verde Units (blue), Pacific DC Intertie (red), 2 San Onofre Units (green), 2 Diablo Units (black).....	3.17
Figure 3-17. COI Interface FFT Results for Loss of Two Palo Verde Generators.....	3.18
Figure 3-18. COI Interface FFT Results for Loss of Pacific DC Intertie.....	3.18
Figure 3-19. COI Interface FFT Results for Loss of Two San Onofre Generators.....	3.19
Figure 3-20. COI Interface FFT Results for Loss of Two Diablo Canyon Generators.....	3.19
Figure 3-21. System Response to Palo Verde Generation Trip with and without 1,500 MW, 0.2 Hz Stimulus.....	3.22
Figure 3-22. System Response to Palo Verde Generation Trip, with 2,000 MW Stimulus at 0.2 Hz (blue), 0.4 Hz (red), 0.63 Hz (green) and 1 Hz (black).....	3.23
Figure 4-1. ΔV of CAISO Monitored Buses For ΔP In Arizona, All Lines in Service.....	4.3
Figure 4-2. ΔV of CAISO Monitored Buses For ΔP In Arizona, N. Gila-Imperial Valley 500 kV Line Out.....	4.3
Figure 4-3. $\Delta V/\Delta P_{gen}$ of CAISO Monitored Buses Values per 100 MW of ΔP In Arizona, All Lines in Service.....	4.4
Figure 4-4. $\Delta V/\Delta P_{gen}$ of CAISO Monitored Buses per 100 MW of ΔP in Arizona, N. Gila-Imperial Valley 500 kV Line Out.....	4.4
Figure 4-5. ΔV of Pisgah 500 kV Bus Voltage For ΔP in Arizona, All Lines In Service.....	4.5
Figure 4-6. ΔV of Pisgah 500 kV Bus Voltage For ΔP in Arizona, All Lines In Service, Plotted Against WOR Flow.....	4.5
Figure 4-7. ΔV of Pisgah 500 kV Bus Voltage For ΔP in Arizona, North Gila-Imperial Valley 500 kV Line Out of Service.....	4.6
Figure 4-8. ΔV of Pisgah 500 kV Bus Voltage For ΔP in Arizona, North Gila-Imperial Valley 500 kV Line Out of Service, Plotted Against WOR Flow.....	4.6

Figure 4-9. ΔV of CAISO Monitored Buses For ΔP In Arizona, with Different Outages.	4.9
Figure 4-10. ΔV of Pisgah 500 kV Bus Voltage For ΔP in Arizona, All Lines In Service and Three Worst-Case CAISO Contingencies, Plotted Against WOR Flow.	4.10
Figure 4-11. ΔV of CAISO Monitored Buses For ΔP in Arizona, Redispatch All CAISO Units (blue) vs. Redispatch of Non-Base-load Units (pink).	4.10
Figure 4-12. ΔV of CAISO Monitored Buses For ΔP in Arizona, Spring (blue) vs. Summer (pink).	4.11
Figure 4-13. $\Delta V/\Delta P_{gen}$ of CAISO Monitored Buses per 100 MW of ΔP in Arizona, Spring (blue) vs. Summer (pink).	4.11
Figure 4-14. 10-Minute Deltas in 15,000 MW DC (11,550 MW AC) Solar PV Profile.	4.13
Figure 4-15. Individual Arizona 100 MW DC/77 MW AC Solar PV Profiles.	4.13
Figure 4-16. 10-Minute Negative Deltas in 15,000 MW DC (11,550 MW AC) Solar PV Profile.	4.14
Figure 4-17. WOR Interface Flow Response to N. Gila-Imperial Valley 500 kV Line Event.	4.17
Figure 4-18. WOR Interface Flow Response to Critical Fault Events: N. Gila-Imperial Valley 500kV (blue), Palo Verde-Colorado River 500kV (red), 2 San Onofre Units (green).	4.17
Figure 4-19. WOR Interface FFT Results for N. Gila-Imperial Valley 500 kV Line Event.	4.18
Figure 4-20. WOR Interface FFT Results for Palo Verde - Colorado River 500 kV Line Event.	4.18
Figure 4-21. WOR Interface FFT Results for Loss of Two San Onofre Units.	4.19
Figure 4-22. System Response to N. Gila-Imperial Valley 500 kV Line Event, with and without 7,000 MW, 0.6 Hz Stimulus.	4.21
Figure 4-23. System Response to N. Gila-Imperial Valley 500 kV Line Event, with 8,000 MW Stimulus at 0.47 Hz (blue), 0.6 Hz (red) and 1.5 Hz (green).	4.22
Figure 4-24. Marketplace SVC Response to N. Gila-Imperial Valley 500 kV Line Event, with 0 MW (blue), 3,000 MW (red), and 6,000 MW (green) Stimulus at 0.6 Hz.	4.23

Table of Tables

Table 2-1. Summary of COI and WOR Spring Databases.....	2.3
Table 2-2. Summary of COI and WOR Summer Databases.....	2.3
Table 2-3. Individual Units Selected for Redispatch in COI Sensitivity Analysis.....	2.5
Table 2-4. COI Interface Definition.....	2.6
Table 2-5. COI Interface Series Compensation (% of Line Impedance) in Spring and Summer Databases.....	2.6
Table 2-6. Voltage Controlled Shunt Capacitors by COI Interface in Spring Database.....	2.6
Table 2-7. Voltage Controlled Shunt Capacitors by COI Interface in Summer Database.....	2.7
Table 2-8. WOR Interface Flows in Spring Database.....	2.8
Table 2-9. WOR Interface Flows in Summer Database.....	2.9
Table 2-10. WOR Interface Series Compensation (% of Line Impedance) in Spring Database.....	2.9
Table 2-11. WOR Interface Series Compensation (% of Line Impedance) in Summer Database.....	2.10
Table 2-12. 500 kV Voltage Controlled Shunt Capacitors by WOR Interface in Spring Database.....	2.10
Table 2-13. 500 kV Voltage Controlled Shunt Capacitors by WOR Interface in Summer Database..	2.10
Table 2-14. SVCs by WOR Interface in Spring Database.....	2.10
Table 2-15. Critical Contingency List For COI Interface Analysis.....	2.11
Table 2-16. Critical Contingency List For WOR Interface Analysis.....	2.11
Table 2-17. Critical Dynamic Disturbances Evaluated For COI Interface.....	2.13
Table 2-18. Critical Dynamic Disturbances Evaluated For WOR Interface.....	2.14
Table 2-19. Aggregate Wind Profile Summary.....	2.14
Table 2-20. Aggregate PV Solar Profile Summary.....	2.15
Table 3-1. $\Delta V/\Delta P$ at Round Mountain 500 kV, All Lines In. Values Are Per Unit per 100 MW of ΔP on COI and ΔP Northwest Generation.....	3.7
Table 3-2. $\Delta V/\Delta P$ at Round Mountain 500 kV, Captain Jack-Olinda 500 kV line Out of Service. Values Are Per Unit per 100 MW of ΔP on COI and ΔP Northwest Generation.....	3.7
Table 3-3. ΔV at Selected Buses with Switched Shunt Capacitors. ΔV Shown for 1,521 MW and 1,106 MW Change in NW Generation.....	3.8
Table 3-4. Aggregate Wind Profile 10-Minute Delta Statistics.....	3.13
Table 3-5. Expected 10-Minute Negative Wind Deltas.....	3.14
Table 3-6. Expected 10-Minute Positive Wind Deltas.....	3.14
Table 3-7. Expected Frequency and Magnitude of ΔV at Round Mtn 500 kV for 5,000 MW Wind Profile for Spring Cases.....	3.15
Table 3-8. Expected Frequency and Magnitude of ΔV at Round Mtn 500 kV for 5,000 MW Wind Profile for Summer Sensitivity Case.....	3.15
Table 3-9. Dominant Swing Modes Across COI Interface.....	3.20
Table 3-10. $\Delta V/\Delta P_{gen}$ at Maxwell 500 kV for Palo Verde Outage, +/-2,000 MW Stimulus. Values are Per Unit per 100 MW of Stimulus.....	3.21
Table 4-1. $\Delta V/\Delta P$ at Pisgah 500 kV for Base System (n-0) and North Gila-Imperial Valley Outage. Values Are Per Unit per 100 MW of ΔP on WOR and ΔP Arizona Generation.....	4.2
Table 4-2. ΔV at Selected Buses with Switched Shunt Capacitors. ΔV Shown for 2,410 MW and 3,250MW Change in Arizona Generation.....	4.8
Table 4-3. Aggregate Solar PV Profile 10-Minute Delta Statistics.....	4.14
Table 4-4. Expected 10-Minute Negative Solar PV Deltas.....	4.15
Table 4-5. Expected 10-Minute Positive Solar PV Deltas.....	4.15
Table 4-6. Expected Frequency and Magnitude of ΔV at Pisgah 500 kV for 15,000 MW DC/11,550 MW AC Solar PV Profile for Spring Cases.....	4.15
Table 4-7. Dominant Swing Modes Across WOR Interface.....	4.19

Table 4-8. $\Delta V/\Delta P$ at Pisgah 500 kV for North Gila-Imperial Valley 500 kV line Outage, +/-8,000 MW Stimulus. Values are Per Unit per 100 MW of Stimulus..... 4.24

Legal Notice

This report was prepared by General Electric International, Inc. as an account of work sponsored by California ISO (CAISO). Neither CAISO nor GEI, nor any person acting on behalf of either:

1. Makes any warranty or representation, expressed or implied, with respect to the use of any information contained in this report, or that the use of any information, apparatus, method, or process disclosed in the report may not infringe privately owned rights.
2. Assumes any liabilities with respect to the use of or for damage resulting from the use of any information, apparatus, method, or process disclosed in this report.

Copyright©2010 GE Energy. All rights reserved

Executive Summary

The objective of this study was to explore the impact of dynamic scheduling of renewable generation across interfaces into CAISO. Dynamic scheduling was narrowly defined to include only wind or solar PV variability. Other potential components of dynamic scheduling, such as hourly or sub-hourly schedule changes, were not considered. Two technical aspects of system performance were evaluated:

- Steady-state voltage changes
- Oscillatory response

Two interfaces were evaluated:

- California Oregon Interface (COI)
- West of River (WOR)

To begin, aggregate wind and solar PV profiles were analyzed to statistically characterize their expected variability. This statistical analysis evaluated the change in wind or PV solar generation from one 10-minute point to the next. These statistics provide a measure of how often relatively severe changes in power can be expected. For example, when 99% of changes in power (ΔP) per MW of dynamically scheduled wind or solar generation are within a given range, the statistical expectation is that more severe events will occur, on average, less than once per day. Daily tap motions and capacitor switching are presently expected during system operations. Wind and solar variations that result in normal switching or other control actions over a similar period were judged acceptable. The statistics of wind variation dictate that faster variations, i.e. on a period shorter than 10 minutes, will be of smaller amplitude.

From the power flow analysis, the change in voltage (ΔV) associated with such a change in power was calculated, as well as the potential impact of that ΔV on transformer LTC tap motion and shunt capacitor switching. Since the power flow analysis was performed with the COI and WOR interfaces near maximum, the focus was on the negative changes in power.

Finally, the impact of wind and solar PV variability on small signal oscillatory performance was examined. The dynamic performance evaluation incorporated extremely conservative assumptions. Specifically, all variable renewable generation in a given area (i.e., wind in the Northwest, solar PV in the Southwest) was oscillated at a single bus at one of the identified power swing frequencies. This test, which has negligible risk of occurrence, provided maximum impact on grid oscillations. The assumption underlying this test is that common-mode oscillation of the renewable generation will be worse than any variation that might occur in operation, and therefore provides a conservative upper bound.

The specific conclusions associated with each interface are discussed below.

COI Interface

The maximum power flow allowed across the COI interface is 4,800 MW. Therefore, the theoretical maximum dynamic schedule is also 4,800 MW. This maximum dynamic schedule was represented by a 5,000 MW aggregate wind profile in this study.

The statistical analysis showed that 99% of the time, the expected 10-minute drop in wind generation would be 301 MW or less (Table 3-5). The power flow analysis showed that this would result in at most a 0.012 pu change in voltage (Table 3-7) on the 500 kV system near COI. Changes on the lower voltage system, i.e., closer to served loads, are considerably smaller - too small to result in additional transformer LTC tap motion or shunt capacitor switching. The maximum 10-minute drop was 1,672 MW, which occurred once in the year of data. The power flow analysis showed that this would result in up to a 0.065 pu ΔV , which would likely cause some LTC tap motion and shunt capacitor switching. The wind data shows that voltage changes of this magnitude will be rare, and will not occur in rapid succession. There is no significant risk of LTC tap hunting or rapid on/off cycling of shunt devices.

The dynamic analysis showed that an extreme test, driving all of the dynamically scheduled wind generation at a characteristic frequency with a peak-to-peak magnitude that exceeded the interface limit, still resulted in damped oscillations. At magnitudes greater than 3,000 MW peak-to-peak, some protective relays operated depending upon the system condition and fault event. There is no credible wind variation that can cause oscillatory destabilization of an otherwise stable system.

WOR Interface

The maximum power flow allowed across the WOR interface is 10,100 MW (WECC 2006 Path Rating Catalog). Therefore, the theoretical maximum dynamic schedule is also 10,100 MW. This maximum dynamic schedule was represented by a 15,000 MW DC/11,550 MW AC aggregate solar PV profile in this study.

The statistical analysis showed that 99% of the time, the expected 10-minute drop in solar PV generation would be 412 MW or less (Table 4-4). The power flow analysis showed that this would result in a 0.004 pu change in voltage (Table 4-6), which is too small to result in additional transformer LTC tap motion or shunt capacitor switching. The maximum 10-minute drop was 523 MW, which occurred once in the year of data. The power flow analysis showed that this would also result in relatively small (0.005 pu) change in voltage. Industry experience with large scale PV, including data measurement and development, is considerably less than that with wind power. As field and analytical experience grows, these results will likely benefit from refinement.

The dynamic analysis showed that the extreme test, driving all of the dynamically scheduled solar PV generation at a characteristic frequency with a peak-to-peak magnitude that exceeded the interface limit, still resulted in damped oscillations. At magnitudes greater than the 10,100 MW WOR limit, some protective relays operated and nearby SVC duty increased depending upon the system condition and fault event.

Conclusion

Under extreme conditions (e.g., combinations of 500 kV line or multiple generation unit outages, once-a-year changes in dynamically schedule renewable generation output, and unrealistically monolithic aggregate wind and/or solar PV behavior), it may be possible to trigger excessive shunt capacitor switching, transformer LTC motion, SVC response, and/or protective relay operation. However, the expected variability from the wind and solar PV generation when dynamically scheduled up to the overall maximum currently applied to each interface will not result in large changes in voltage nor excessive duty on voltage regulating devices (e.g., LTC transformers and shunt capacitors). Therefore, this analysis shows that no additional limits are required on dynamically scheduled variable generation when the existing maxima are applied to each interface.

The expected change in voltage caused by dynamic scheduling is somewhat sensitivity to CAISO generation redispatch and to system operating condition (spring vs summer peak). However, the sensitivity is relatively low and does not change the conclusions of the study.

Note: The above conclusions are based on voltage and oscillatory performance of substation equipment within the ISO's footprint under high levels of import of intermittent resources during both normal and abnormal operating conditions. Neighboring Balancing Authorities may have limitations within their systems that could impact the level of import of renewable resources through dynamic transfers into the ISO.

1 Introduction

The objective of this study was to explore the impact of dynamic scheduling of renewable generation across interfaces into CAISO. Dynamic scheduling was narrowly defined to include only wind or solar PV variability. Other potential components of dynamic scheduling, such as hourly or sub-hourly schedule changes, were not considered. Two technical aspects of system performance (steady-state voltage changes and oscillatory response) were evaluated for two interface (California Oregon Interface (COI) and West of River (WOR)).

To begin, aggregate wind and solar PV profiles were analyzed to statistically characterize their expected variability. This statistical analysis evaluated the change in wind or PV solar generation from one 10-minute point to the next. These statistics provide a measure of how often relatively severe changes in power can be expected. For example, when 99% of changes in power (ΔP) per MW of dynamically scheduled wind or solar generation are within a given range, the statistical expectation is that more severe events will occur, on average, less than once per day. Daily tap motions and capacitor switching are presently expected during system operations. Wind and solar variations that result in normal switching or other control actions over a similar period were judged acceptable. The statistics of wind variation dictate that faster variations, i.e. on a period shorter than 10 minutes, will be of smaller amplitude.

From the power flow analysis, the change in voltage (ΔV) associated with such a change in power was calculated, as well as the potential impact of that ΔV on transformer LTC tap motion and shunt capacitor switching. Since the power flow analysis was performed with the COI and WOR interfaces near maximum, the focus was on the negative changes in power.

Finally, the impact of wind and solar PV variability on small signal oscillatory performance was examined. The dynamic performance evaluation incorporated extremely conservative assumptions. Specifically, all variable renewable generation in a given area (i.e., wind in the Northwest, solar PV in the Southwest) was oscillated at a single bus at one of the identified power swing frequencies. This test, which has negligible risk of occurrence, provided maximum impact on grid oscillations. The assumption underlying this test is that common-mode oscillation of the renewable generation will be worse than any variation that might occur in operation, and therefore provides a conservative upper bound.

The details of the study approach are described in Section 2, COI analysis results are reported in Section 3, and WOR analysis results are reported in Section 4. The study conclusions are discussed in Section 5.

2 Study Approach

An overview of the study approach, assumptions, power system, wind and solar PV data is provided in this section. All power system analysis was performed using GE's PSLF software.

2.1 Steady-State Model

CAISO modified a standard WECC 2018 heavy spring database to develop the two primary study databases. The following changes were made to create the COI spring database:

- Added 1,074 MW of wind generation at Solano
- Replaced the SCE area with the SCE area from the 2020 heavy summer case of the 2011 CAISO Transmission Expansion Plan and scaled the load down to the level of the 2018 heavy spring case
- Added the following upgrades in the Tehachapi area to represent the Tehachapi Renewable Transmission Project as shown in Figure 2-1:
 - Added 3,961 MW of wind generation at Tehachapi
 - Added four additional 34.5 kV transmission lines to accommodate the renewable project connected to the Tehachapi Whirlwind 230 kV substation
 - Added two additional 34.5/0.69 kV transformers to accommodate the renewable project connected to the Tehachapi Windhub 230 kV substation
 - Added second 230 kV transmission line between Tehachapi and Skyriver
 - Added second and third 230 kV transmission lines between Tehachapi P and East-West-WILD
 - Added second 230 kV transmission line between East-West-WILD and Vincent
 - Added second Tehachapi 230/66/12 kV transformer
 - Added second 66 kV line between Tehachapi P and Tehachapi M
 - Added fourth Tehachapi M 66/12.5 kV transformer
 - Added second Midwind 66/12.5 kV transformer
 - Added two additional Tehachapi P 230/66 kV transformers
 - Added two additional Tehachapi M 230/66 kV transformers
 - Added another Northwind 66/12 kV transformer

Starting with the above COI study database, CAISO performed a generation redispatch to develop the WOR spring database, as follows:

- Added 3,128 MW generation in Arizona
- Added 200 MW generation in Nevada
- Added 795 MW generation in SCE
- Reduced Northwest generation by 2,034 MW
- Reduced British Columbia generation by 684 MW
- Reduced LADWP generation by 893 MW
- Reduced PG&E generation by 708 MW

A summary of the two primary spring databases is shown in Table 2-1, including overall generation, load, and selected path flows.

CAISO also provided two 2020 summer peak databases for the sensitivity analysis. The original case was the 2020 Summer Peak Portfolio 1 case from the CAISO Comprehensive Transmission Plan with 33% renewable resource integration. This case was used as-is for the WOR sensitivity analysis. To create the COI sensitivity database, Northwest generation was increased by 1,242 MW and SCE generation was decreased by 1,012 MW. A summary of the two summer sensitivity cases is shown in Table 2-2, including overall generation, load, and selected path flows.



Figure 2-1. Tehachapi Renewable Transmission Project.

Table 2-1. Summary of COI and WOR Spring Databases.

	COI Database	WOR Database
CAISO* generation	29,842 MW	30,184 MW
CAISO* load	38,565 MW	38,602 MW
WECC generation	145,692 MW	145,120 MW
WECC load	140,462 MW	140,499 MW
COI flow	4,787 MW	2,003 MW
WOR flow	5,467 MW	9,315 MW
PDCI flow	2,000 MW	2,000 MW
Path 15 flow	-917 MW	1,899 MW
Path 26 flow	3,331 MW	264 MW
EOR flow	3,582 MW	5,872 MW
SCIT flow	13,010 MW	13,490 MW

*For this table CAISO was defined by power flow areas 22 (San Diego Gas & Electric), 24 (Southern California Edison), and 30 (Pacific Gas & Electric)

Table 2-2. Summary of COI and WOR Summer Databases.

	COI Database	WOR Database
CAISO* generation	53,358 MW	54,299 MW
CAISO* load	62,689MW	62,689 MW
WECC generation	199,274 MW	198,973 MW
WECC load	192,413 MW	192,413 MW
COI flow	4,800 MW	3,972 MW
WOR flow	11,482 MW	11,246 MW
PDCI flow	1,550 MW	1,550 MW
Path 15 flow	1,822 MW	2,642 MW
Path 26 flow	1,140 MW	304 MW
EOR flow	5,692 MW	5,438 MW
SCIT flow	11,913 MW	11,119 MW

*For this table CAISO was defined by power flow areas 22 (San Diego), 24 (Southern California Edison), and 30 (PG&E)

2.2 Steady-State Analysis

The objective of the steady-state analysis was to evaluate the impact of dynamic scheduling on the voltage performance of the COI and WOR interfaces. Specifically, the goal was to determine the impact of variations in imports (ΔP) on delta voltage (ΔV) and the resulting

impact on equipment – i.e., shunt capacitor or reactor switching events and LTC transformer tap motions.

Since the original power flow cases had the study interfaces at or near their limits, ΔP was in the downward direction (i.e. a reduction in imports). This was achieved by tripping remote generation. For ΔP on COI, generation at John Day was tripped, and for ΔP on WOR, generation at Navajo and Springerville was tripped. These sites are relatively far from the interface, but provide a large change in interface flow per MW of generation tripped (i.e., a high distribution factor). This minimizes the impact of the lost reactive support (due to the tripped generation) on ΔV , and provides a more accurate measure of ΔV based on ΔP across the interface.

The tripped generation was balanced by increasing generation within CAISO as defined by the PG&E, San Diego, and SCE areas. Three redispatch procedures were used. In the first, individual units were redispatched in proportion to their MVA rating, while not exceeding their maximum power output (Pmax in the powerflow data set). A second type of redispatch excluded units identified as baseload in the powerflow (gens table BL flag set to 1), and also respected the power limits.

The third redispatch used individual units selected by CAISO, and was only applied to the COI interface sensitivity analysis. These units are shown in Table 2-3, with their initial status, initial power output and maximum power output, for the COI spring and summer databases. Note that most of the selected units were out of service in the spring case, and many are near their maxima in the summer case. Units that were initially out-of-service (i.e., status = 0) were turned on and allowed to contribute to the redispatch. The redispatch was implemented by splitting the needed generation equally until each unit reached its power limit.

For all redispatch procedures, losses were balanced by the system swing generator, Pittsburg, which is located in PG&E territory.

The change in flow across the study interface will be less than the amount of generation tripped. For example, loss of 1,100 MW at John Day and a corresponding increase in generation within CAISO results in a reduction of 760 MW of flow across COI, or about 70% of the delta generation. The remaining 340 MW flow across other interfaces or are accommodated by a change in losses. Throughout this report, both the delta generation and delta interface flow are reported.

The $\Delta V/\Delta P$ characteristics were calculated for six control-action conditions:

- No action: No regulation other than generator voltage control
- Continuous SVD action: Only SVCs with continuous action regulating (PSLF type 2 SVDs)
- LTC action: Only LTC transformers regulating
- All SVD action: SVCs with continuous action and switched shunts regulating (PSLF type 2 and 4 SVDs)

- SVC and LTC: SVCs, switched shunts and LTC transformers regulating
- SVC, LTC and PAR: SVCs, switched shunts, LTC transformers and phase angle regulating transformers acting

For all of the above control action combinations, each generator was allowed to regulate the voltage on its terminal bus within its given reactive capability.

Table 2-3. Individual Units Selected for Redispatch in COI Sensitivity Analysis.

#	Name	kV	ID	Spring			Summer		
				Status	Initial Output	Maximum Output	Status	Initial Output	Maximum Output
1	DEC STG1	24	1	0	0 MW	320 MW	1	280 MW	320 MW
2	DEC CTG2	18	1	0	0 MW	215 MW	1	200 MW	215 MW
3	DEC CTG2	18	1	0	0 MW	215 MW	1	200 MW	215 MW
4	DEC CTG3	18	1	0	0 MW	215 MW	1	200 MW	215 MW
5	ELKHIL1G	18	1	0	0 MW	199 MW	0	0 MW	199 MW
6	ELKHIL2G	18	1	0	0 MW	199 MW	0	0 MW	199 MW
7	ELKHIL3G	18	1	0	0 MW	225 MW	0	0 MW	225 MW
8	MOSSLND6	22	1	0	0 MW	750 MW	0	0 MW	750 MW
9	MOSSLND7	22	1	1	750 MW	750 MW	0	0 MW	750 MW
10	LMECST1	18	1	0	0 MW	280 MW	1	250 MW	280 MW
11	LMECCT1	18	1	0	0 MW	199 MW	1	170 MW	199 MW
12	LMECCT2	18	1	0	0 MW	199 MW	1	170 MW	199 MW
13	MEC STG1	18	1	0	0 MW	215 MW	1	200 MW	215 MW
14	MEC CTG1	18	1	0	0 MW	180 MW	1	170 MW	180 MW
15	MEC CTG2	18	1	0	0 MW	180 MW	1	170 MW	180 MW
16	HELMS 1	18	1	0	0 MW	404 MW	1	404 MW	404 MW
17	HELMS 2	18	1	0	0 MW	404 MW	1	404 MW	404 MW
18	HELMS 3	18	1	1	390 MW	404 MW	1	404 MW	404 MW

2.2.1 COI Interface Study Area

The COI interface consists of three 500 kV lines across the Oregon-California border as shown in Table 2-4. Each of those lines is series compensated. The amount of series compensation in the spring database is shown in Table 2-5. Shunt capacitors and reactors are also located near the COI interface. In particular, 1,079 MVar of line connected shunt reactors are in-service in power flow zone 300, which is in the PG&E area and titled "Intertie". These reactors will switch with their associated lines and do not respond to voltage

variations. There are no fixed shunt capacitors represented as PSLF SHUNT devices in zone 300. The voltage controlled mechanically switched shunt capacitors in zone 300 are shown in Table 2-6. All of these shunt capacitors are modeled as type 4 SVDs, which means they switch in steps when the voltage goes outside a deadband.

The amount of series compensation in the summer database is identical to the amount of series compensation in the spring database, as shown in Table 2-5. The summer case also has 1,079 MVar of line connected shunt reactors in-service and no fixed shunt capacitors in zone 300. The voltage controlled shunt capacitors in zone 300 for the summer case are shown in Table 2-7. All of these shunt capacitors are modeled as type 4 SVDs, which means they switch in steps when the voltage goes outside a deadband.

Table 2-4. COI Interface Definition.

From Bus			To Bus			ID	P (MW)	Q (MVar)
#	Name	kV	#	Name	kV			
40687	Malin	500	30025	Round Mt	500	1	1,528	-62
40687	Malin	500	30025	Round Mt	500	2	1,549	-82
40535	Capt Jack	500	30020	Olinda	500	1	1,715	-205
Total							4,793	-350

Table 2-5. COI Interface Series Compensation (% of Line Impedance) in Spring and Summer Databases.

From Bus			To Bus			ID	Location	%	Location	%
#	Name	kV	#	Name	kV					
40687	Malin	500	30025	Round Mt	500	1	Malin	31	Round Mt	31
40687	Malin	500	30025	Round Mt	500	2	Malin	35	Round Mt	29
45035	Capt Jack	500	30020	Olinda	500	1	Capt Jack	31	Olinda	31

Table 2-6. Voltage Controlled Shunt Capacitors by COI Interface in Spring Database.

#	Name	kV	ID	B (MVar)	Scheduled Voltage	Voltage Deadband
30042	Metcalf	500	V	350	1.037 pu	+/- 0.02 pu
30015	Table Mt	500	V	454	1.060 pu	+/- 0.08 pu
30020	Olinda	500	V	200	1.079 pu	+/- 0.02 pu
30035	Tracy	500	V	600	1.070 pu	+/- 0.02 pu

Table 2-7. Voltage Controlled Shunt Capacitors by COI Interface in Summer Database.

#	Name	kV	ID	B (MVAR)	Scheduled Voltage	Voltage Deadband
30042	Metcalf	500	V	350	1.050 pu	0.03 +/- pu
30015	Table Mt	500	V	454	1.060 pu	0.08 +/- pu
30020	Olinda	500	V	200	1.079 pu	0.02 +/- pu
30035	Tracy	500	V	600	1.070 pu	0.02 +/- pu

2.2.2 WOR Interface Study Area

The WOR interface is defined by eight 500 kV lines and eight lower voltage lines across the Arizona-California border as shown in Table 2-8 for the spring case and Table 2-9 for the summer case. Many of these lines are series compensated. The amount of compensation in the spring database is shown in Table 2-10 and the amount of compensation in the summer case is shown in Table 2-11.

Shunt capacitors and reactors are also located near the WOR interface, which was defined as zones 210, 227, 240, 241, 248, 254, 260 and 270. In particular, about 234 MVAR shunt reactors are in-service near the WOR interface in the spring case and 280 MVAR in the summer case. There are also about 2,800 MVAR of fixed shunt capacitors in the area in the spring case and 4,900 MVAR in the summer case.

About 550 MVAR of voltage controlled shunts (SVDs) are in-service in the spring case, with about another 3,000 MVAR available to respond to voltage changes. The 500 kV voltage controlled shunt capacitors are shown in Table 2-12. The Valley SC and Miraloma shunt capacitors are modeled as type 4 SVDs, which means they switch in steps when the voltage goes outside a deadband. The Vincent 500 kV shunt capacitor is locked at 400 MVAR.

In the summer, about 2,650 MVAR of voltage controlled shunts (SVDs) are in-service, with about another 3,750 MVAR available to respond to voltage changes. The 500 kV voltage controlled shunt capacitors are shown in Table 2-13. The Valley SC and Miraloma shunt capacitors are again modeled as type 4 SVDs. The Vincent 500 kV shunt capacitor is turned off (status = 0).

Static Var Compensators (SVCs) at the Devers, Marketplace and Adelanto 500 kV buses, as shown in Table 2-14, are modeled as generators in the power flow and with svcwsc models in the spring dynamic database. In the spring and summer power flows, the reactive limits are set to 0, so none of these SVCs contribute reactive support in the steady-state analysis.

Table 2-8. WOR Interface Flows in Spring Database.

From Bus			To Bus			ID	P (MW)
#	Name	kV	#	Name	kV		
28195	Red Bluff	500	24801	Devers	500	1	1,015
28195	Red Bluff	500	24801	Devers	500	2	1,014
24042	El Dorado	500	84226	Pisgah	500	1	1,265
24041	El Dorado	230	24219	Pisgah	230	2	104
24041	El Dorado	230	24627	Cima	230	1	106
22356	Imperial Valley	230	21025	El Centro	230	1	195
27204	HL Tap	500	26003	Adelanto	500	1	851
26048	McCullough	500	26105	Victorville	500	2	884
26048	McCullough	500	26105	Victorville	500	1	894
26501	Mead	287	26104	Victorville	287	1	160
21076	Ramon	230	24806	Mirage	230	1	128
21007	Coachella	230	24806	Mirage	230	1	179
25406	J. Hinds	230	24806	Mirage	230	1	56
24097	Mohave	500	24086	Lugo	500	1	613
22536	N. Gila	500	22360	Imperial Valley	500	1	1,853
Total							9,315

Table 2-9. WOR Interface Flows in Summer Database.

From Bus			To Bus			ID	P (MW)
#	Name	kV	#	Name	kV		
28195	Red Bluff	500	24801	Devers	500	1	1,594
28195	Red Bluff	500	24801	Devers	500	2	1,594
24042	El Dorado	500	84226	Pisgah	500	1	1,085
24041	El Dorado	230	24219	Pisgah	230	2	46
24041	El Dorado	230	24627	Cima	230	1	48
21025	El Centro	230	22356	Imperial Valley	230	1	250
27204	HL Tap	500	26003	Adelanto	500	1	1,056
26048	McCullough	500	26105	Victorville	500	2	1,069
26048	McCullough	500	26105	Victorville	500	1	1,079
26501	Mead	287	26104	Victorville	287	1	207
21076	Ramon	230	24806	Mirage	230	1	248
21007	Coachella	230	24806	Mirage	230	1	299
25406	J. Hinds	230	24806	Mirage	230	1	330
24097	Mohave	500	24086	Lugo	500	1	729
22536	N. Gila	500	22360	Imperial Valley	500	1	1,612
Total							11,246

Table 2-10. WOR Interface Series Compensation (% of Line Impedance) in Spring Database.

From Bus			To Bus			ID	Location	%	Location	%
#	Name	kV	#	Name	kV					
24042	El Dorado	500	84226	Pisgah	500	1	El Dorado	55		
26044	Marketplace	500	27204	HL Tap	500	1	Marketplace	55		
26048	McCullough	500	26105	Victorville	500	1			Victorville	35
26048	McCullough	500	26105	Victorville	500	2	McCullough	35		
24097	Mohave	500	24086	Lugo	500	1			Lugo	35
22536	N. Gila	500	22360	Imperial Valley	500	2			Imperial Valley	54

Table 2-11. WOR Interface Series Compensation (% of Line Impedance) in Summer Database.

From Bus			To Bus							
#	Name	kV	#	Name	kV	ID	Location	%	Location	%
24801	Devers	500	28195	RedBluff	500	1			RedBluff	70
24801	Devers	500	28195	RedBluff	500	2			RedBluff	70
24042	El Dorado	500	84226	Pisgah	500	1	El Dorado	55		
26044	Marketplace	500	27204	HL Tap	500	1	Marketplace	55		
26048	McCullough	500	26105	Victorville	500	1			Victorville	35
26048	McCullough	500	26105	Victorville	500	2	McCullough	35		
24097	Mohave	500	24086	Lugo	500	1	Mohave	35	Lugo	35
22536	N. Gila	500	22360	Imperial Valley	500	2			Imperial Valley	54

Table 2-12. 500 kV Voltage Controlled Shunt Capacitors by WOR Interface in Spring Database.

#	Name	kV	ID	B (MVar)	Scheduled Voltage	Voltage Deadband
24156	Vincent	500	1	400	1.000 pu	locked
24151	Valley SC	500	ei	300	1.038 pu	+/- 0.012 pu
24092	Miraloma	500	ei	300	1.052 pu	+/- 0.008 pu

Table 2-13. 500 kV Voltage Controlled Shunt Capacitors by WOR Interface in Summer Database.

#	Name	kV	ID	B (MVar)	Scheduled Voltage	Voltage Deadband
24156	Vincent	500	1	0	off	off
24151	Valley SC	500	ei	300	1.038 pu	+/- 0.020 pu
24092	Miraloma	500	ei	300	1.052 pu	+/- 0.02 pu

Table 2-14. SVCs by WOR Interface in Spring Database.

#	Name	kV	ID	Steady-State Output (MVar)	Dynamic Capability (MVar)
24999	Devers	500	1	0	275
24999	Devers	500	2	0	387.5
26120	Marketplace	500	1	0	387.5
26119	Adelanto	500	1	0	387.5

2.2.3 Performance Criteria and Monitoring

The pre-contingency power flow solution allowed static VAR devices (SVDs, i.e., SVCs and automatically switched voltage controlled capacitors), phase angle regulators (PARs), and load tap changing transformers (LTCs) to move. The post-contingency solution parameters varied.

All bus voltages at 230 kV or above were monitored in WECC. The focus, however, was on the buses in the COI interface zones (300 and 405) and the WOR interface zones (210, 227, 240, 241, 248, 254, 260 and 270). Bus voltages at 115 kV and above were monitored in those zones. Pre- and post-contingency voltages less than 0.95 pu or more than 1.10 pu were recorded. Voltage changes from pre- to post-contingency greater than 0.001 pu were also recorded. All interface flows were monitored as well as area flows in PG&E, San Diego and Southern California Edison. All SVC and LTC movements were also monitored.

2.2.4 Contingency Lists

CAISO identified the most critical contingencies for each interface, as shown in Table 2-15 and Table 2-16.

Table 2-15. Critical Contingency List For COI Interface Analysis.

Contingency
Loss of 2 Palo Verde units, including SPS tripping of 120 MW load in Arizona
Loss of PDCI, including SPS tripping of Northwest generation
Loss of 2 San Onofre units
Loss of 2 Diablo Canyon units

Table 2-16. Critical Contingency List For WOR Interface Analysis.

Contingency
Loss of N. Gila-Imperial Valley 500 kV line
Loss of Palo Verde – Colorado River 500 kV line*
Loss of 2 San Onofre units

*The Palo Verde-Colorado River 500 kV outage was the most critical of the three line section outages in the Palo Verde-Colorado River-Red Bluff-Devers 500 kV corridor.

2.3 Dynamic Analysis

The objective of the dynamic analysis was to evaluate the impact of variable renewable power generation on the small signal oscillatory performance of the COI and WOR interfaces. Specifically, the goals were to characterize the frequency components of interface power swings in response to critical faults, to test whether renewable generation oscillating at those frequencies could adversely affect system damping, and therefore, to

identify the need, if any, for a limit on the amount of dynamic scheduling across the interfaces.

The dominant swing modes across the two interfaces were identified using PSLF dynamic simulations. CAISO identified the critical disturbances for each interface and provided descriptions in the form of swt files. These critical fault events, described in Section 2.3.2, were used to stimulate power swings across each interface. This provided a benchmark for determining the effect of dynamic transfers on small-signal stability. A Fast Fourier Transform (FFT) was then used to find the frequency components of these power swings.

To test whether renewable generation could adversely affect power swing damping under challenging conditions, it was assumed that:

- All variable renewable generation in a given area (i.e., wind in the Northwest, solar PV in the Southwest) would oscillate together at one of the identified power swing frequencies
- All variable renewable generation would be located at a single bus near the study interface (i.e., Malin 500 kV bus for the COI analysis, Eldorado 500 kV bus for the WOR analysis) to maximize its impact

The variable renewable generation driving function was a sine wave at a characteristic frequency with a selected magnitude. Additional tests were performed with the driving function at different magnitudes, and at different frequencies. The worst-case fault events were then simulated while the driving function was applied. The results were analyzed to determine the impact on power swing damping, whether WECC voltage and frequency criteria were met, and whether any protective relays operated (e.g., under frequency load shedding, generating unit protection). Adverse impacts were used to establish limits on the dynamic schedule.

The same spring power flow databases developed by CAISO for the steady-state analysis, and described in Section 2.1, were used in the dynamic analysis. The oscillating of renewable generation was implemented by varying the power consumption of a load specifically added for that purpose (i.e., initially at 0 MW).

Minor changes to the associated dynamic data were made to achieve an adequate initialization, i.e., a flat line response in a no-disturbance simulation. Five generators (51576 "DKW 35T1", 37317 "UNIONVLY", 22124 "CHCARITA", 40671 "LONGVIEW", and 44052 "TDA F1F2") were netted as negative load. Six power system stabilizer (PSS) models (21081 "NLNDGT#1", 21083 "NLNDGT#2", 26154 "HYN1112G" ID 11, 26154 "HYN1112G" ID 12, 57274 "MACKAY2", and 38357 "WOODMID2") were switched off.

All under-voltage or under-frequency relays modeled as tlin1 and under-frequency load shedding (UFLS) relays modeled as lsd9 in Alberta (area 54) and British Columbia (area 50) were switched off. This was done in order to avoid spurious results, i.e., limiting overall system performance due to relay operations at small, remote loads.

2.3.1 Performance Criteria and Monitoring

The transient performance criteria were drawn from Western Electricity Coordinating Council Reliability Criteria [1].

The transient voltage dip standard for Category B contingencies is summarized as follows:

- The voltage dip must not exceed 25% at load buses or 30% at non-load buses
- The voltage dip must not exceed 20% for more than 20 cycles at load buses

The minimum transient frequency standard for Category B contingencies is summarized as follows:

- The frequency must not fall below 59.6 Hz for 6 cycles or more at load buses

The transient voltage dip standard for Category C contingencies is summarized as follows:

- The voltage dip must not exceed 30% at any bus
- The voltage dip must not exceed 20% for more than 40 cycles at load buses

The minimum transient frequency standard for Category C contingencies is summarized as follows:

- The frequency must not fall below 59.0 Hz for 6 cycles or more at load buses

For the dynamic analysis, all buses at 345 kV and above were monitored. The more stringent load bus criteria were applied to all buses, even those without loads.

2.3.2 Disturbance List

CAISO identified the most critical dynamic disturbances for each interface, as shown in Table 2-17 and Table 2-18.

Table 2-17. Critical Dynamic Disturbances Evaluated For COI Interface.

Tripped Elements	Other Actions
2 Palo Verde generators	SPS trips 120 MW load in Arizona
Pacific DC Intertie	SPS trips Northwest generation
2 San Onofre generators	None
2 Diablo Canyon generators	None

Table 2-18. Critical Dynamic Disturbances Evaluated For WOR Interface.

Fault Type	Faulted Bus	Tripped Elements	Other Actions
3- ϕ , 4 cy	N. Gila 500 kV	N. Gila-Imperial Valley 500 kV line	None
3- ϕ , 4 cy	Palo Verde 500 kV	Palo Verde-Colorado River 500 kV line	Apply/remove fault damping on PV units
None	None	2 San Onofre generators	None

2.4 Wind and PV Solar Statistical Analysis

Aggregate wind and PV solar profiles were developed from a year (2006) of 10-minute wind and PV solar power profile data from the NREL Western Wind and Solar Integration Study (WWSIS) [2].

For the COI interface evaluation, aggregate wind profiles were developed from about 2,700 wind sites in Oregon and Washington. The individual 30-MW sites were sorted from best to worst, on the basis of their capacity factors. Then the top sites were selected and combined into aggregate profiles of various ratings - approximately 2,500 MW, 5,000 MW, 10,000 MW, and 15,000 MW. The profiles were cumulative, such that the 5,000 MW profile consisted of the 2,500 MW profile plus the next best 2,500 MW of wind sites, and the 10,000 MW profile consisted of the 5,000 MW profile plus the next best 5,000 MW of sites. For simplicity, the profiles are described in round numbers, the actual profiles were integer multiples of the 30-MW plant size. An overview of the aggregate wind profiles is shown in Table 2-19.

Table 2-19. Aggregate Wind Profile Summary.

	2,500 MW	5,000 MW	10,000 MW	15,000 MW
Maximum Output	2,447 MW	4,889 MW	9,775 MW	14,663 MW
Minimum Output	0 MW	3 MW	13 MW	16 MW
# of Oregon Sites	24	39	90	187
# of Washington Sites	59	127	243	313
Total # of Sites	83	166	333	500
Total Rating	2,490 MW	4,980 MW	9,990 MW	15,000 MW

Significantly fewer PV solar sites were available from the WWSIS. The aggregate solar PV profiles were developed from about 275 sites across WECC for the WOR interface evaluation. Each site had a nominal DC rating of 100 MW. The sixteen sites in Arizona were sorted from best to worst, followed by 71 sorted California sites, and then the remaining sorted WECC sites. Again, the ranking was based on capacity factor. The top sites were selected and combined into aggregate cumulative profiles of various ratings. The nominal DC ratings, however, do not account for inverter, transformer, soiling and other losses. As described in Section 2.4.2, the rated AC power is 77% of the DC rating. Therefore, both the AC and DC ratings are used to identify the aggregate profiles. An overview of the aggregate solar PV profiles is shown in Table 2-20.

Table 2-20. Aggregate PV Solar Profile Summary.

	2,500 MW DC 1,925 MW AC	5,000 MW DC 3,850 MW AC	10,000 MW DC 7,700 MW AC	15,000 MW DC 11,550 MW AC
Maximum Output	1,813 MW	3,581 MW	7,040 MW	10,624 MW
Minimum Output	0 MW	0 MW	0 MW	0 MW
# of Arizona Sites	16	16	16	16
# of Other WECC Sites	9	34	84	134
Total # of Sites	25	50	100	150

The aggregate profiles were analyzed to statistically characterize their expected variability. Specifically, this statistical analysis evaluated the change in wind or PV solar generation from one 10-minute point to the next. From this, a statistical expectation of the change in power (ΔP) per MW of rated wind or solar generation was determined, and then an expected ΔP per MW of dynamic scheduling.

A measure of the ΔV per MW of dynamic schedule was determined from this ΔP per MW of dynamic schedule and the $\Delta V/\Delta P$ characteristic calculated in the power flow analysis. The ΔV per MW of dynamic schedule across COI was based on the aggregate wind profile, and the statistical expectation of ΔV per MW of dynamic schedule across WOR was based on the aggregate PV solar profile.

2.4.1 Wind Data Development

An overview of the wind data development for the WWSIS is provided below. A detailed description of the wind data is available from the NREL website [3].

3TIER Group developed the wind dataset for the WWSIS. Lacking sufficient measured data to represent the necessary level of wind generation (over 75 GW), the wind resource across the entire western United States was modeled to generate a consistent wind dataset in space and time. 3TIER Group used the Weather Research and Forecasting (WRF) mesoscale Numerical Weather Prediction Model (NWP) over the western United States at a 2-km, 10-minute resolution for years 2004-2006. In order to do this, it was necessary to run four independent geographical domains in 3-day blocks, merge them together and smooth the seams. While the seams were smoothed so that variability did not exceed realistic limits, the days with seams unfortunately exhibited significantly more variability than the days without seams. Therefore, the wind data from every third day (starting with day one) were eliminated from the 10-minute statistical analysis.

Each 2-km x 2-km grid cell was assumed to contain 10 Vestas V90 3-MW wind turbines, yielding a 30-MW rating per grid cell. Actual wind plants, however, do not exhibit a deterministic wind plant power curve. Therefore, 3TIER Group's stochastic SCORE (Statistical Correction to Output from a Record Extension) and SCORE-lite methodologies were used for power conversion, instead of using the sum of ten Vestas V90 wind turbine power curves.

3TIER Group, NREL, and NAU validated the dataset against meteorological tower measurements of wind speed. NREL also validated the dataset against wind plant output for over 1 GW of actual wind plants for which NREL could access historic data.

2.4.2 Solar Data Development

An overview of the PV solar data development for the WWSIS is provided below. A detailed description of the PV solar data is available from the NREL website [4].

The State University of New York (SUNY) at Albany, Clean Power Research, developed the solar resource dataset (SolarAnywhere) for the study. They used a satellite cloud cover model to simulate the United States at a 10-km, hourly resolution. This dataset includes global horizontal, direct normal and diffuse radiation.

The hourly PV data was modeled as distributed generation on rooftops, because sufficient measurements and modeling information for large, central station PV plants were not available at the time of the study. Weather stations in the western United States were modeled using PV Watts to create PV output in block sizes of 100-MW DC. Default settings of PV Watts were used for inverter and transformer losses, soiling and other losses, and system availability, for a total derating factor of 0.77. That means that the total AC output under standard temperature conditions was 77% of the DC rating. In order to model distributed generation from multiple, dispersed resources, PV Watts was run using 11 different system configurations of tilt, orientation, and tracking/flat-plate selection. The outputs were aggregated.

To refine the PV output from the above hourly data to a 10-minute resolution, NREL developed a model that compared the hourly average PV output to the clear sky (no clouds) PV output and added sub-hourly variability. The amount of variability added was based on measured PV output from many small PV plants in Arizona Public Service's Solar Test and Research (STAR) program, the Springerville system, and several small PV plants in Colorado.

3 COI Interface

The objective of this analysis was to identify any dynamic schedule limitations on the COI interface due to steady-state voltage and/or oscillatory performance.

3.1 Voltage Performance

The objective of the steady-state analysis was to evaluate the impact of dynamic scheduling on the voltage performance of the COI interface. Specifically, the goal was to determine the impact of variations in imports (ΔP) on delta voltage (ΔV) and the resulting impact on equipment – i.e., shunt capacitor or reactor switching events and LTC transformer tap motions.

3.1.1 Steady-state $\Delta V/\Delta P$ Characteristic

The steady-state $\Delta V/\Delta P$ characteristics of the COI interface were calculated for two spring system conditions; all lines in and with the Captain Jack-Olinda 500 kV line out of service. The Captain Jack-Olinda 500 kV line was the most heavily loaded line on the COI interface. Calculations were made for 553 MW, 1,106 MW and 1,521 MW changes in Northwest generation, which was implemented at John Day.

Figure 3-1 shows a scatter plot of ΔV for the monitored buses for the three delta generation (ΔP_{gen}) conditions, for all six of the voltage control options as defined in Section 2.2. All CAISO buses at 230 kV and above were monitored. In addition, 115 kV buses near the interface were monitored. The plot shows groupings of voltage changes (ΔV) for each delta generation condition. The delta voltages are sorted from highest to lowest independently for each control option.

The x-axis is a count of data points, corresponding to the number of voltages recorded for each scenario. Note that there are fewer recorded voltages for the lower ΔP_{gen} cases than the higher. This is due to the monitoring logic used to record bus voltages. The higher levels of ΔP_{gen} result in larger ΔV s, which means that more buses will meet the recording criteria.

The initial condition for all scenarios is a stressed COI case. When imports are reduced, system voltages will increase. Thus, nearly all ΔV values are positive. The control option with only LTC action shows the largest ΔV at nearly every bus for all delta generation conditions. This is followed by the No Action, and Continuous Action control options. Options with switched shunts active (All SVD Action, SVC & LTC Action, and SVD, LTC, PAR Action) have lower voltages, and in some cases ΔV is negative. This is primarily due to shunt capacitors switching off following the reduction in imports.

The 500 kV buses in Northern CA and Southern OR have the largest ΔV . This includes the Maxwell, Round Mountain, Olinda, Malin, and Captain Jack 500 kV buses. For a 1,521 MW reduction in Northwest generation, the Round Mountain 500 kV bus voltage increases by 0.034 pu with no control action, 0.038 pu with LTC control only and 0.033 pu with continuous

SVD. The majority of buses have a ΔV of less than 0.02 pu for the 1,521 MW change in generated power.

Figure 3-2 shows a similar scatter plot of ΔV with the Captain Jack-Olinda 500 kV line out of service. For these scenarios, the line was taken out of service and the powerflow case was solved with all control actions (LTC, SVCs, switched shunts, and PARs) active. The dispatch was not modified to reduce CAISO imports or COI path flows. The three delta generation scenarios were then implemented with the six different control options.

With the 500 kV line out of service, ΔV is greater. Again, the largest changes in voltages are seen at the 500 kV buses in Northern CA. Round Mountain 500 kV voltages increased by 0.047 pu with no control action, and 0.051 pu with only LTC action for a 1,521 MW generation shift. However, the majority of buses see a voltage change of less than 0.02 pu.

Figure 3-3 is a scatter plot of $\Delta V/\Delta P_{gen}$ with all lines in service. The points represent ΔV per 100 MW of ΔP generation in the Northwest. $\Delta V/\Delta P_{gen}$ is less than 0.002 pu per 100 MW of ΔP_{gen} for nearly every bus in the CAISO system, with the majority of buses less than 0.001 pu/100 MW of ΔP_{gen} . Figure 3-4 shows $\Delta V/\Delta P_{gen}$ with Captain Jack-Olinda out of service. $\Delta V/\Delta P_{gen}$ for the majority of buses does not change significantly with the line out. However, for the most effected buses, $\Delta V/\Delta P_{gen}$ increases by about 0.001 pu per 100 MW of ΔP_{gen} .

Another way to view the $\Delta V/\Delta P$ of the different scenarios is for an individual bus. Figure 3-5 is a plot of the Round Mountain 500 kV bus voltage plotted against ΔP generation. The ΔV for six control options is shown. At a 553 MW reduction in Northwest generation, ΔV is between 0.012 and 0.014 pu for the different control options. With increased reduction in generation, ΔV increases and the spread between the control options increases. For a 1,512 MW reduction in generation, ΔV ranges from 0.025 pu for full SVD & LTC Action, to 0.038 pu with only LTC Action. This is the largest ΔV for any of the monitored CAISO buses.

Figure 3-6 shows the same ΔV as Figure 3-5, but they are plotted against the change in flow on COI (ΔP_{coi}). Every 1 MW of generation shifted from John Day to CAISO reduces the flow on COI by about 0.67 MW. Thus, the three test generation levels (553 MW, 1,106 MW and 1,521 MW) result in 368 MW, 750 MW and 1,042 MW reductions in COI flow.

Figure 3-7 and Figure 3-8 show similar graphs of Round Mountain ΔV with the Captain Jack-Olinda 500 kV line out. As expected, the range of ΔV is larger with a major line out than with all lines in. The ΔV ranges from 0.036 pu for All SVD Action to 0.051 pu for LTC Action.

Given the change in Northwest generation, change in COI flow and change in voltage, the range of $\Delta V/\Delta P$ at Round Mountain is shown in Table 3-1. The values shown are for no control action, continuous SVD (SVC's) Action, LTC Action and SVC & LTC Action. These show the widest range in $\Delta V/\Delta P$. Similar data with the Captain Jack-Olinda 500 kV line out are shown in Table 3-2. The variations in $\Delta V/\Delta P$ reflect the non-linearity of the system. These include generator reactive range (i.e. when a unit runs into a reactive limit and can no longer regulate voltage), SVC reactive range, LTC tap movements and shunt capacitor/reactor switching. The value of $\Delta V/\Delta P$ at Round Mountain with only SVC control action is slightly lower than that with no control action.

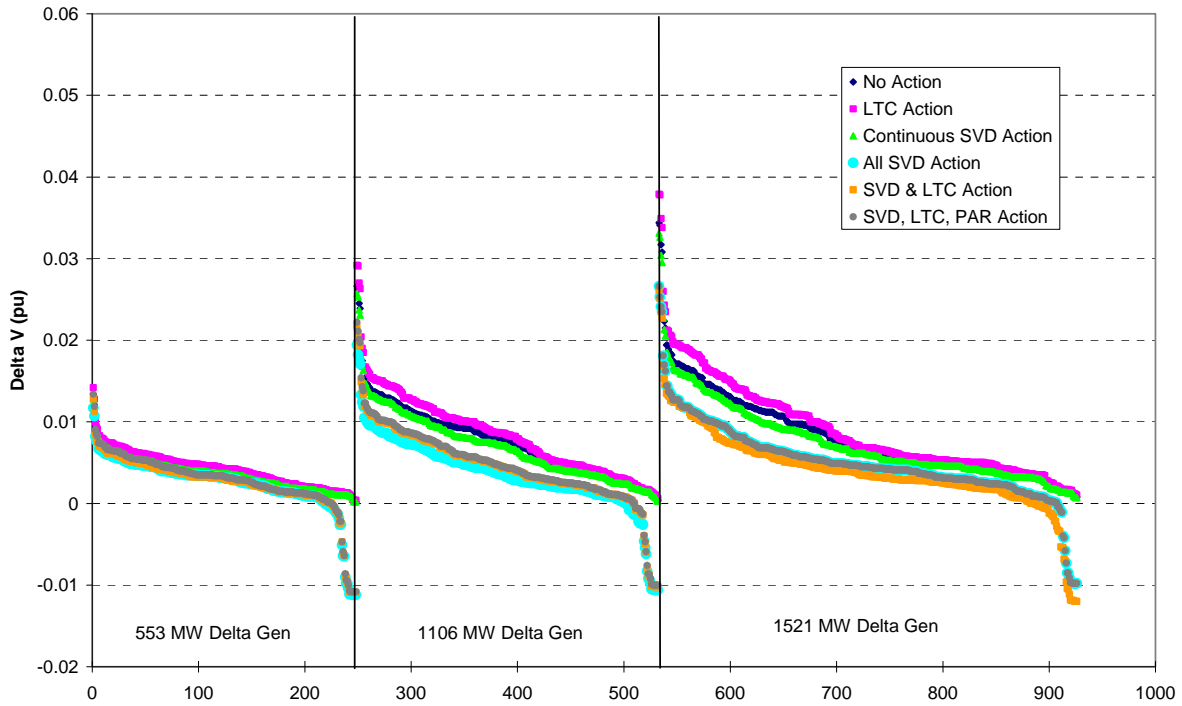


Figure 3-1. ΔV of CAISO Monitored Buses For ΔP in Northwest, All Lines In.

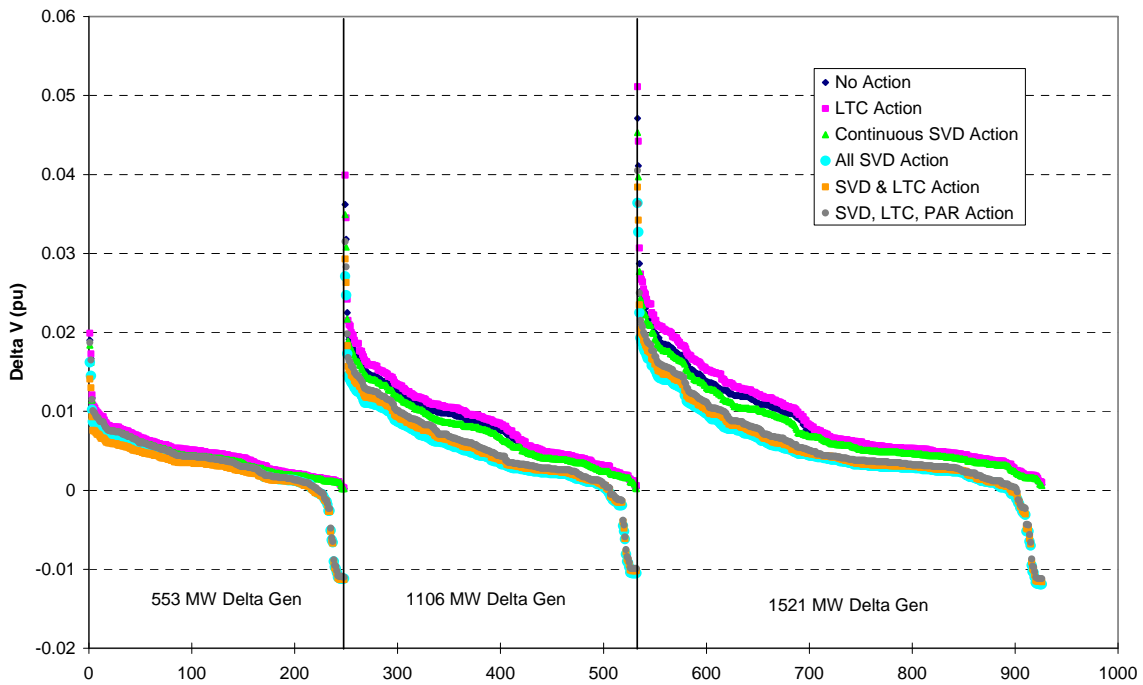


Figure 3-2. ΔV of CAISO Monitored Buses For ΔP in Northwest, Captain Jack-Olinda Out of Service Pre Generation Shift.

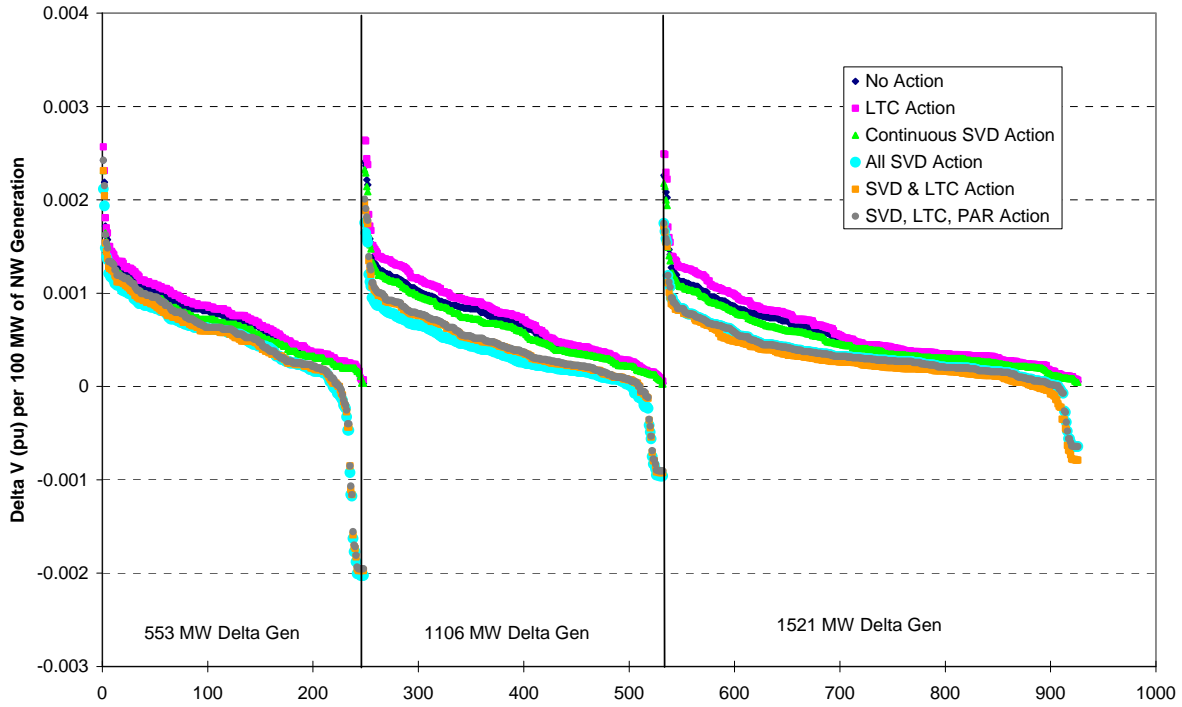


Figure 3-3. $\Delta V/\Delta P_{gen}$ of CAISO Monitored Buses per 100 MW of ΔP in Northwest, All Lines In.

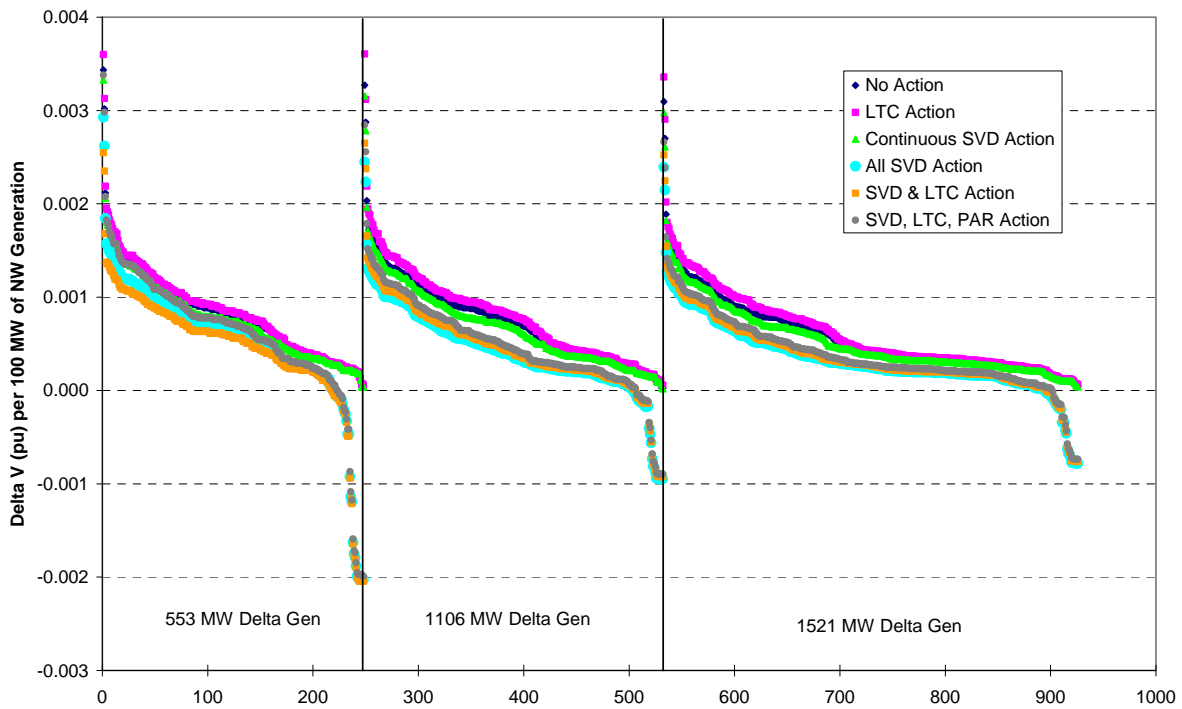


Figure 3-4. $\Delta V/\Delta P_{gen}$ of CAISO Monitored Buses per 100 MW of ΔP in Northwest, Captain Jack-Olinda Out of Service Pre Generation Shift.

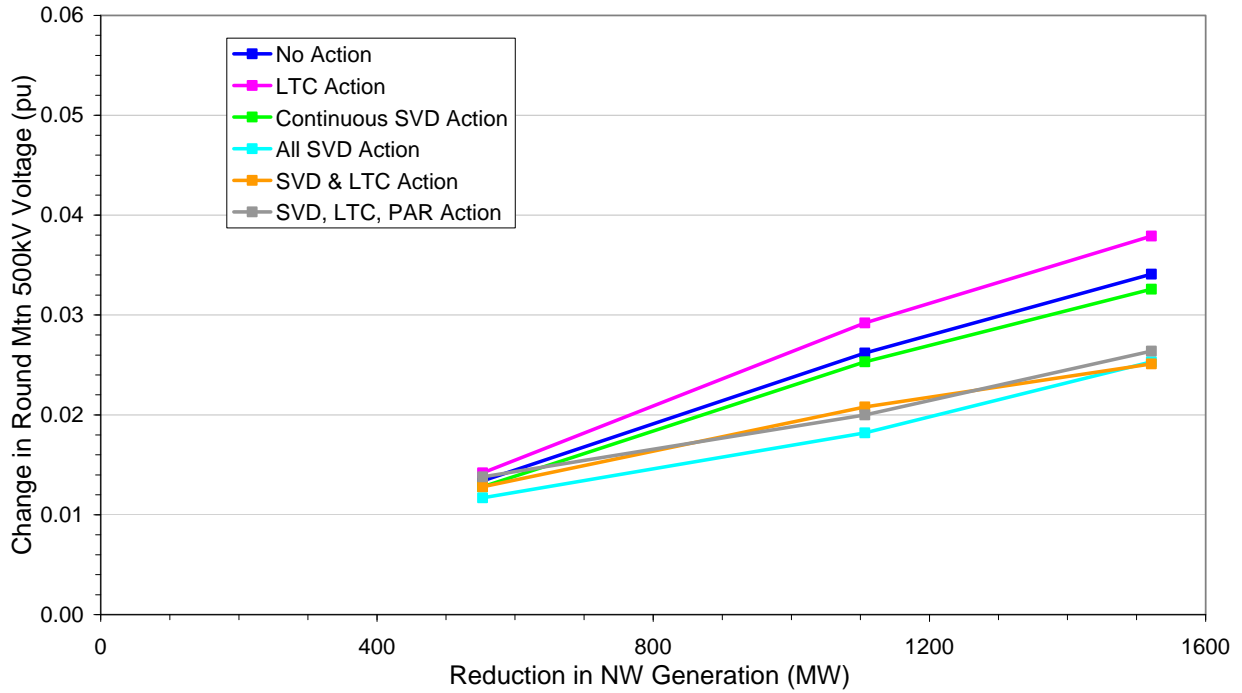


Figure 3-5. ΔV of Round Mountain 500 kV Bus Voltage For ΔP in Northwest, All Lines In Service.

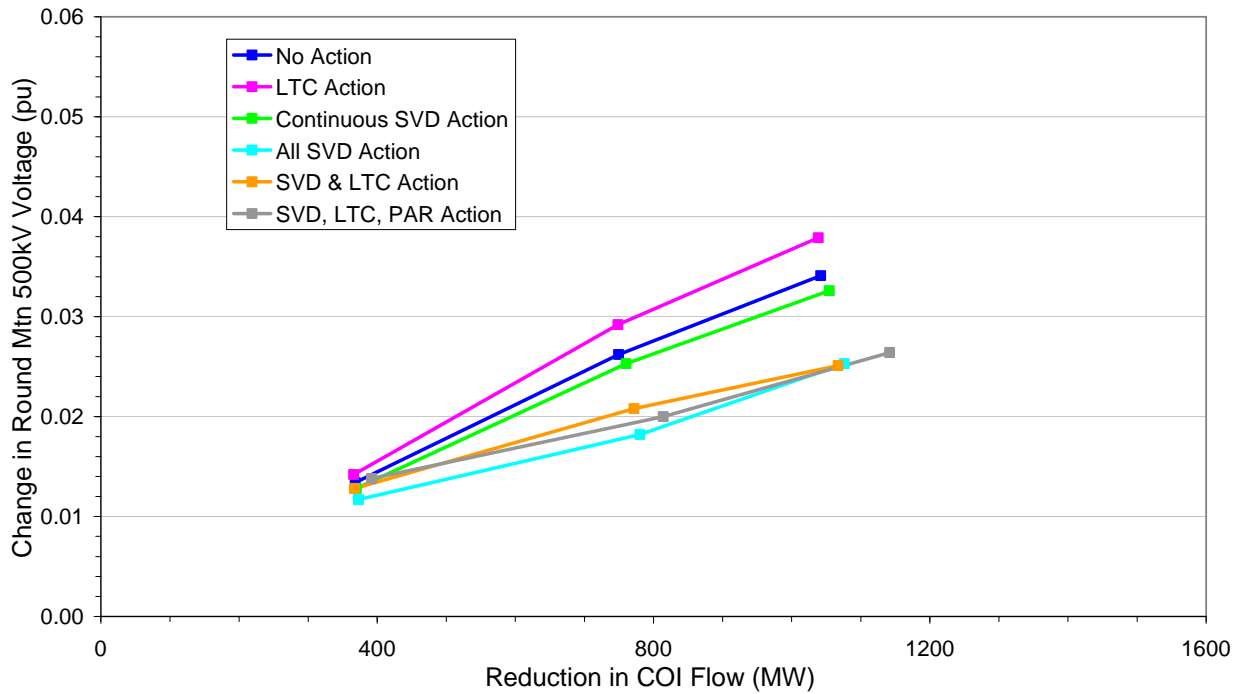


Figure 3-6. ΔV of Round Mountain 500 kV Bus Voltage For ΔP in Northwest, All Lines In Service, Plotted Against COI Flow.

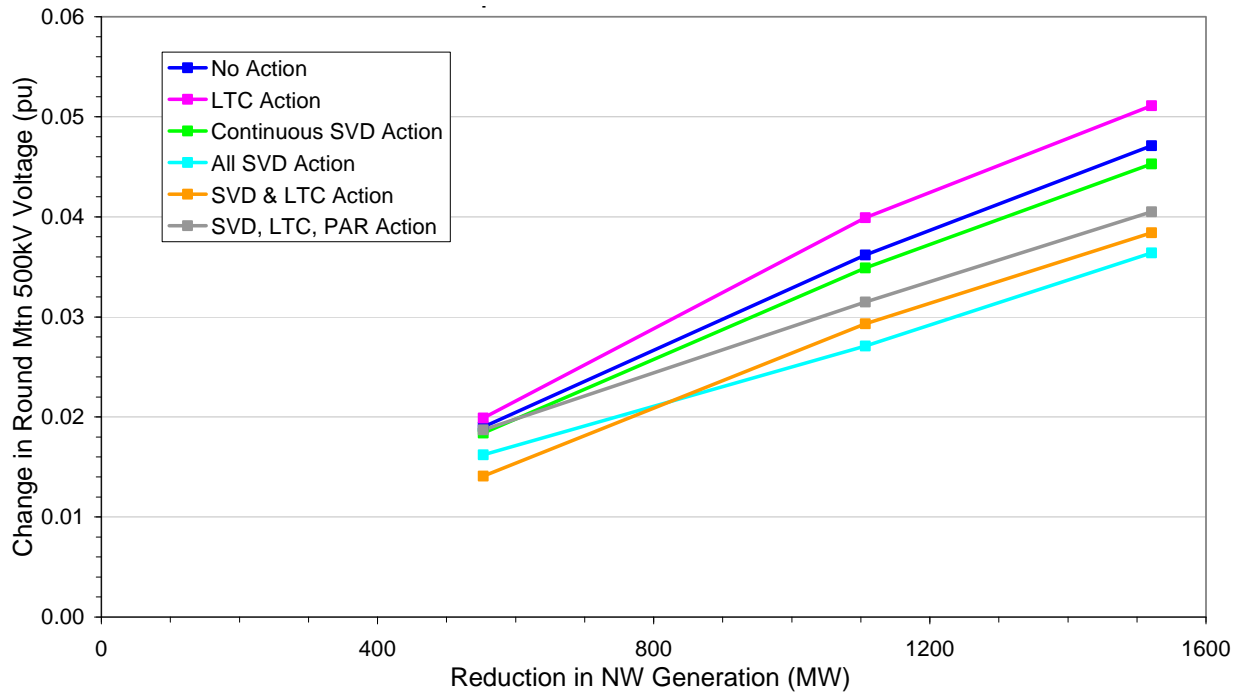


Figure 3-7. ΔV of Round Mountain 500 kV Bus Voltage For ΔP in Northwest, Captain Jack-Olinda 500 kV Line Out of Service.

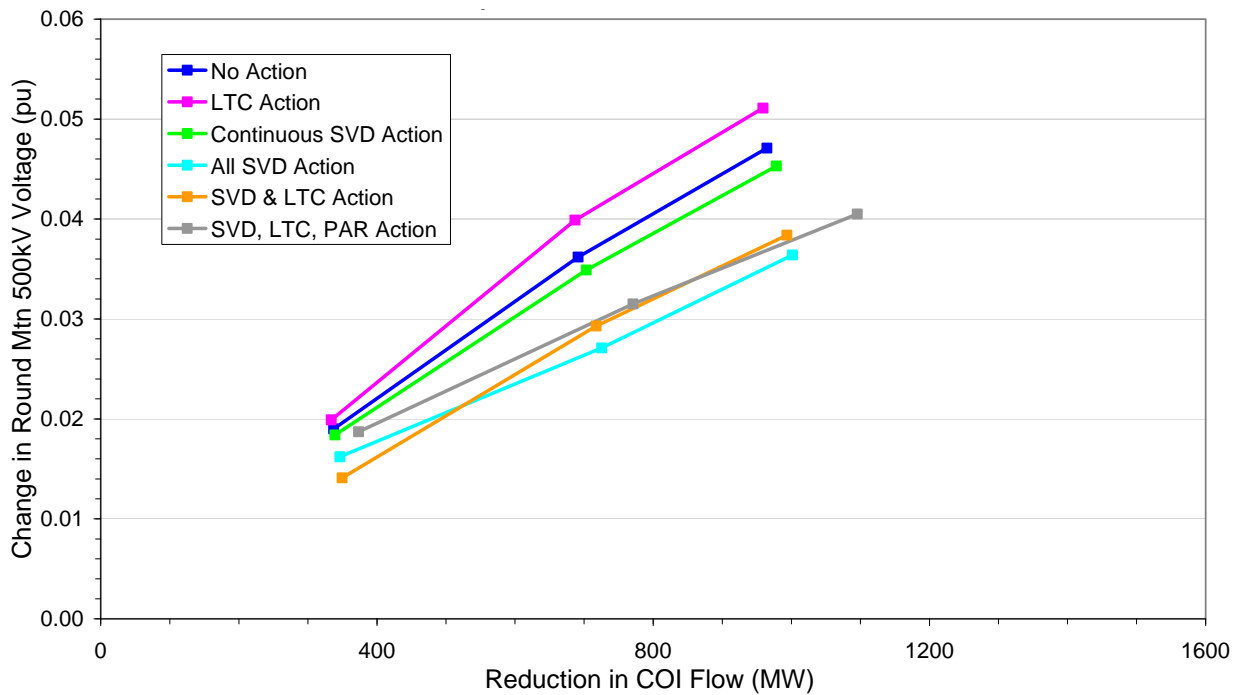


Figure 3-8. ΔV of Round Mountain 500 kV Bus Voltage For ΔP in Northwest, Captain Jack-Olinda 500 kV Line Out of Service, Plotted Against COI Flow.

Table 3-1. $\Delta V/\Delta P$ at Round Mountain 500 kV, All Lines In. Values Are Per Unit per 100 MW of ΔP on COI and ΔP Northwest Generation.

No Action		SVC Action		LTC Action		SVD & LTC Action _I	
$\Delta V/\Delta P_{COI}$	$\Delta V/\Delta P_{GEN}$	$\Delta V/\Delta P_{COI}$	$\Delta V/\Delta P_{GEN}$	$\Delta V/\Delta P_{COI}$	$\Delta V/\Delta P_{GEN}$	$\Delta V/\Delta P_{COI}$	$\Delta V/\Delta P_{GEN}$
0.0033 to 0.0036	0.0022 to 0.0024	0.0031 to 0.0035	0.0021 to 0.0023	0.0037 to 0.0039	0.0025 to 0.0026	0.0024 to 0.0035	0.0017 to 0.0023

Table 3-2. $\Delta V/\Delta P$ at Round Mountain 500 kV, Captain Jack-Olinda 500 kV line Out of Service. Values Are Per Unit per 100 MW of ΔP on COI and ΔP Northwest Generation.

No Action		SVC Action		LTC Action		SVD & LTC Action	
$\Delta V/\Delta P_{COI}$	$\Delta V/\Delta P_{GEN}$						
0.0049 to 0.0056	0.0031 to 0.00344	0.0047 to 0.0055	0.0030 to 0.0033	0.0053 to 0.0059	0.0034 to 0.0036	0.0040 to 0.0042	0.0025 to 0.0026

3.1.2 Shunt Capacitor and LTC Switching

One of the concerns with the voltage variations caused by dynamic scheduling is excessive LTC tap motion and shunt capacitor/reactor switching. For example, a sudden reduction in imports from the Northwest will cause CA voltage to increase. If the change in voltage is great enough, it will cause capacitors to switch off. A subsequent increase in Northwest imports will reduce voltages in CA, and could cause the capacitors to switch back on.

Excessive capacitor switching will only be an issue when ΔV caused by the change in imports plus ΔV caused by capacitor switching exceeds the voltage control deadband. The values of ΔV for capacitor switching will vary depending on system conditions. However, it is reasonable to assume that the control deadband of any automatically switched capacitor will be set to at least two times the ΔV for capacitor switching. Under this assumption, the largest ΔV for capacitor switching would be 50% of the voltage control deadband. This leaves another 50% of the deadband for import variations.

Table 3-3 shows the 230 kV and above CAISO buses with switched shunt capacitors where the ΔV for the 1,521 MW reduction in NW generation exceeds 50% of the control deadband. This table shows the voltage control deadband modeled in the powerflow (e.g., 2*SVD vband), ΔV for 1,106 MW and 1,521 MW reduction in NW generation, and ΔV in percent of the control deadband for the two generation reductions. The ΔV values are with only SVCs active, since they will regulate before shunt capacitors and LTCs switch.

By the logic described above, all eight shunt capacitors listed in Table 3-3 could experience off/on switching cycles for 1,521 MW decrease/increase cycles in imports. At 1,106 MW, only three of the shunt capacitors would switch on and off. The $\Delta V/\Delta P_{gen}$ with the Captain Jack-Olinda 500 kV line out is higher than for the base system. The ΔV is generally about 0.01 to 0.02 pu higher for the contingency condition than for the normal condition on the 500 kV

buses near COI for 1,521 MW ΔP . On 230 kV buses, the increase in ΔV is about 0.002 to 0.005 pu . Thus, for the outage, additional 500 kV capacitors could experience off/on switching, and it could occur at lower levels of ΔP_{gen} . However, the outage should not significantly increase the likelihood of repeated off/on switching for the majority of capacitors on the 230 kV and lower system.

The control deadbands for the 230 kV shunt capacitors are set at 0.018 pu in the powerflow supplied. This is a tight control range and may not represent actual equipment settings.

Table 3-3. ΔV at Selected Buses with Switched Shunt Capacitors. ΔV Shown for 1,521 MW and 1,106 MW Change in NW Generation.

Bus #	Name	kV	Control Vband (pu)	1,106 MW ΔP_{gen}		1,521 MW ΔP_{gen}	
				ΔV (pu)	ΔV (% of Vband)	ΔV (pu)	ΔV (% of Vband)
30020	OLINDA	500	0.04	0.0237	59	0.0304	76
30035	TRACY	500	0.04	0.0168	42	0.0213	53
30765	LOSBANOS	230	0.018	0.008	44	0.0103	57
30735	METCALF	230	0.018	0.0087	48	0.0108	60
30705	MONTAVIS	230	0.018	0.0083	46	0.0102	57
30630	NEWARK D	230	0.018	0.0082	46	0.0098	54
30625	TESLA D	230	0.018	0.0118	66	0.0146	81
30460	VACA-DIX	230	0.018	0.0131	73	0.0162	90

Similar analysis was performed for the LTC transformers in the CAISO area. The largest change in bus voltages at any 230 kV bus is 0.0073 pu for 553 MW, 0.0141 pu for 1,106 MW, and 0.018 pu for 1,521 MW. The tightest voltage control band width for all LTC transformers in CAISO is 0.008 pu, and most have a control band width of 0.015 pu or more. Given this, it is possible that repeated decrease/increase cycles in imports of 500 MW or more could cause LTC tap switching. However, most LTCs in CAISO are regulating lower voltage buses, where the change in voltage is significantly lower than on the 230 kV system. Therefore, the number of transformers susceptible to repeated LTC switching should be limited.

Simulations run with LTC transformer and switched shunt controls active show little switching within CAISO. This is as much a function of the initial condition in the powerflow case as the ΔV of the dynamic imports. However, it does indicate that even large changes in imports should not cause excessive equipment switching.

3.1.3 Sensitivity Analysis

Three types of sensitivities were explored – additional transmission line or generating unit outages, different generation redispatch procedures, and a higher system load level (i.e., summer peak).

The analysis above concentrated on normal operation and operation with Captain Jack-Olinda 500 kV line out of service. Figure 3-9 shows a sorted scatter plot of ΔV vs. ΔP_{gen} for the spring base system and five critical outages:

- Loss of Captain Jack-Olinda 500 kV line
- Loss of two Palo Verde units, including SPS tripping of 120 MW Arizona load
- Loss of PDCI, including SPS tripping of Northwest generation
- Loss of two San Onofre units
- Loss of two Diablo Canyon units

The plot shows ΔV for the control option with only SVCs active (LTC taps and switched shunts fixed). In general, ΔV for the additional outages is slightly higher than ΔV for the Captain Jack-Olinda outage. However, the single largest ΔV is for the Captain Jack-Olinda outage.

In the analysis presented to this point, redispatching of tripped Northwest generation was distributed across all CAISO units, proportional to their MVA and up to their maximum power limit. Two redispatch sensitivities were performed. In one, units identified as baseload in the powerflow (gens table BL flag set to 1) did not participate in the redispatch. In the custom dispatch, individual units selected by CAISO were redispatched. In the spring case, most of the selected units were out of service. These units were turned on and allowed to contribute to the redispatch. A sorted scatter plot of the base and two sensitivity redispatches is shown in Figure 3-10. The plot shows ΔV for the control option with only generator control and SVCs active. LTC taps and switched shunts were fixed.

ΔV is slightly lower when baseload units do not participate in the redispatch. This change is likely due to the change in flow patterns caused by the different generation redispatch.

ΔV is both somewhat higher and lower with the custom dispatch. Because the custom dispatch required turning on out-of-service units, it also adds reactive power to the system. Therefore, the ΔV changes are due to that as well as to the change in flow patterns caused by the different generation redispatch.

Both variations on the redispatch procedure show that there is some sensitivity of ΔV to the units that are redispatched to meet dynamic scheduling.

The final sensitivity examined the voltage performance of a summer case. A sorted scatter plot of the spring and summer ΔV results, with the original redispatch approach, is shown in Figure 3-11. Figure 3-12 is a scatter plot of $\Delta V/\Delta P_{gen}$ for the spring and summer cases with all lines in service. The points represent ΔV per 100 MW of ΔP generation in the Northwest. In both figures the summer results are lower than the spring results. This is likely due to the significantly higher number of generators in the summer case – more generation means more reactive capability, which results in better voltage control.

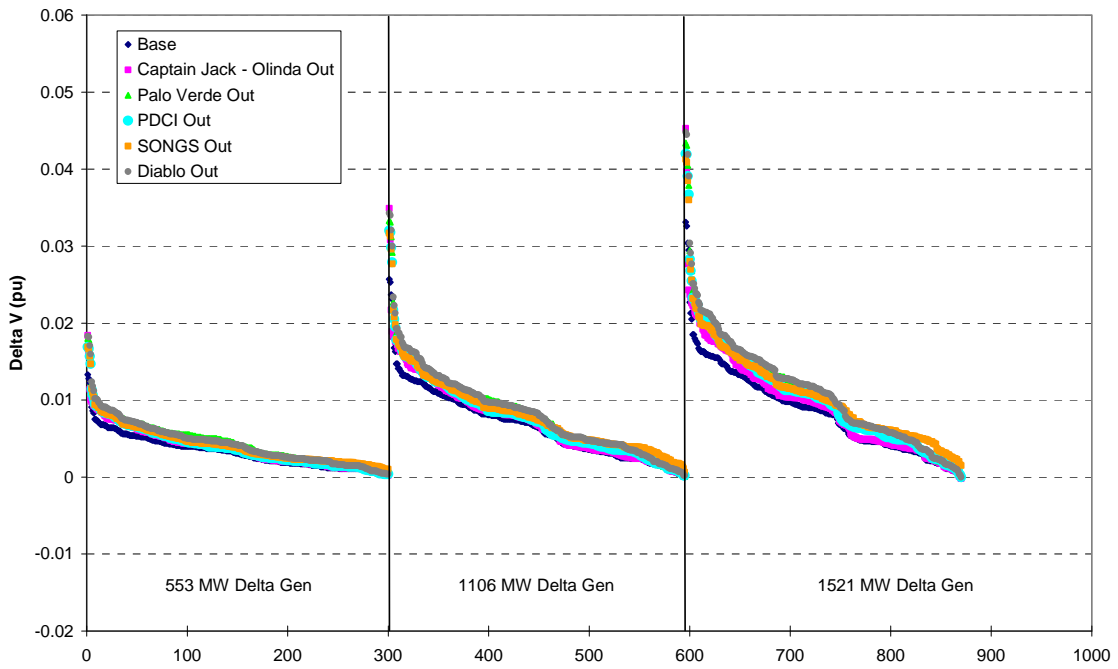


Figure 3-9. ΔV of CAISO Monitored Buses For ΔP in Northwest, Base System and Five Worst-Case Outages.

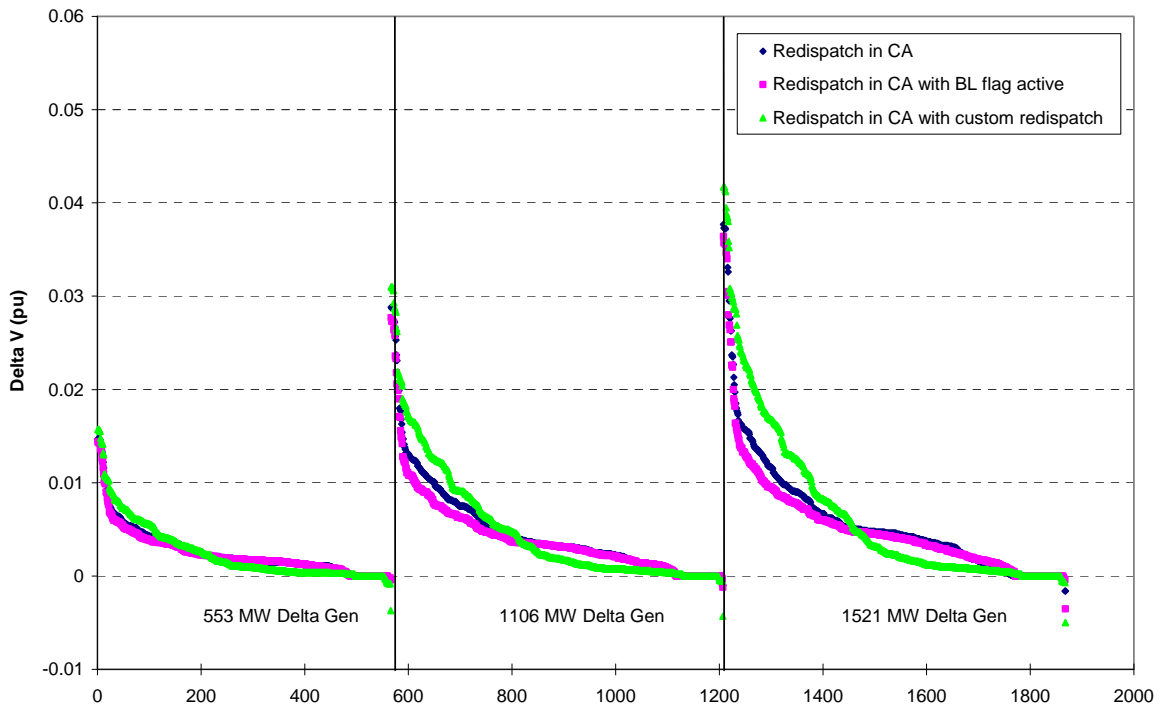


Figure 3-10. ΔV of CAISO Monitored Buses For ΔP in Northwest, Redispatch All CAISO Units (blue), Redispatch of Non-Base-load Units (pink), Redispatch Selected Units (green).

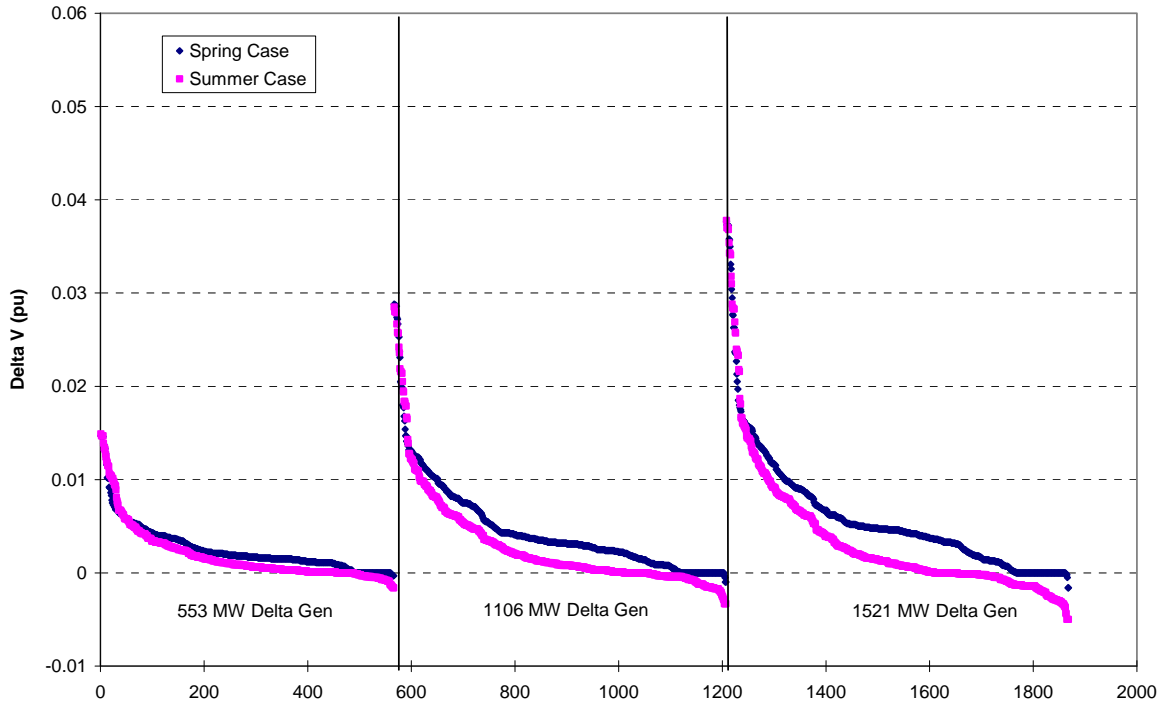


Figure 3-11. ΔV of CAISO Monitored Buses For ΔP in Northwest, Spring (blue) vs. Summer (pink).

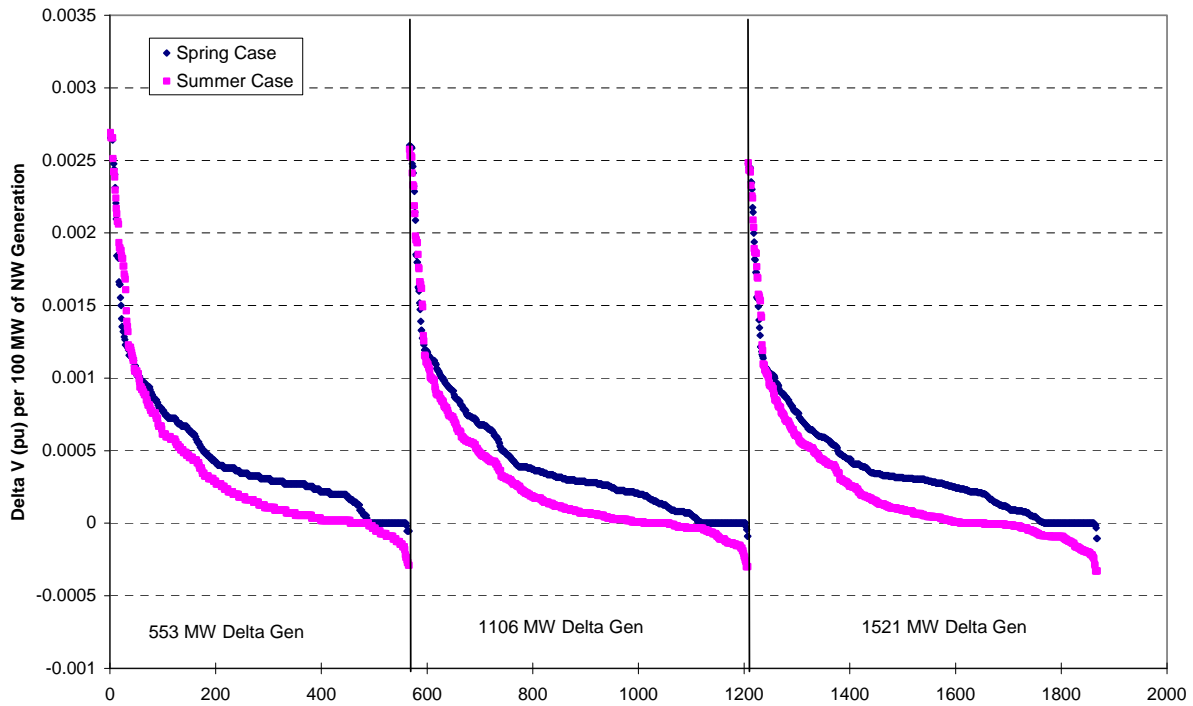


Figure 3-12. $\Delta V/\Delta P_{gen}$ of CAISO Monitored Buses per 100 MW of ΔP in Northwest, Spring (blue) vs. Summer (pink).

3.1.4 Statistical Analysis of Wind Profiles

The aggregate wind profiles, as described in Section 2.4, were analyzed to statistically characterize their expected variability. Specifically, this statistical analysis evaluated the change in wind generation from one 10-minute point to the next. This 10-minute difference in wind generation is called the 10-minute wind delta throughout this report.

A scatter plot of the 10-minute wind deltas for the 5,000 MW aggregate wind profile is shown in Figure 3-13. As expected, there is more variability (i.e., larger 10-minute deltas) in the mid-range of wind power output. In this region, changes in wind speed are reflected as changes in wind power output which is proportional to the cube of the wind speed. At wind speeds above rated, the wind turbines are already at maximum power output and changes in wind speed do not have as much impact on the power output. In this aggregate wind profile, the maximum positive 10-minute change in power is about 1,400 MW and occurs at about 2,000 MW of output (~40% of rated) after the change. The maximum negative 10-minute change in power is about -1,700 MW and occurs at about 1,000 MW of output (~20% of rated) after the change.

A summary of the wind delta statistics is shown in Table 3-4. They are split between positive deltas and negative deltas. Since the power flow analysis was performed with the COI interface near maximum, the focus will be on the negative deltas. As an example, the 5,000 MW wind profile shows a maximum negative delta (i.e., a drop in wind generation) of -1,672 MW. However, the average negative delta is only -46 MW, and the median (i.e., 50% of the negative deltas are greater than this value and 50% are less than this value) is even less at -26 MW.

This maximum and median are also highlighted in the duration curve of negative deltas for the 5,000 MW profile shown in Figure 3-14. This figure shows that the majority of the negative deltas are below about -300 MW. In fact, 99% of the negative deltas are below -301 MW. This means that once every day and a half, wind farms with a total rating of 5,000 MW would be expected to produce one 10-minute drop in power of more than 301 MW. Additional negative wind delta expectation percentages, and their frequencies, are shown in Table 3-5. Positive wind delta expectation percentages are shown in Table 3-6.

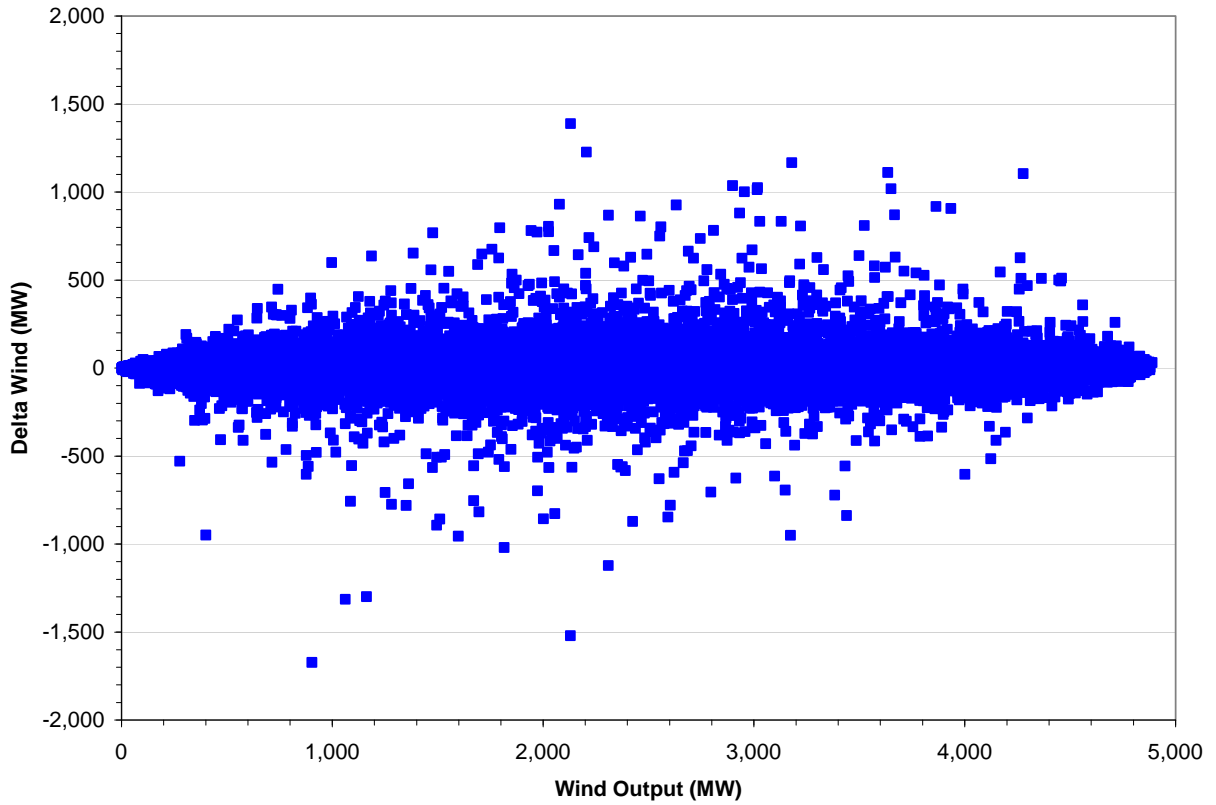


Figure 3-13. 10-Minute Deltas in 5,000 MW Wind Profile.

Table 3-4. Aggregate Wind Profile 10-Minute Delta Statistics.

	2,500 MW	5,000 MW	10,000 MW	15,000 MW
Maximum Output	2,447 MW	4,889 MW	9,775 MW	14,663 MW
Maximum Positive Delta	695 MW	1,388 MW	2,363 MW	2,896 MW
Average Positive Delta	26 MW	48 MW	81 MW	107 MW
Median Positive Delta	14 MW	24 MW	42 MW	57 MW
% of Positive Deltas	49%	48%	48%	48%
Maximum Negative Delta	-785 MW	-1,672 MW	-2,554 MW	-3,199 MW
Average Negative Delta	-25 MW	-46 MW	-78 MW	-104 MW
Median Negative Delta	-14 MW	-26 MW	-45 MW	-62 MW
% of Negative Deltas	51%	52%	52%	52%

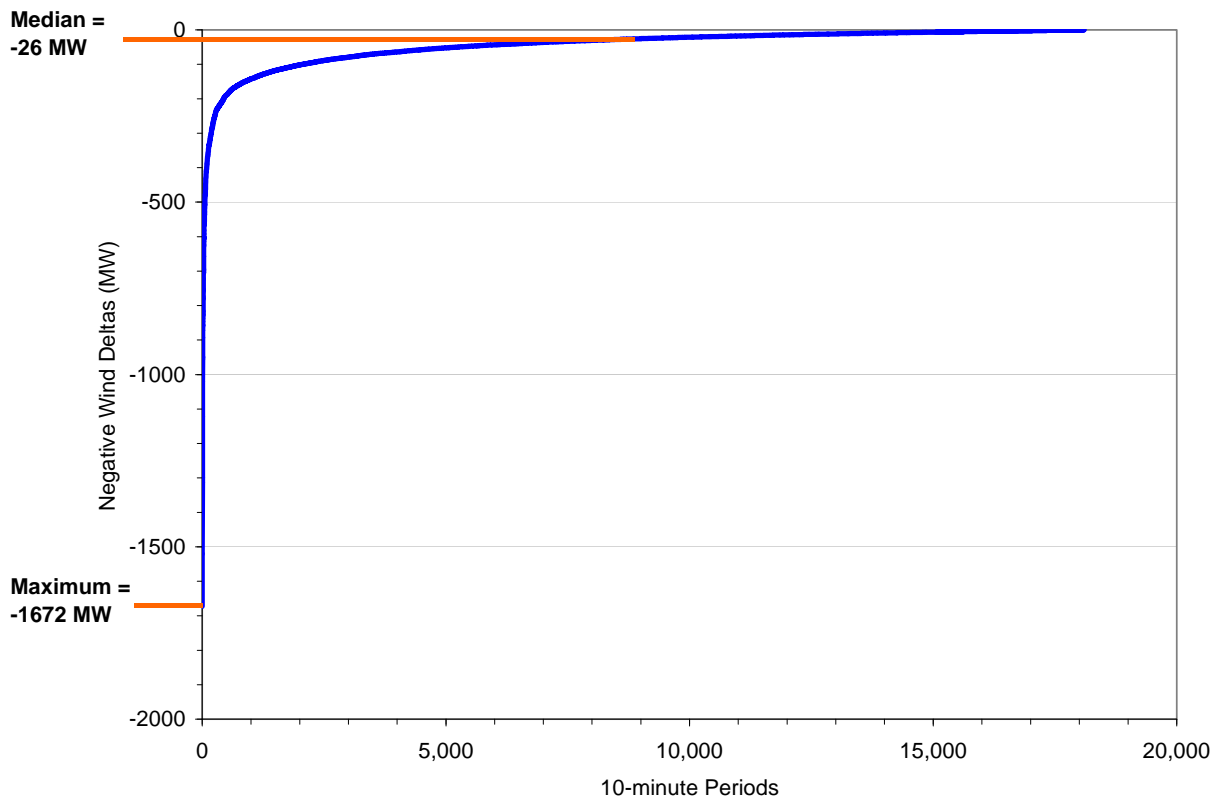


Figure 3-14. 10-Minute Negative Deltas in 5,000 MW Wind Profile.

Table 3-5. Expected 10-Minute Negative Wind Deltas.

% Expectation	Frequency	2,500 MW	5,000 MW	10,000 MW	15,000 MW
-	Once per year	-785 MW	-1,672 MW	-2,554 MW	-3,199 MW
99.9%	Once every 2 weeks	-393 MW	-780 MW	-1,257 MW	-1,543 MW
99%	Once every 1.5 days	-155 MW	-301 MW	-495 MW	-611 MW
95%	Four times per day	-80 MW	-148 MW	-250 MW	-324 MW
90%	Eight times per day	-57 MW	-108 MW	-182 MW	-239 MW

Table 3-6. Expected 10-Minute Positive Wind Deltas.

% Expectation	Frequency	2,500 MW	5,000 MW	10,000 MW	15,000 MW
-	Once per year	695 MW	1,388 MW	2,363 MW	2,896 MW
99.9%	Once every 2 weeks	461 MW	868 MW	1,412 MW	1,752 MW
99%	Once every 1.5 days	191 MW	376 MW	628 MW	825 MW
95%	Four times per day	86 MW	166 MW	285 MW	366 MW
90%	Eight times per day	57 MW	108 MW	186 MW	247 MW

From the steady-state analysis with all lines in service under spring conditions, the largest $\Delta V/\Delta P_{gen}$ occurs at the Round Mountain 500 kV bus. With no control action, $\Delta V/\Delta P_{gen}$ is 0.0024 pu/100 MW of ΔP_{gen} . With only LTC controls active, the value is 0.0039 pu/100 MW. The expected ΔV can be calculated based on these values and on the expected 10-minute negative wind deltas. The ΔV range is show in Table 3-7.

Once every two weeks a drop in wind of 780 MW or more will result in a voltage change of 0.02 pu or greater. This could result in a shunt capacitor or LTC switching cycle (e.g. cap switches off when generation drops, then back on when generation picks up). One time per year, a more significant change in voltage can be expected.

Table 3-8 lists the expected frequency and magnitude of ΔP_{gen} and ΔV at Round Mountain 500 kV for the summer sensitivity case. Since the statistical analysis is based on an entire year of wind data, rather than a seasonal subset, ΔP_{gen} is the same for spring and summer. $\Delta V/\Delta P_{gen}$ for the summer sensitivity cases is slightly lower than for the spring study case. Therefore, the expected ΔV is slightly lower for the sensitivity case.

The ΔV with a line out-of-service would be higher, but the frequency of occurrence would be lower due to the low likelihood of both a line outage and a large change in wind generation.

Table 3-7. Expected Frequency and Magnitude of ΔV at Round Mtn 500 kV for 5,000 MW Wind Profile for Spring Cases.

% Expectation	Frequency	ΔP_{gen}	ΔV No Action	ΔV SVC Action	ΔV LTC Action	ΔV SVD & LTC Action
-	Once per year	-1,672 MW	0.040 pu	0.038 pu	0.065 pu	0.038 pu
99.9%	Once every 2 weeks	-780 MW	0.019 pu	0.018 pu	0.030 pu	0.018 pu
99%	Once every 1.5 days	-301 MW	0.007 pu	0.007 pu	0.012 pu	0.007 pu
95%	Four times per day	-148 MW	0.004 pu	0.003 pu	0.006 pu	0.004 pu
90%	Eight times per day	-108 MW	0.003 pu	0.002 pu	0.004 pu	0.003 pu

Table 3-8. Expected Frequency and Magnitude of ΔV at Round Mtn 500 kV for 5,000 MW Wind Profile for Summer Sensitivity Case.

% Expectation	Frequency	ΔP_{gen}	ΔV SVC Action
-	Once per year	-1,672 MW	0.037 pu
99.9%	Once every 2 weeks	-780 MW	0.017pu
99%	Once every 1.5 days	-301 MW	0.007 pu
95%	Four times per day	-148 MW	0.003 pu
90%	Eight times per day	-108 MW	0.002 pu

3.2 Oscillatory Performance

The objective of this task was to evaluate the impact of variable wind generation on the small signal oscillatory performance of the COI interface. Specifically, the goals were to characterize the frequency components of interface power swings in response to critical faults, to test whether renewable generation oscillating at those frequencies could adversely affect system damping, and therefore, to identify the need, if any, for a limit on the amount of dynamic scheduling across the interface.

3.2.1 Swing Mode Identification

The dominant swing modes across the COI interface were identified using PSLF dynamic simulations and a Fast Fourier Transform (FFT) analysis.

The critical fault events, described in Section 2.3.2, were used to stimulate power oscillations across the COI interface. As an example, COI power flow response to the loss of two Palo Verde units is shown in Figure 3-15. At 1 second, two Palo Verde units were tripped. The event stimulates power swings on the COI interface. Shortly after the units trip, the magnitude of the swing is about 430 MW (5,770 MW at 3.1 seconds minus 5,342 MW at 5.2 seconds). The swing is reduced to near 0 MW by about 15 seconds. These simulation results will act as a benchmark for determining the effect of dynamic transfers on small-signal stability.

Figure 3-16 shows the COI power flow response to four critical fault events. The blue line represents the response to the loss of two Palo Verde units, the red line represents the response to the loss of Pacific DC Intertie, the green line shows the response to the loss of two San Onofre units and the black line shows the response to the loss of two Diablo Canyon units. The loss of two Palo Verde units is the worst-case outage in terms of the magnitude and damping of the power swing.

An FFT (Fast Fourier Transform) analysis was then used to identify the frequency components of the power oscillations across the interface. The FFT is an efficient version of the DFT (Discrete Fourier Transform), which takes a discrete signal in the time domain and transforms that signal into its discrete frequency domain. Results of the FFTs for each of the four critical disturbances are shown in Figure 3-17 to Figure 3-20. The dominant swing modes are summarized in Table 3-9. These frequencies are consistent with those observed in the WECC grid.

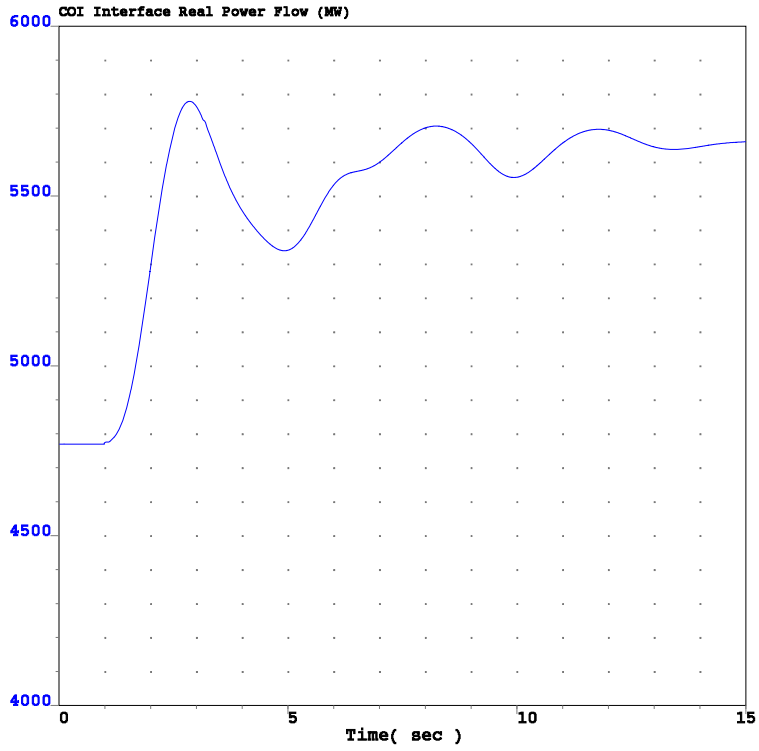


Figure 3-15. COI Interface Flow in Response to Loss of Two Palo Verde Generators.

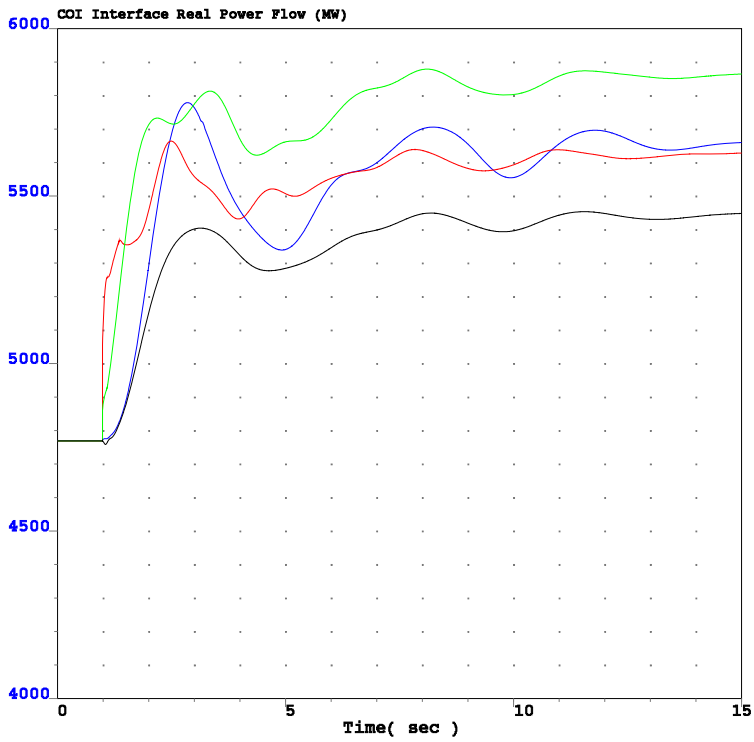


Figure 3-16. COI Interface Flow in Response to Critical Fault Events: 2 Palo Verde Units (blue), Pacific DC Intertie (red), 2 San Onofre Units (green), 2 Diablo Units (black).

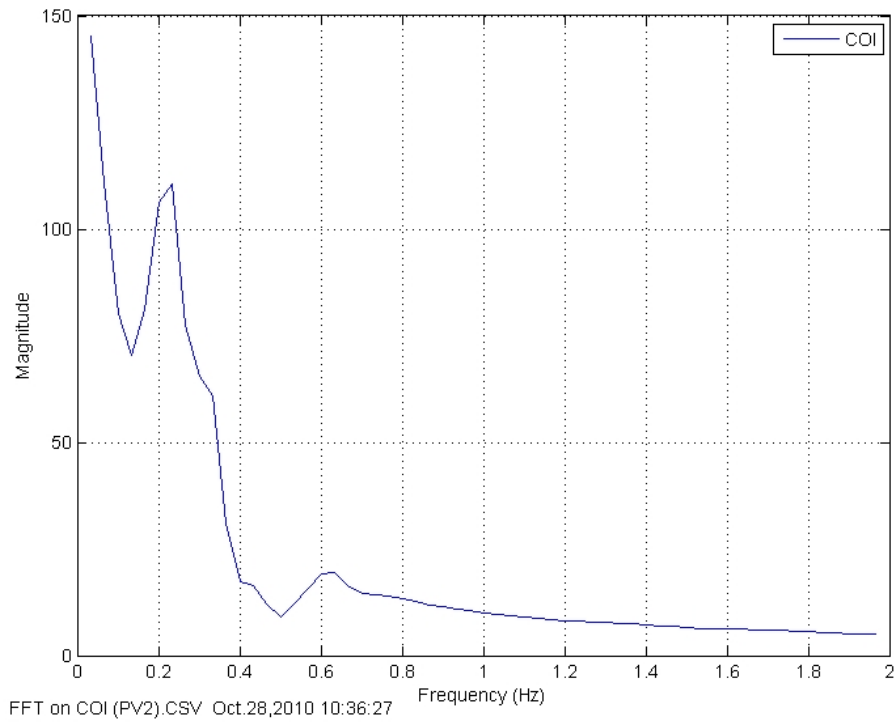


Figure 3-17. COI Interface FFT Results for Loss of Two Palo Verde Generators.

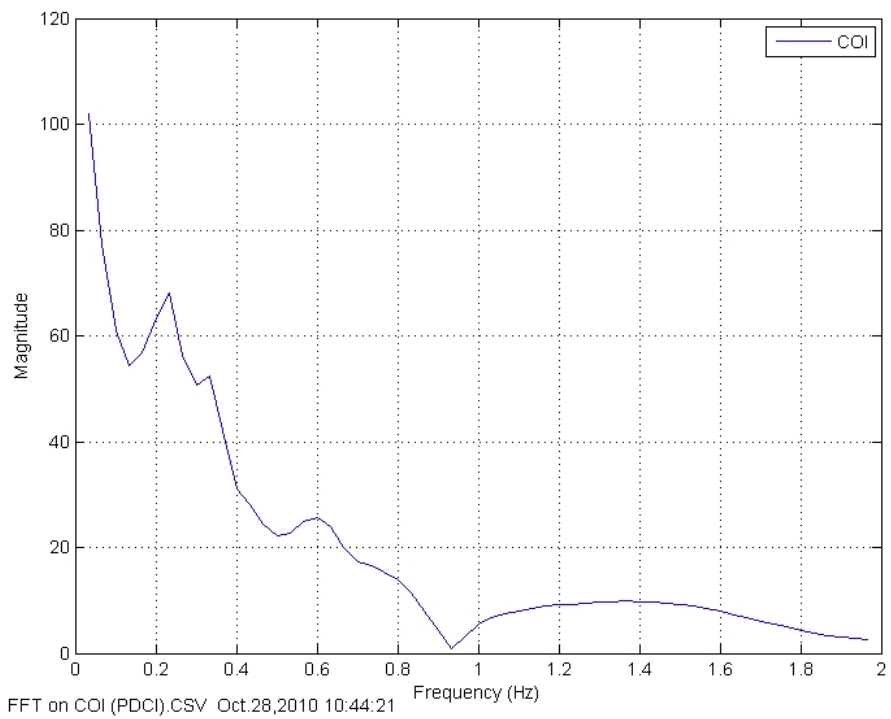


Figure 3-18. COI Interface FFT Results for Loss of Pacific DC Intertie.

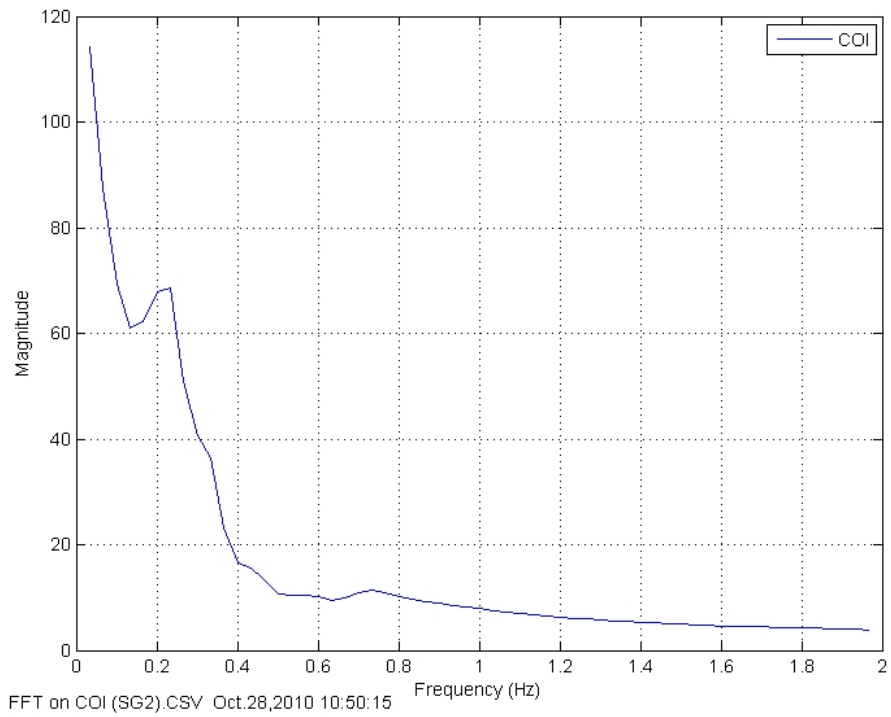


Figure 3-19. COI Interface FFT Results for Loss of Two San Onofre Generators.

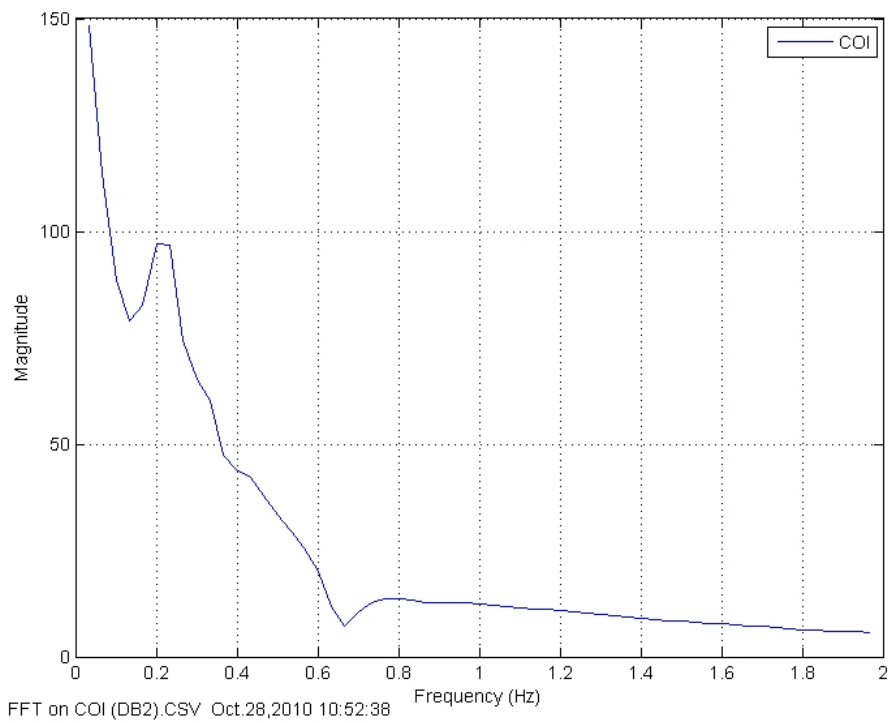


Figure 3-20. COI Interface FFT Results for Loss of Two Diablo Canyon Generators.

Table 3-9. Dominant Swing Modes Across COI Interface.

Loss of 2 Palo Verde Units	Loss of Pacific DC Intertie	Loss of 2 San Onofre Units	Loss of 2 Diablo Canyon Units
0.20-0.23 Hz 0.63 Hz	0.23 Hz 0.33 Hz 0.60 Hz	0.20-0.23 Hz 0.73 Hz	0.20-0.23 Hz 0.80 Hz

3.2.2 Impact of Wind Variability on Small-Signal Stability

To test whether renewable generation could adversely affect power swing damping under challenging conditions, tests were devised in which all wind generation in the Northwest oscillated together at the Malin 500 kV bus near the COI interface. This test, which has negligible risk of occurrence, provides maximum impact on grid oscillations. The assumption underlying this test is that common-mode oscillation of the wind generation will be worse than any variation that might occur in operation, and therefore provides a conservative upper bound. The variable renewable generation driving function was a sine wave at a selected frequency with a selected magnitude in increments of 500 MW.

The worst-case fault events were then simulated while the driving function was applied. As described in Section 3.2.1, the worst of all four events was the loss of two Palo Verde units, so the following figures and discussion will focus on that disturbance.

Figure 3-21 shows the COI interface flow, Maxwell 500 kV bus voltage and Maxwell 500 kV bus frequency in response to the loss of two Palo Verde units. The blue line represents the benchmark system response, and the red line represents the system response with a 1,500 MW, 0.2 Hz stimulus. A 0.2 Hz oscillation was selected, instead of the 0.23 Hz shown in the FFT, to match the peak of the stimulus with the post-fault peak swing across the COI interface.

As expected, the magnitudes of the swings observed on the COI interface are less than the magnitude of the stimulus. Also, the power swings sparked by the disturbance decay such that only the stimulus signal remains by the end of the simulation. The system meets the WECC voltage and frequency criteria, described in Section 2.3.1, and no protective relays operated with a 1,500 MW magnitude. With a 2,000 MW stimulus, the Colstrip plant acceleration trend relay operated at about 20 seconds.

A sensitivity analysis was performed with a 2,000 MW oscillation to investigate the impact of various stimulus frequencies. Figure 3-22 shows the system response to the loss of two Palo Verde units with a 2,000 MW magnitude at 0.2 Hz, 0.4 Hz, 0.63 Hz and 1.0 Hz. The blue line represents the system response at 0.2 Hz, the red line represents the response at 0.4 Hz, the green line represents 0.63 Hz, and the black line represents 1.0 Hz.

In general, the magnitudes of the power, voltage and frequency swings are less at the lower frequencies (e.g., 0.2 Hz, 0.4 Hz) due to the system's ability to respond in that slower time frame. Conversely, the swings are greater at the higher frequencies (e.g., 1.0 Hz) where the system response is too slow to compensate for the stimulus. At 0.63 Hz, the stimulus

frequency aligns with a system natural frequency, and the magnitude of the system response is amplified. As noted above, the system does not meet criteria for 2,000 MW at 0.2 Hz. The system also fails to meet criteria for 2,000 MW at 0.63 Hz – again due to the operation of the Colstrip plant acceleration trend relay at about 2 seconds. The system meets criteria for 2,000 MW at both 0.4 Hz and 1.0 Hz, which are not frequency components of the COI power swings.

The voltage changes of this dynamic analysis were compared to those observed in the steady-state analysis. Values of $\Delta V/\Delta P_{gen}$ are shown in Table 3-10 for the Maxwell 500 kV bus in response to the Palo Verde outage and a +/-2,000 MW stimulus. The values are shown for 0.2 Hz, 0.4 Hz, 0.63 Hz and 1.0 Hz oscillation frequencies. As previously noted, when the stimulus frequency aligns with a system natural frequency, the magnitude of the system response is amplified. This is clear in the $\Delta V/\Delta P_{gen}$ values, which are highest for the 0.63 Hz stimulus. Values of $\Delta V/\Delta P_{gen}$ for oscillations at other frequencies range from 0.002 to 0.003, similar to those calculated in the steady-state analysis.

Table 3-10. $\Delta V/\Delta P_{gen}$ at Maxwell 500 kV for Palo Verde Outage, +/-2,000 MW Stimulus. Values are Per Unit per 100 MW of Stimulus.

Oscillation Frequency	$\Delta V/\Delta P_{gen}$ (pu/100MW)
0.20 Hz	0.003
0.40 Hz	0.0025
0.63 Hz	0.0075
1.00 Hz	0.002

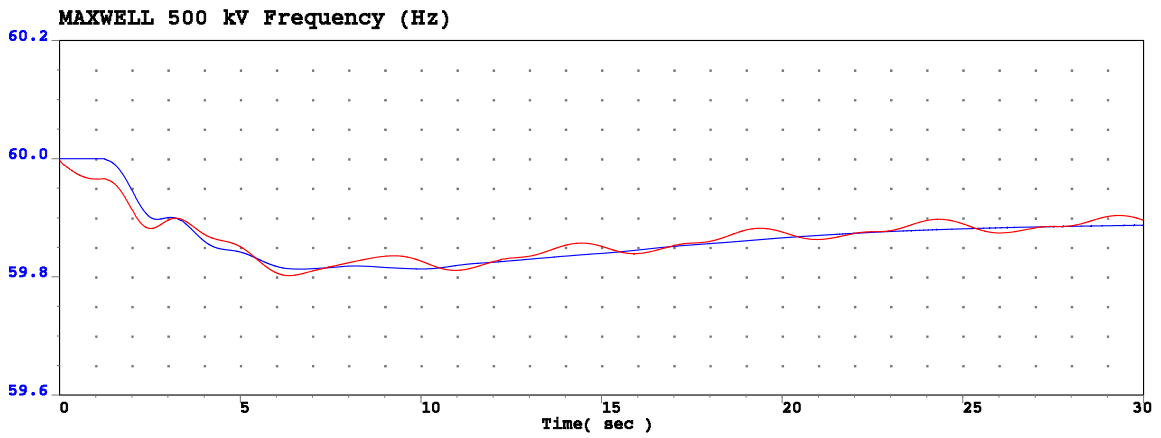
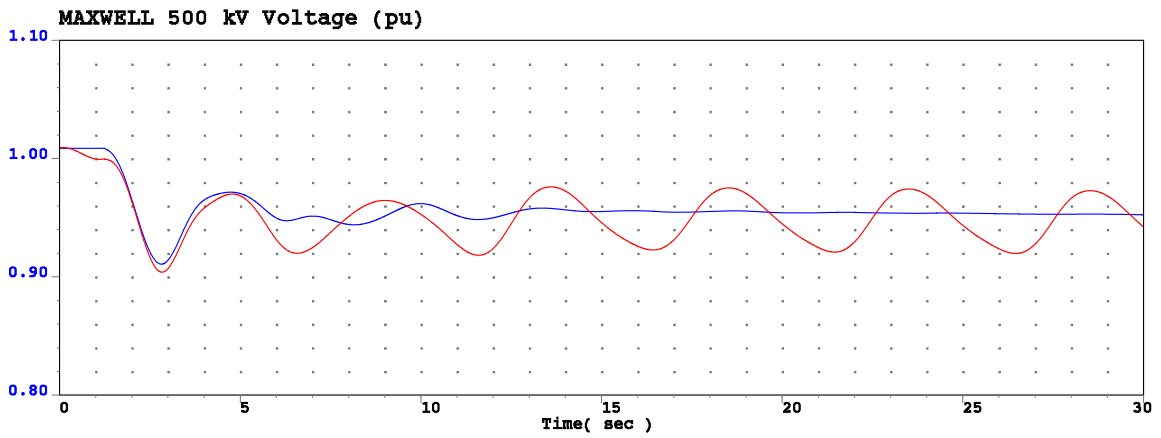
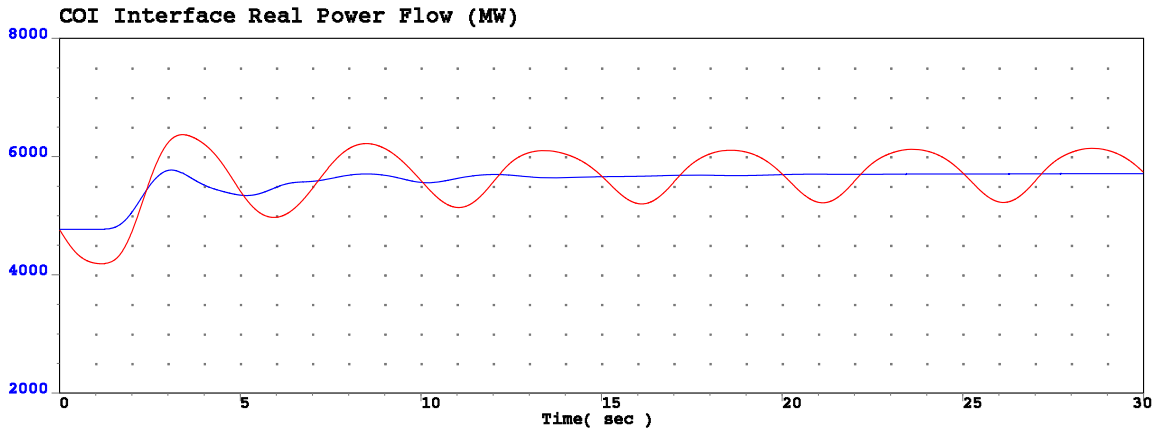


Figure 3-21. System Response to Palo Verde Generation Trip with and without 1,500 MW, 0.2 Hz Stimulus.

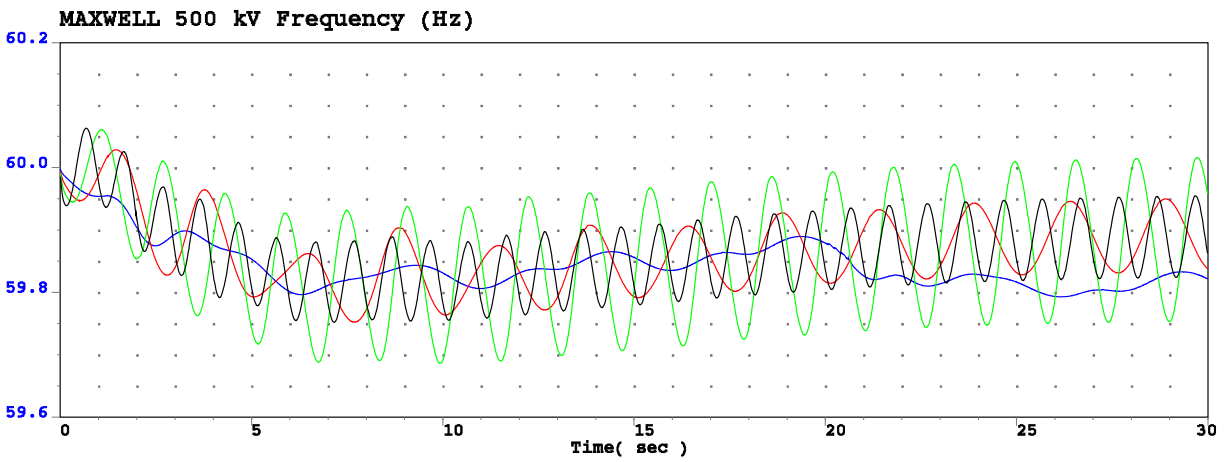
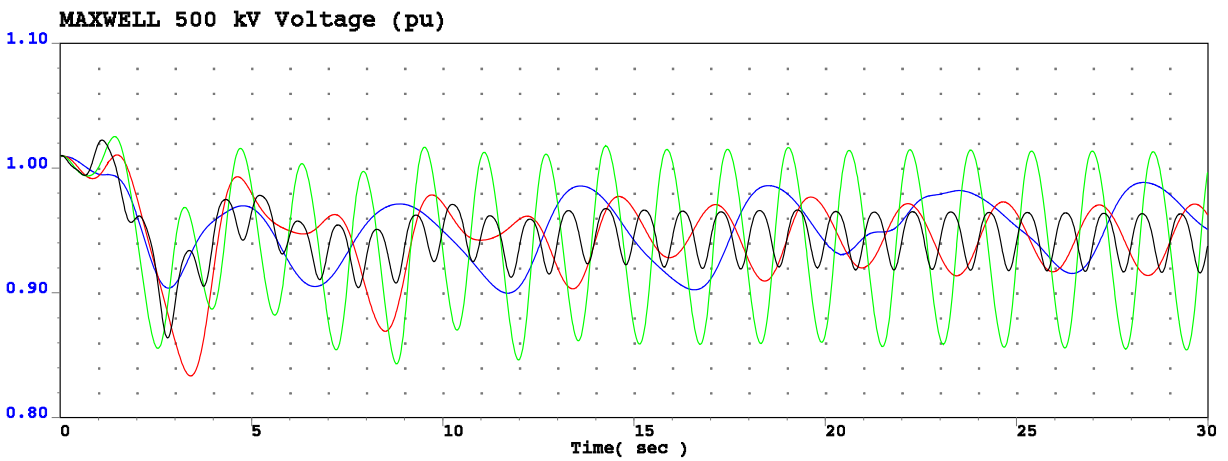
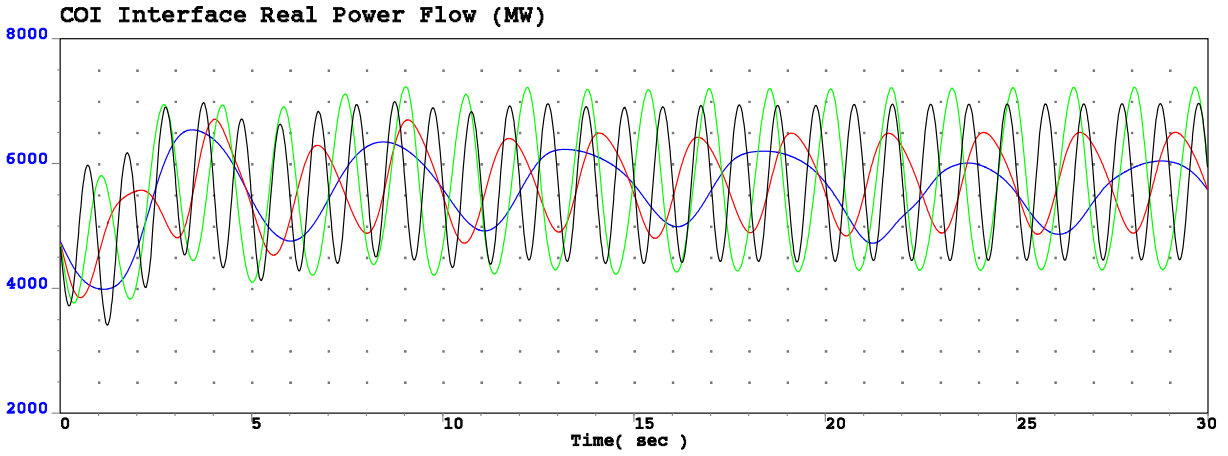


Figure 3-22. System Response to Palo Verde Generation Trip, with 2,000 MW Stimulus at 0.2 Hz (blue), 0.4 Hz (red), 0.63 Hz (green) and 1 Hz (black).

4 WOR Interface

The objective of this analysis was to identify any dynamic schedule limitations on the WOR interface due to steady-state voltage and/or oscillatory performance.

4.1 Voltage Performance

The objective of the steady-state analysis was to evaluate the impact of dynamic scheduling on the voltage performance of the COI interface. Specifically, the goal was to determine the impact of variations in imports (ΔP) on delta voltage (ΔV) and the resulting impact on equipment – i.e., shunt capacitor or reactor switching events and LTC transformer tap motions.

4.1.1 Steady-state $\Delta V/\Delta P$ Characteristic

The steady-state $\Delta V/\Delta P$ characteristics of the WOR interface were calculated for two spring system conditions; all lines in and with the North Gila-Imperial Valley 500 kV line out of service. The North Gila-Imperial Valley 500 kV line was the most heavily loaded line on the WOR interface. Calculations were made at 805 MW, 1,605 MW, 2,410 MW and 3,250 MW of delta generation in Arizona, implemented at Navajo and Springerville. The initial condition for all scenarios was a high WOR flow case. When imports are reduced, system voltages will increase. Thus, nearly all ΔV values are positive.

Figure 4-1 is a sorted scatter plot of ΔV on monitored buses for the four different levels of generation change (ΔP_{gen}). All CAISO buses at 230 kV and above were monitored. In addition, 115 kV and 161 kV buses near the interface were monitored. Note that there were no LTC tap actions for any of the simulations. Therefore, only four control options are shown. These are No movement, continuous SVD (SVCs), all SVDs (SVCs plus switched capacitors), and all SVDs and phase angle regulating transformers (PAR). The plot shows groupings of ΔV for each delta generation condition. The ΔV are sorted from highest to lowest independently for each control option.

The x-axis is a count of data points, corresponding to the number of voltages recorded for each scenario. Note that there are fewer recorded voltages for the lower ΔP_{gen} cases than the higher. This is due to the monitoring logic used to reported bus voltages. The higher levels of ΔP_{gen} result in larger ΔV s, which means that more buses will meet the reporting criteria.

The values of ΔV are significantly lower than those observed for the COI interface. Nearly all buses see a voltage change of less than 0.02 pu, even with the highest ΔP_{gen} . Furthermore, the values do not change significantly with different control options. This is likely due to the abundant generation in the Eldorado Valley. Note that the large SVCs at Devers, Adelanto and Marketplace were modeled with zero reactive capability for the steady-state analysis. Therefore, they do not participate in voltage regulation. With these SVCs regulating voltage, the actual ΔV will be less than this analysis shows.

Figure 4-2 shows a similar scatter plot of ΔV with the North Gila-Imperial Valley 500 kV line out of service. For these scenarios, the line was taken out of service and the powerflow case was solved with all control actions (LTC, SVCs, switched shunts and PARs) active. The dispatch was not modified to reduce CAISO imports or WOR path flows. The four delta generation scenarios were then implemented with the six different control options. Again, no LTC switching action occurred so plots with LTC enabled are not included.

With the 500 kV line out of service, ΔV s are higher. Even with a line out, most of the buses see a voltage change of less than 0.02 pu. The largest change in voltage, 0.0385 pu, is seen at the Pisgah 500 kV bus for a 3,250 MW change in generation (with SVCs active). With all lines in, the same bus has a ΔV of 0.0218 pu.

Figure 4-3 shows another sorted scatter plot for the base system, but of $\Delta V/\Delta P_{gen}$. These values are ΔV per 100 MW of AZ generation. Figure 4-4 shows $\Delta V/\Delta P_{gen}$ with the North Gila Imperial Valley line out. $\Delta V/\Delta P_{gen}$ is generally below 0.001 pu/100 MW throughout the system.

The Pisgah 500 kV bus consistently has the highest ΔV . This is expected, since Pisgah is located in the middle of the WOR lines. Figure 4-5 is a plot of the Pisgah 500 kV bus voltage plotted against ΔP generation with the North Gila-Imperial Valley 500 kV line out of service. The ΔV for the four control options is shown. At a 3,250 MW reduction in Arizona generation, ΔV is 0.0218 pu for all of the control options.

Figure 4-6 shows the same ΔV as Figure 4-5, but they are plotted against the change in flow on WOR (ΔP_{wor}). Every 1 MW of generation shifted from Navajo and Springerville to CAISO reduces the flow on WOR by about 0.7 MW. Thus, the four test generation levels (805 MW, 1,605 MW, 2,410 MW and 3,250 MW) result in about 570 MW, 1,100 MW, 1,580 MW and 2,110 MW reductions in WOR flow. Figure 4-7 and Figure 4-8 show similar plots of Pisgah 500 kV ΔV with the North Gila-Imperial Valley 500 kV line out.

Given the change in Arizona generation, change in WOR flow and change in voltage, the range of $\Delta V/\Delta P$ at Pisgah 500 kV bus is shown in Table 4-1. The values are for the base system (n-0) and with the North Gila-Imperial Valley line out, with only SVCs regulating.

Table 4-1. $\Delta V/\Delta P$ at Pisgah 500 kV for Base System (n-0) and North Gila-Imperial Valley Outage. Values Are Per Unit per 100 MW of ΔP on WOR and ΔP Arizona Generation.

Base System (n-0)		N. Gila-Imperial Valley Out	
$\Delta V/\Delta P_{WOR}$	$\Delta V/\Delta P_{GEN}$	$\Delta V/\Delta P_{WOR}$	$\Delta V/\Delta P_{GEN}$
0.0010 to 0.0014	0.0007 to 0.0010	0.0015 to 0.0028	0.0010 to 0.0018

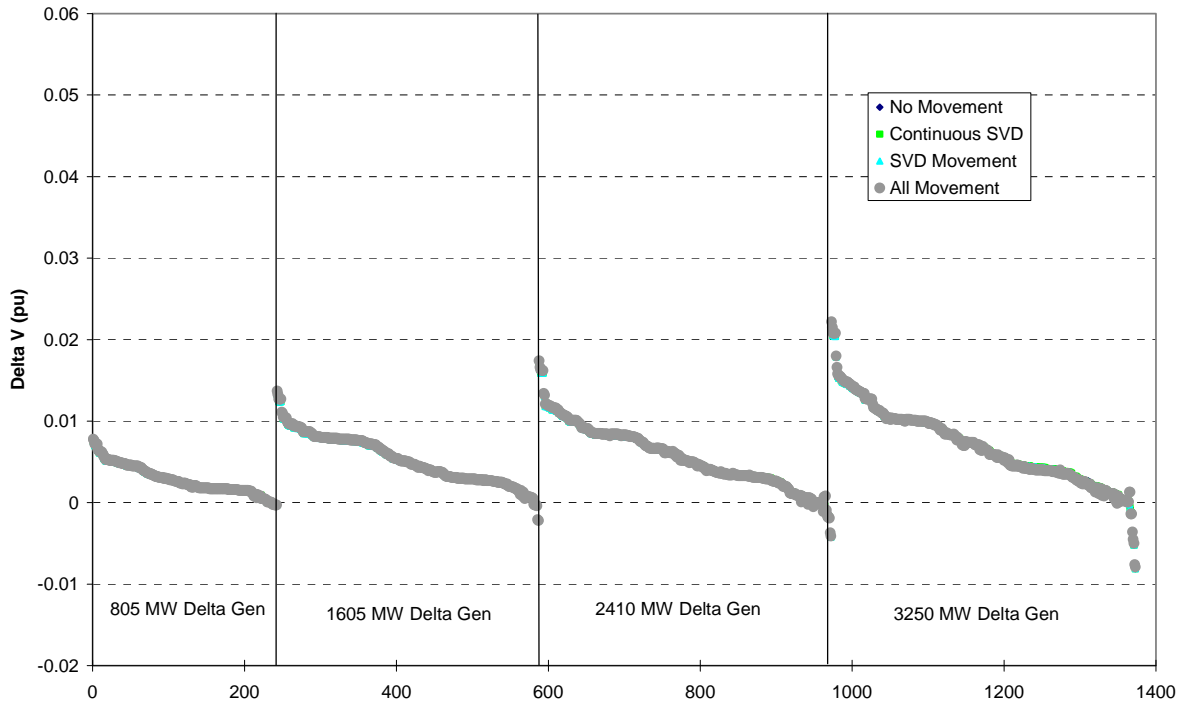


Figure 4-1. ΔV of CAISO Monitored Buses For ΔP In Arizona, All Lines in Service.

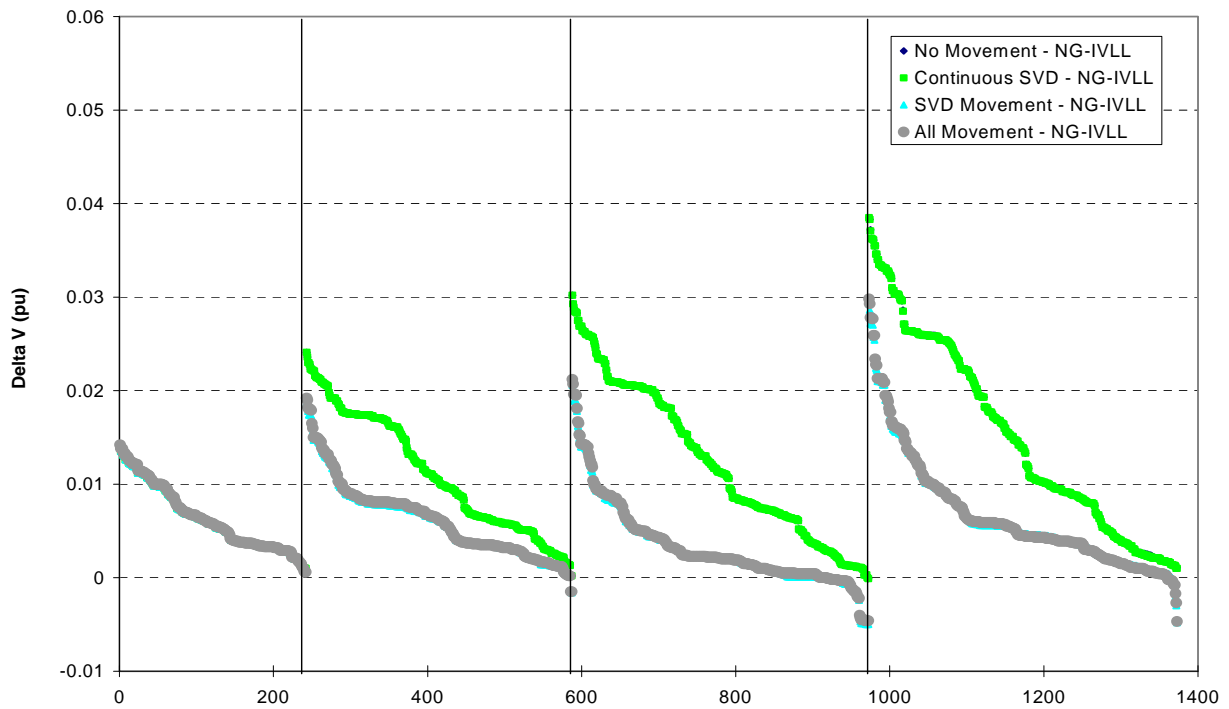


Figure 4-2. ΔV of CAISO Monitored Buses For ΔP In Arizona, N. Gila-Imperial Valley 500 kV Line Out.

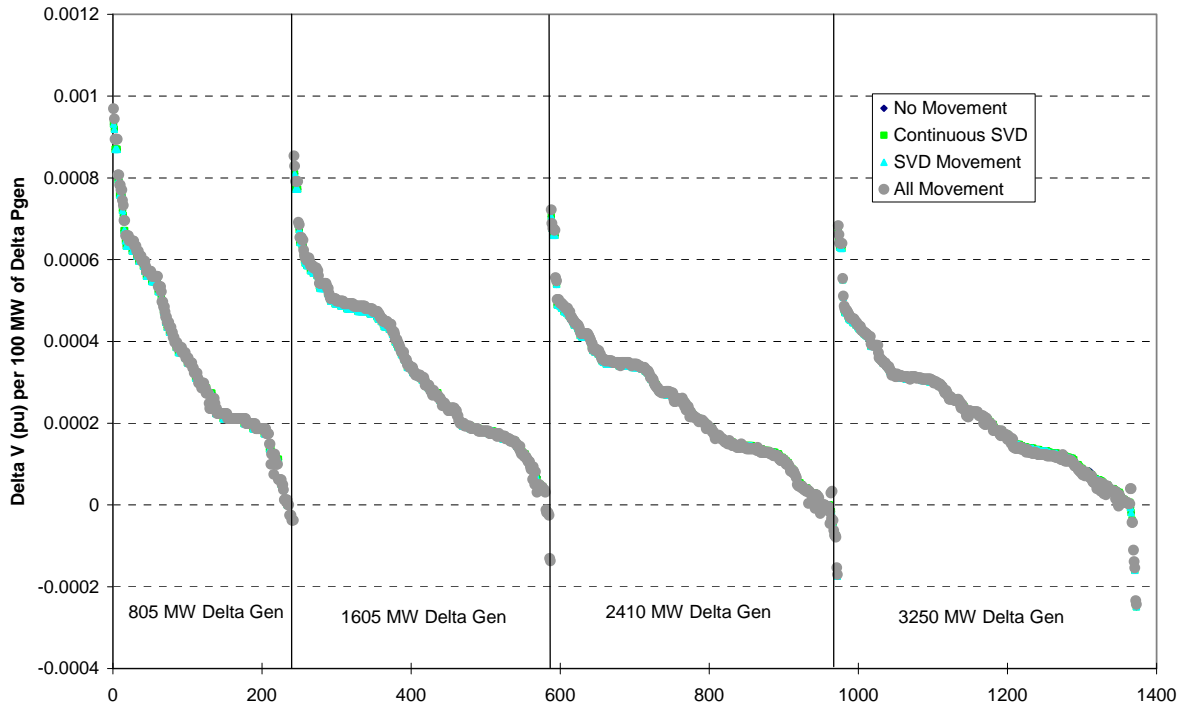


Figure 4-3. $\Delta V/\Delta P_{gen}$ of CAISO Monitored Buses Values per 100 MW of ΔP In Arizona, All Lines in Service.

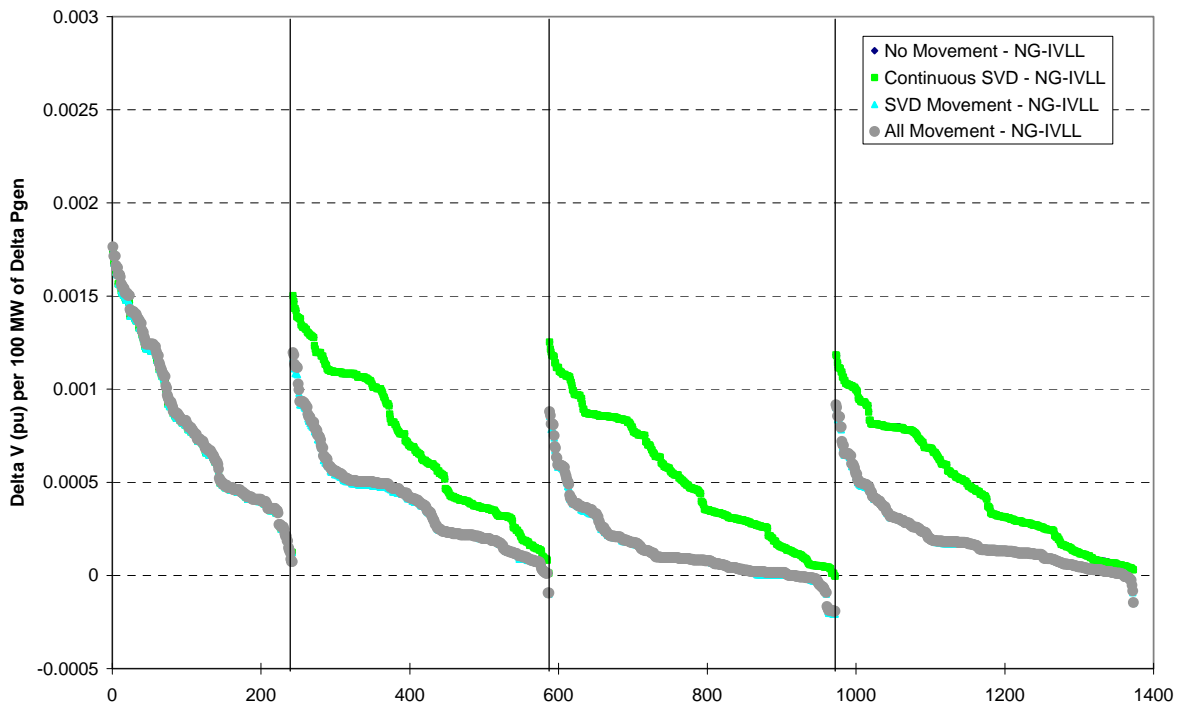


Figure 4-4. $\Delta V/\Delta P_{gen}$ of CAISO Monitored Buses per 100 MW of ΔP in Arizona, N. Gila-Imperial Valley 500 kV Line Out.

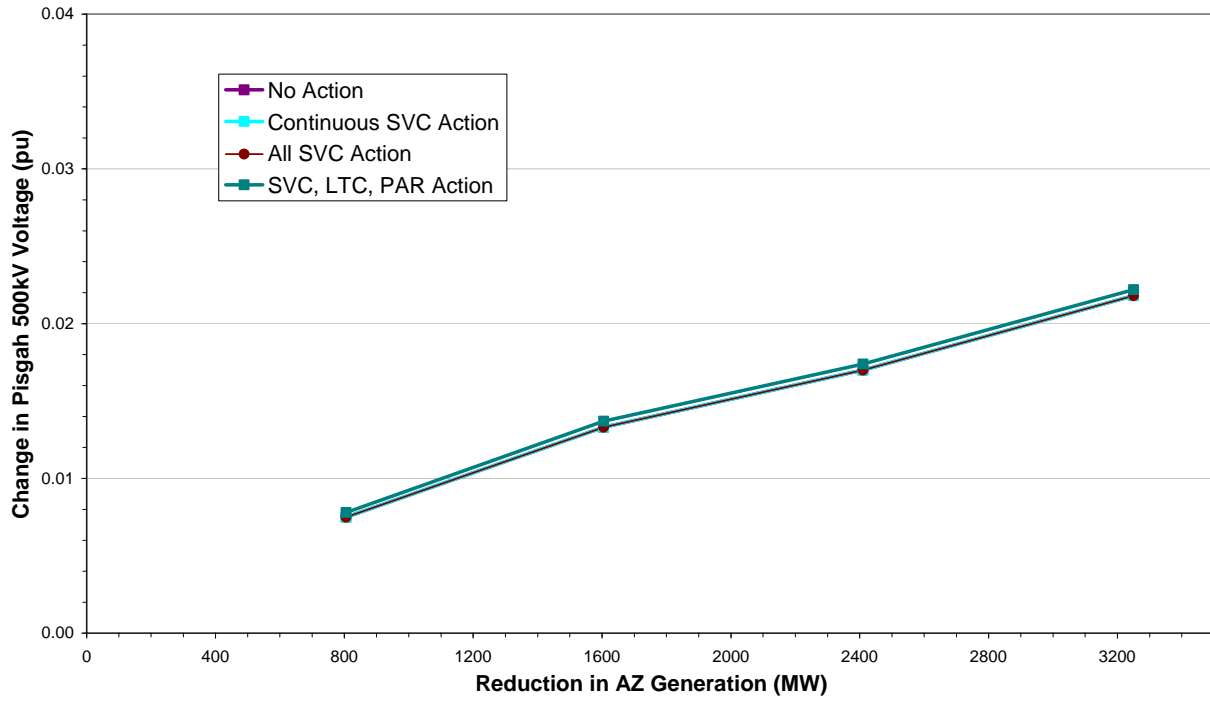


Figure 4-5. ΔV of Pisgah 500 kV Bus Voltage For ΔP in Arizona, All Lines In Service.

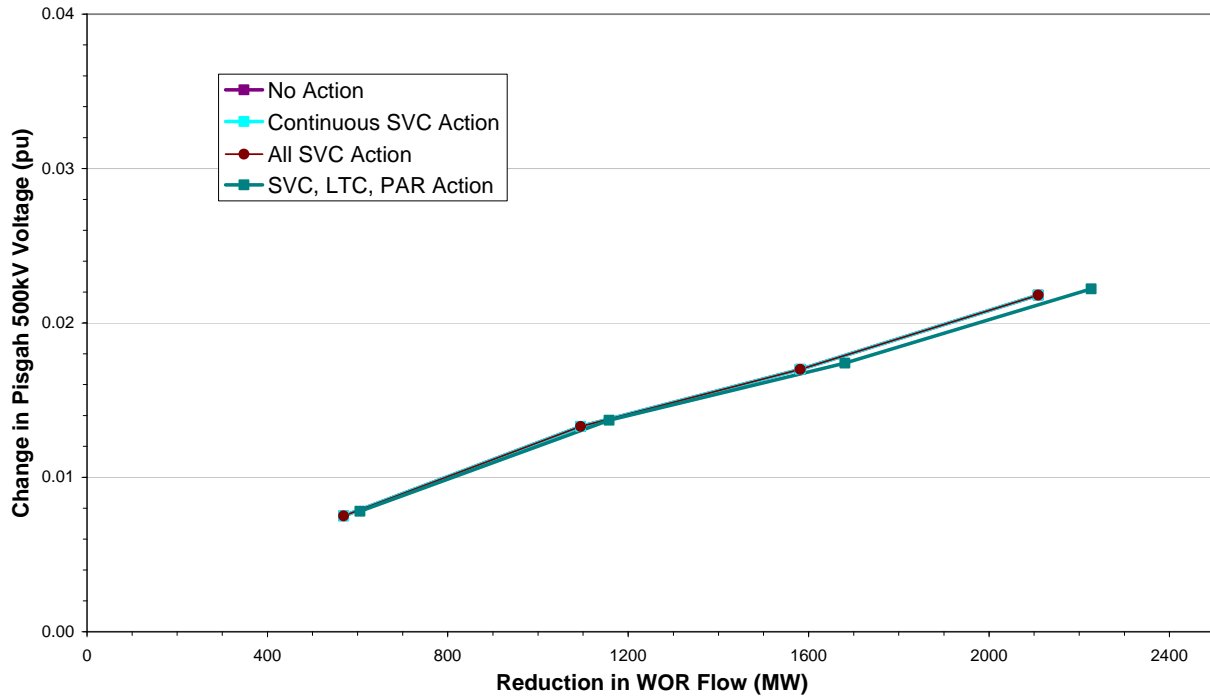


Figure 4-6. ΔV of Pisgah 500 kV Bus Voltage For ΔP in Arizona, All Lines In Service, Plotted Against WOR Flow.

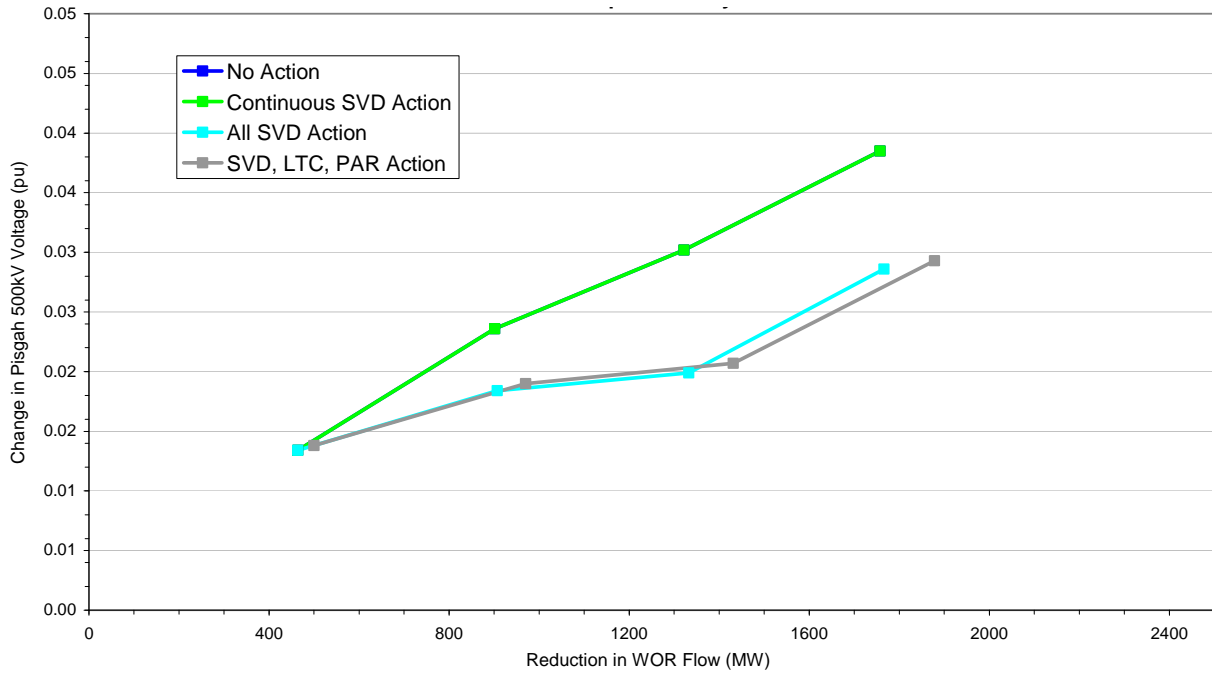


Figure 4-7. ΔV of Pisgah 500 kV Bus Voltage For ΔP in Arizona, North Gila-Imperial Valley 500 kV Line Out of Service.

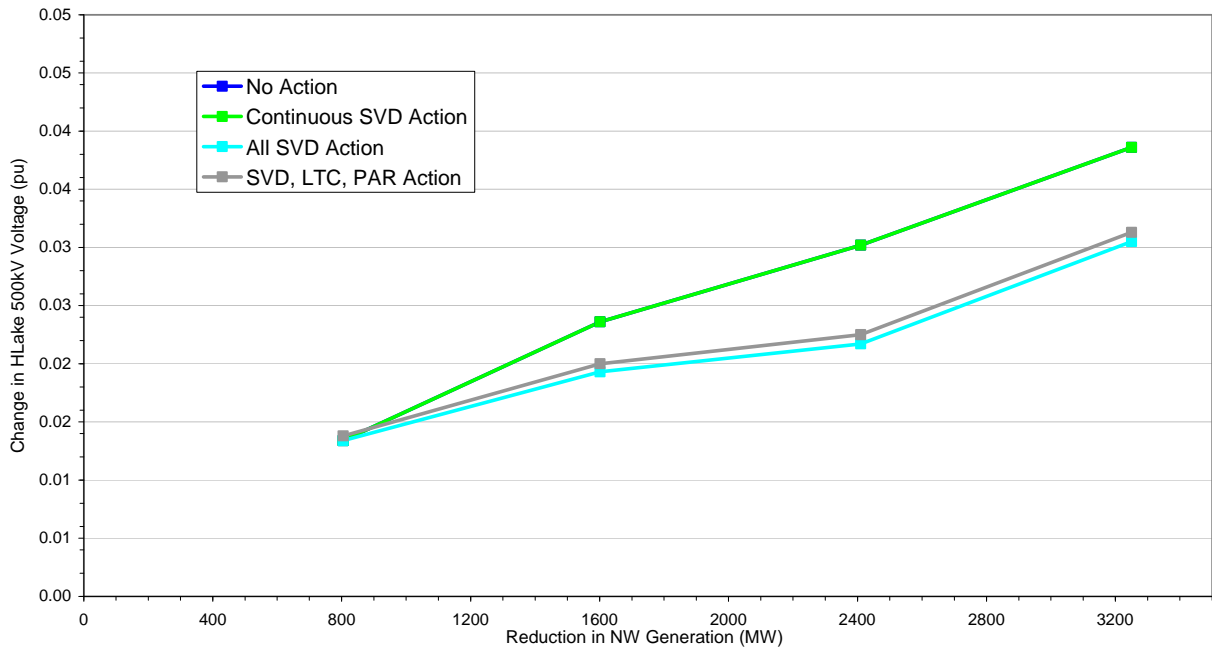


Figure 4-8. ΔV of Pisgah 500 kV Bus Voltage For ΔP in Arizona, North Gila-Imperial Valley 500 kV Line Out of Service, Plotted Against WOR Flow.

4.1.2 Shunt Capacitor and LTC Switching

One of the concerns with the voltage variations caused by dynamic scheduling is excessive LTC tap motion and shunt capacitor/reactor switching. For example, a sudden reduction in imports from Arizona will cause CA voltage to increase. If the change in voltage is great enough, it will cause capacitors to switch off. A subsequent increase in Arizona imports will reduce voltages in CA, and could cause the capacitors to switch back on.

Excessive capacitor switching will only be an issue when ΔV caused by the change in imports plus ΔV caused by capacitor switching exceeds the voltage control deadband. The values of ΔV for capacitor switching will vary depending on system conditions. However, it is reasonable to assume that the control deadband of any automatically switched capacitor will be set to at least two times the ΔV for capacitor switching. Under this assumption, the largest ΔV for capacitor switching would be 50% of the voltage control deadband. This leaves another 50% of the deadband for import variations.

Table 4-2 shows the 230 kV and above CAISO buses with switched shunt capacitors where the ΔV for the 3,250 MW reduction in Arizona generation exceeds 50% of the control deadband. This table shows the voltage control deadband modeled in the powerflow (e.g., $2 \times \text{SVD vband}$), ΔV in per unit, and ΔV in percent of the control deadband. The ΔV values are with SVCs active, since they will regulate before shunt capacitors and LTCs switch, and are shown for the 3,250 MW and 2,410 MW generation reduction cases.

By the logic described above, all 7 shunt capacitors could experience off/on switching for 3,250 MW decrease/increase cycles in imports. Only two of the shunt capacitors could experience off/on switching for 2,410 MW decrease/increase cycles in imports. The ΔV is generally about 0.01 to 0.015 pu higher for the line-out condition than for the normal condition on the buses near WOR for 3,250 MW ΔP . On buses further from the interface, the increase in ΔV with the outage is lower. Therefore, additional capacitors near the interface could experience off/on switching, and it could occur at lower levels of ΔP_{gen} for the line-out condition.

The control deadbands for several of the shunt capacitors are set below 0.02 pu in the powerflow supplied. This is a tight control range and may not represent actual equipment settings.

**Table 4-2. ΔV at Selected Buses with Switched Shunt Capacitors.
 ΔV Shown for 2,410 MW and 3,250MW Change in Arizona Generation.**

Bus #	Name	kV	Control Vband (pu)	2,410 MW ΔP_{gen}		3,250 MW ΔP_{gen}	
				ΔV (pu)	ΔV (% of Vband)	ΔV (pu)	ΔV (% of Vband)
24092	MIRALOMA	500	0.016	0.0110	69	0.0138	86
24151	VALLEYSC	500	0.024	0.0114	46	0.0143	60
24025	CHINO	230	0.018	0.009	50	0.0113	63
24100	OLINDA	230	0.018	0.0082	46	0.0103	57
24112	PADUA	230	0.022	0.0091	41	0.0111	50
24154	VILLA PK	230	0.022	0.0090	41	0.0115	52
24160	VALLEYSC	115	0.016	0.0114	69	0.0143	89

Similar analysis was performed for the LTC transformers in the CAISO area. The largest change in bus voltages at any 230 kV bus is 0.020 pu for 3,250 MW, 0.016 pu for 2,410 MW, 0.012 pu for 1,605 MW, and 0.007 pu for 806 MW. The tightest voltage control band width for all LTC transformers in CAISO is 0.008 pu, and most have a control band width of 0.015 pu or more. Given this, it is possible that repeated decrease/increase cycles in imports of 800 MW or more could cause LTC tap switching. However, most LTCs in CAISO are regulating lower voltage buses, where the change in voltage is significantly lower than on the 230 kV system. Therefore, the number of transformers susceptible to repeated LTC switching should be limited.

Simulations run with LTC transformer and switched shunt controls active show little shunt switching and no LTC switching within CAISO. This is as much a function of the initial condition in the powerflow case as the ΔV of the dynamic imports. However, it does indicate that even large changes in imports should not cause excessive equipment switching.

4.1.3 Sensitivity Analysis

Three types of sensitivities were explored – additional transmission line or generating unit outages, a second generation redispatch procedure, and a higher system load level (i.e., summer peak).

The analysis above concentrated on normal operation and operation with the North Gila-Imperial Valley 500 kV line out of service. Figure 4-9 shows a sorted scatter plot of ΔV vs. ΔP_{gen} with SVC action for the spring base system and three critical outages:

- Loss of North Gila-Imperial Valley 500 kV line
- Loss of Palo Verde-Colorado River 500 kV line
- Loss of two San Onofre (SONGS) units

Figure 4-10 shows the change in Pisgah 500 kV bus voltage for these conditions.

Palo Verde-Colorado River 500 kV is the first of three line sections from Palo Verde to Devers. The other two are Colorado River-Red Bluff, and Red Bluff-Devers. An initial screening showed that the Palo Verde-Colorado River section outage had the biggest impact, so it was chosen.

ΔV for the additional outages is lower than ΔV for the North Gila-Imperial Valley outage.

In the analysis presented to this point, redispatching of tripped Arizona generation was distributed across all CAISO units, proportional to their MVA and up to their maximum power limit. A sensitivity was performed where units identified as baseload in the powerflow (gens table BL flag set to 1) did not participate in the redispatch. A sorted scatter plot of the base and sensitivity redispatches is shown in Figure 4-11. Removing baseload units from the redispatch causes a slight increase in ΔV at the higher ΔP_{gen} levels. This shows that ΔV is somewhat sensitive to the CAISO units that are redispatched to meet dynamic scheduling.

The final sensitivity examined the voltage performance of a summer case. A sorted scatter plot of the spring and summer ΔV results, with the original redispatch approach, is shown in Figure 4-12. Figure 4-13 is a scatter plot of $\Delta V/\Delta P_{gen}$ for the spring and summer cases with all lines in service. The points represent ΔV per 100 MW of ΔP generation in Arizona. In both figures the summer results are generally lower than the spring results. This is likely due to the significantly higher number of generators in the summer case – more generation means more reactive capability, which results in better voltage control.

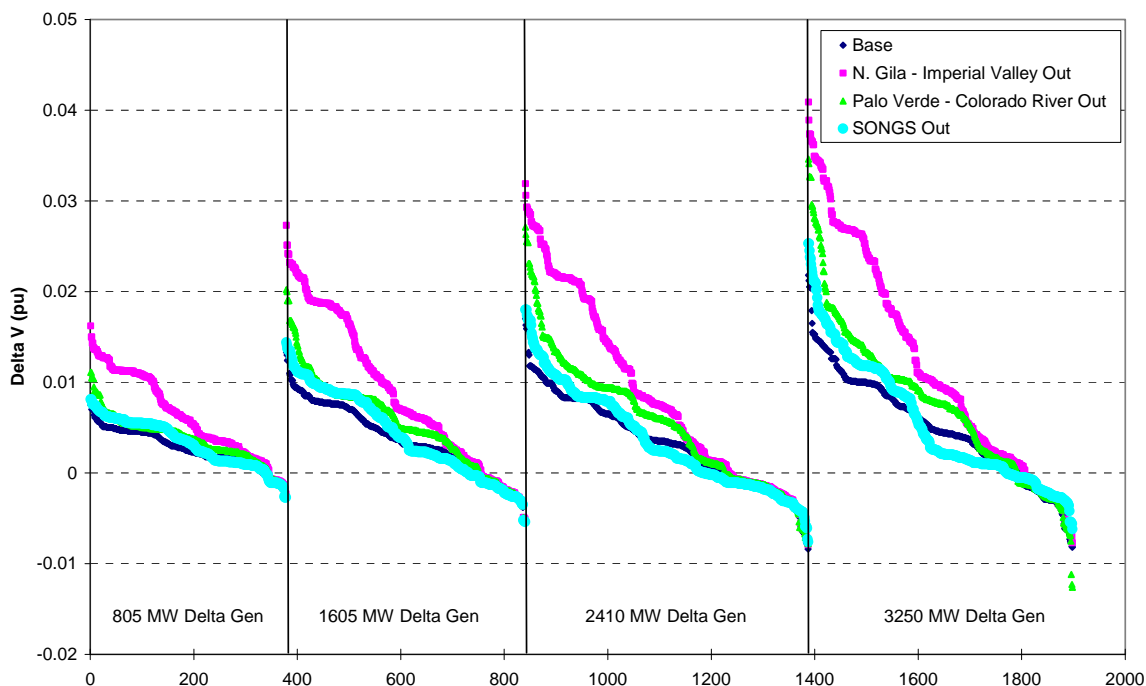


Figure 4-9. ΔV of CAISO Monitored Buses For ΔP In Arizona, with Different Outages.

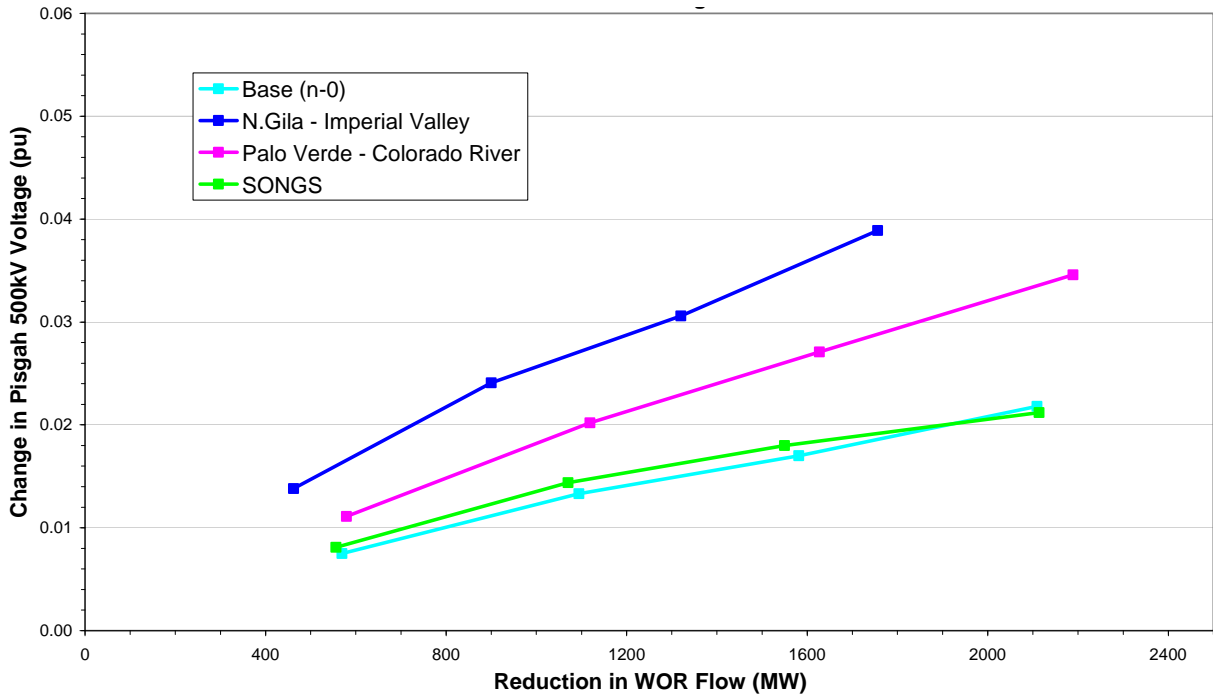


Figure 4-10. ΔV of Pisgah 500 kV Bus Voltage For ΔP in Arizona, All Lines In Service and Three Worst-Case CAISO Contingencies, Plotted Against WOR Flow.

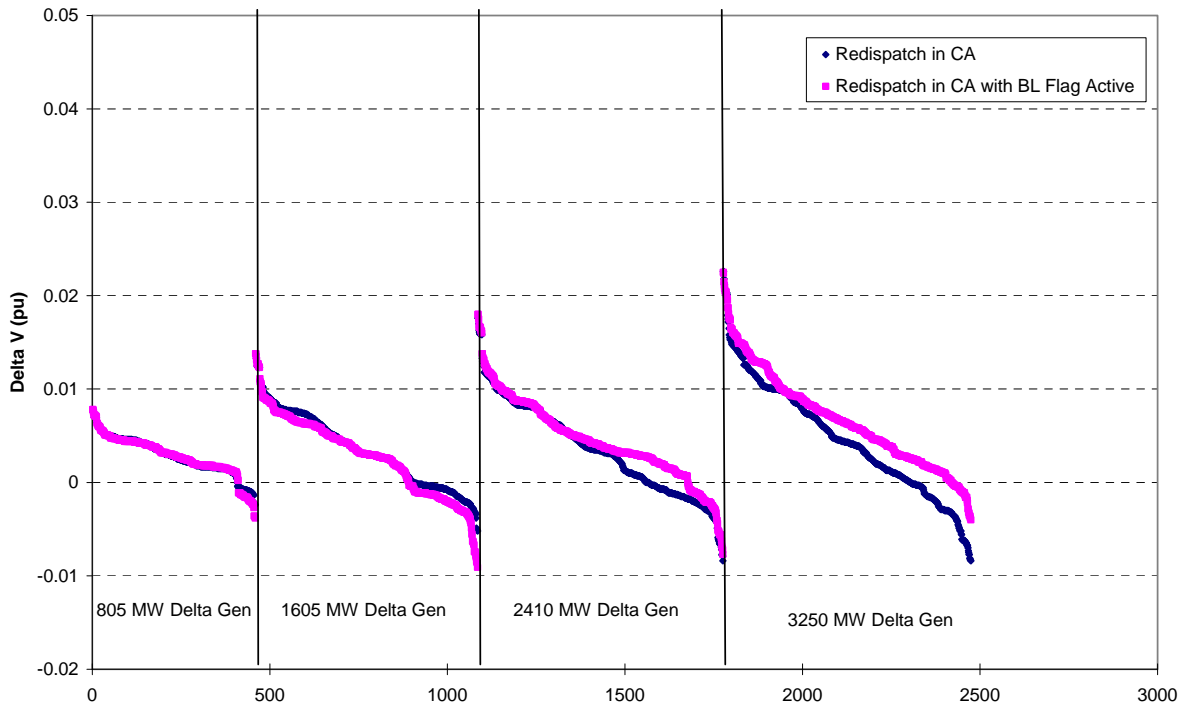


Figure 4-11. ΔV of CAISO Monitored Buses For ΔP in Arizona, Redispatch All CAISO Units (blue) vs. Redispatch of Non-Baseload Units (pink).

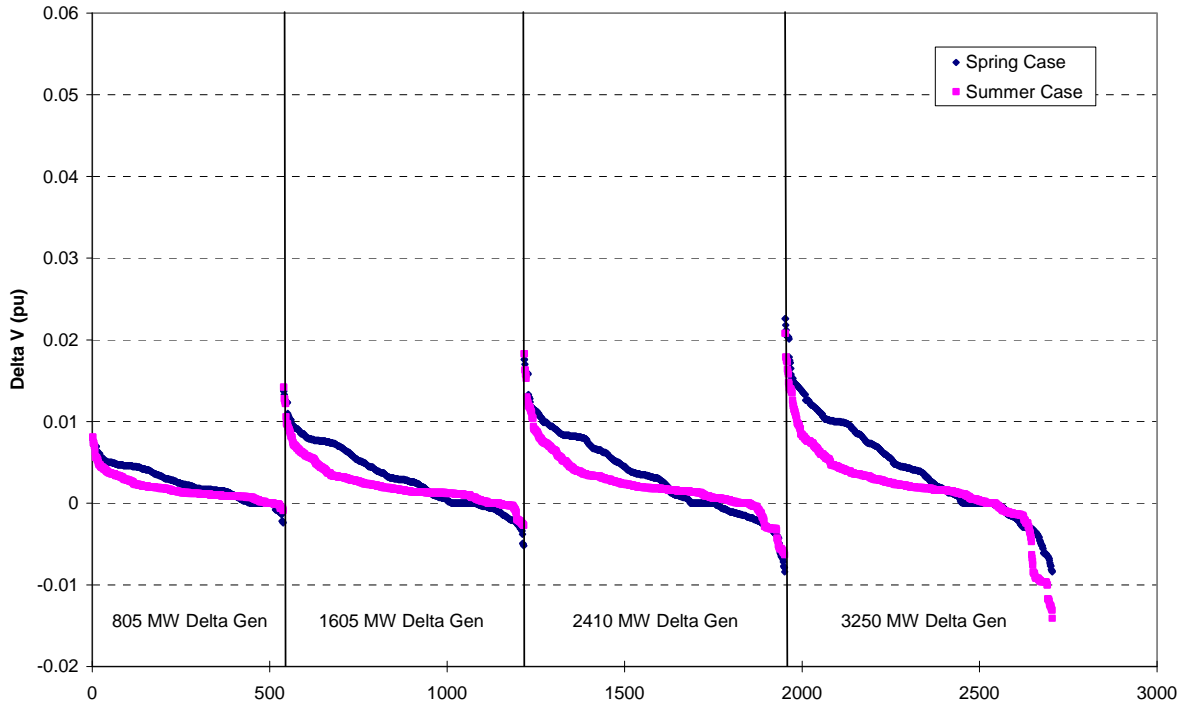


Figure 4-12. ΔV of CAISO Monitored Buses For ΔP in Arizona, Spring (blue) vs. Summer (pink).

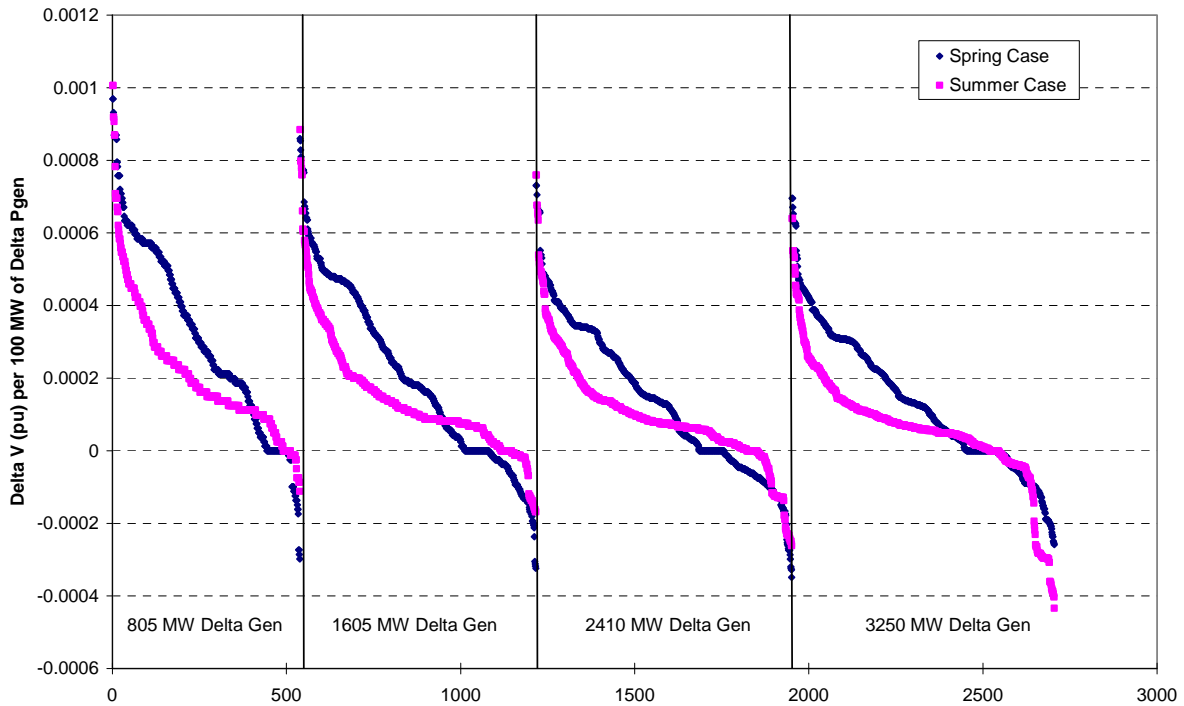


Figure 4-13. $\Delta V/\Delta P_{gen}$ of CAISO Monitored Buses per 100 MW of ΔP in Arizona, Spring (blue) vs. Summer (pink).

4.1.4 Statistical Analysis of Solar Profiles

The aggregate solar profiles, as described in Section 2.4, were analyzed to statistically characterize their expected variability. Specifically, this statistical analysis evaluated the change in solar PV generation from one 10-minute point to the next. This 10-minute difference in solar PV generation is called the 10-minute solar PV delta throughout this report.

A scatter plot of the 10-minute solar PV deltas for the 15,000 MW DC/11,550 MW AC aggregate profile is shown in Figure 4-14. The maximum positive 10-minute change in power for this aggregate profile is about 500 MW, the maximum negative 10-minute delta is about -500 MW. Although this profile has a higher rating than the 5,000 MW aggregate wind profile discussed in Section 3.1.4, the variability is less. As discussed in Section 2.4.2, the PV profile 10-minute variability was based on measured PV output from many small PV plants and superimposed on hourly PV data modeled as distributed generation on rooftops. Whether these profiles appropriately represent both the variability and geographic diversity of a large PV plant is unknown, given the lack of measured data from such a plant.

An example of the variability and geographic diversity in the individual 100 MW DC/77 MW AC PV profiles is shown in Figure 4-15. Sixteen individual PV plant profiles for a single day are shown, as well as the average of the sixteen. The largest 10-minute delta (positive or negative) in any one profile on this day was 47 MW or 61%. This is the largest 10-minute delta for the entire year in this set of sixteen profiles. In contrast, the largest 10-minute delta in the daily average profile was 5 MW or 7% - illustrating the smoothing effect of geographic diversity.

A summary of the solar PV delta statistics for the aggregate profiles is shown in Table 4-3. They are split between positive deltas and negative deltas. Since the power flow analysis was performed with the WOR interface near maximum, the focus will be on the negative deltas. As an example, the 15,000 MW DC/11,550 MW AC profile shows a maximum negative delta (i.e., a drop in solar PV generation) of -523 MW. The average negative delta is -178 MW, and the median is -189 MW. The duration curve of negative deltas for this aggregate profile is shown in Figure 4-16. This curve does not drop as quickly as the wind delta duration curve shown in Figure 3-14.

The negative solar PV delta expectation percentages, and their frequencies, are shown in Table 4-4. As an example, solar PV farms with a total rating of 15,000 MW DC/11,550 MW AC would be expected to produce one 10-minute drop in power of more than 475 MW every three weeks, and one drop of more than 334 MW four times a day. Positive solar PV delta expectation percentages are shown in Table 4-5.

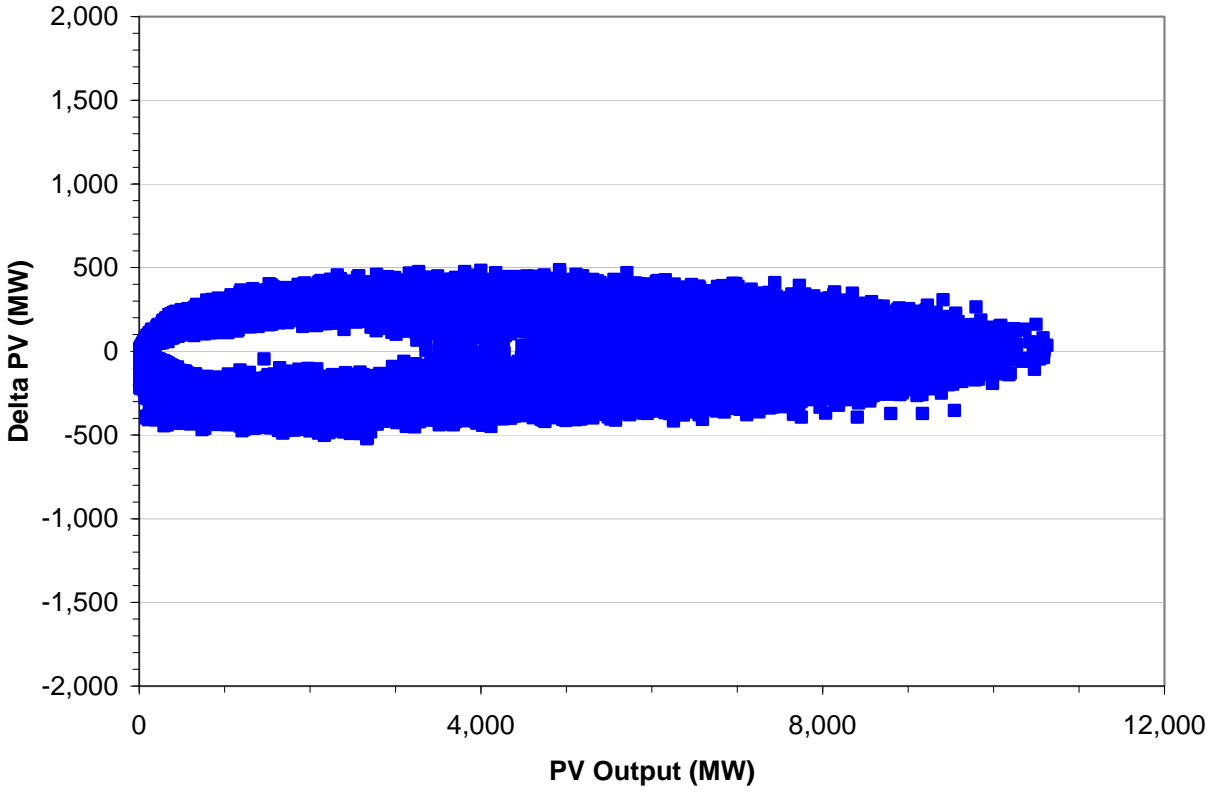


Figure 4-14. 10-Minute Deltas in 15,000 MW DC (11,550 MW AC) Solar PV Profile.

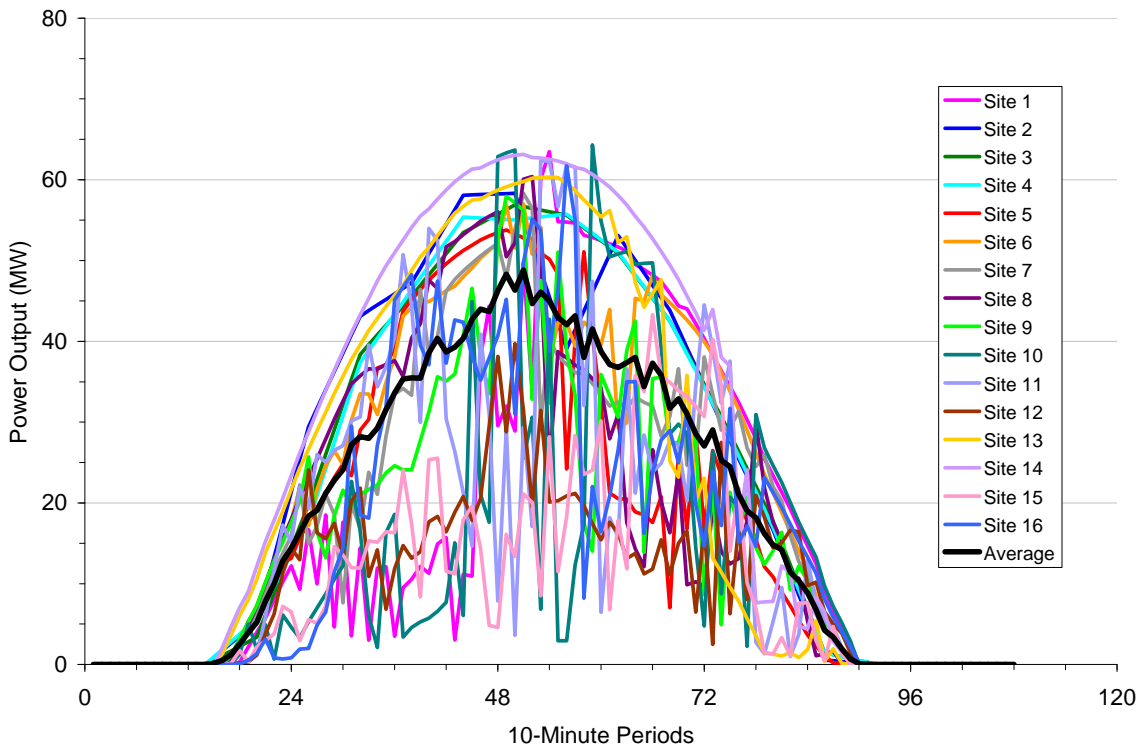


Figure 4-15. Individual Arizona 100 MW DC/77 MW AC Solar PV Profiles.

Table 4-3. Aggregate Solar PV Profile 10-Minute Delta Statistics.

	2,500 MW DC 1,925 MW AC	5,000 MW DC 3,850 MW AC	10,000 MW DC 7,700 MW AC	15,000 MW DC 11,550 MW AC
Maximum Output	1,813 MW	3,581 MW	7,040 MW	10,624 MW
Maximum Positive Delta	198 MW	199 MW	359 MW	488 MW
Average Positive Delta	38 MW	67 MW	121 MW	180 MW
Median Positive Delta	37 MW	66 MW	114 MW	181 MW
% of Positive Deltas	49%	50%	51%	50%
Maximum Negative Delta	-167 MW	-208 MW	-387 MW	-523 MW
Average Negative Delta	-36 MW	-68 MW	-124 MW	-178 MW
Median Negative Delta	-35 MW	-71 MW	-126 MW	-189 MW
% of Negative Deltas	51%	50%	49%	50%

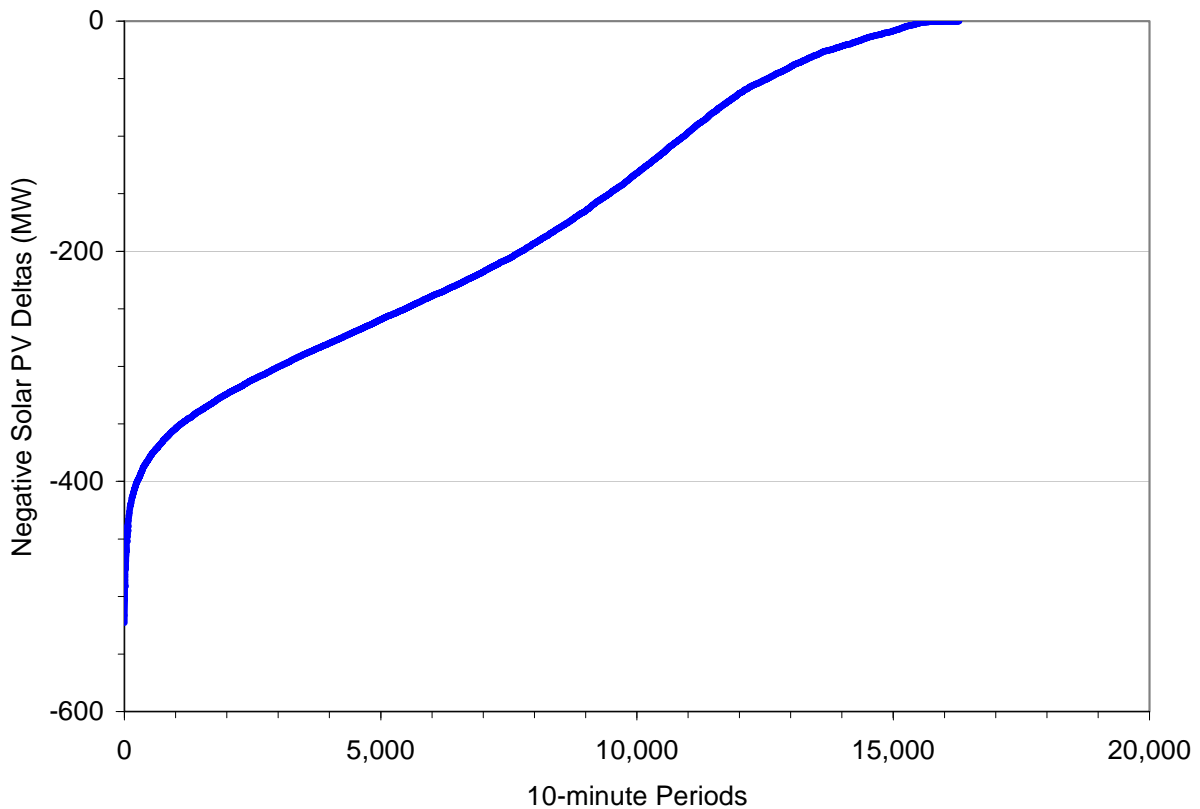


Figure 4-16. 10-Minute Negative Deltas in 15,000 MW DC (11,550 MW AC) Solar PV Profile.

Table 4-4. Expected 10-Minute Negative Solar PV Deltas.

% Expectation	Frequency	2,500 MW DC	5,000 MW DC	10,000 MW DC	15,000 MW DC
		1,925 MW AC	3,850 MW AC	7,700 MW AC	11,550 MW AC
-	Once per year	-167 MW	-208 MW	-387 MW	-523 MW
99.9%	Once every 3 weeks	-124 MW	-200 MW	-372 MW	-475 MW
99%	Once every 2 days	-92 MW	-175 MW	-313 MW	-412 MW
95%	Two times per day	-76 MW	-141 MW	-254 MW	-362 MW
90%	Four times per day	-68 MW	-126 MW	-235 MW	-334 MW

Table 4-5. Expected 10-Minute Positive Solar PV Deltas.

% Expectation	Frequency	2,500 MW DC	5,000 MW DC	10,000 MW DC	15,000 MW DC
		1,925 MW AC	3,850 MW AC	7,700 MW AC	11,550 MW AC
-	Once per year	198 MW	199 MW	359 MW	488 MW
99.9%	Once every 3 weeks	124 MW	176 MW	315 MW	452 MW
99%	Once every 2 days	91 MW	154 MW	288 MW	412 MW
95%	Two times per day	75 MW	140 MW	256 MW	370 MW
90%	Four times per day	70 MW	129 MW	237 MW	345 MW

From the steady-state analysis with all lines in service, the largest ΔV occurs at the Pisgah 500 kV bus. Regardless of control action, the largest $\Delta V/\Delta P_{gen}$ is 0.001 pu/100 MW of ΔP_{gen} . The expected ΔV can be calculated based on this value and on the expected 10-minute negative wind deltas. The range is shown in Table 4-6. Once per year a change in PV will result in a voltage change of about 0.005 pu. This is unlikely to result in a shunt capacitor or LTC switching cycle (e.g. cap switches off when generation drops, then back on when generation picks up).

The largest $\Delta V/\Delta P_{gen}$ for the summer sensitivity case was slightly higher than that for the spring study case. The calculated value of expected ΔV is nearly identical for the spring and summer cases.

The ΔV with a line out-of-service would be higher, but the frequency of occurrence would be lower due to the low likelihood of both a line outage and a large change in solar PV generation.

Table 4-6. Expected Frequency and Magnitude of ΔV at Pisgah 500 kV for 15,000 MW DC/11,550 MW AC Solar PV Profile for Spring Cases.

% Expectation	Frequency	ΔP_{gen}	ΔV
-	Once per year	-523 MW	0.005 pu
99.9%	Once every 2 weeks	-475 MW	0.005 pu
99%	Once every 1.5 days	-412 MW	0.004 pu
95%	Four times per day	-362 MW	0.004 pu
90%	Eight times per day	-334 MW	0.003 pu

4.2 Oscillatory Performance

The objective of this task was to evaluate the impact of variable solar PV generation on the small signal oscillatory performance of the WOR interface. Specifically, the goals were to characterize the frequency components of interface power swings in response to critical faults, to test whether renewable generation oscillating at those frequencies could adversely affect system damping, and therefore, to identify the need, if any, for a limit on the amount of dynamic scheduling across the interface.

4.2.1 Swing Mode Identification

The dominant swing modes across the WOR interface were identified using PSLF dynamic simulations and an FFT analysis.

The critical fault events, described in Section 2.3.2, were used to stimulate power oscillations across the WOR interface. As an example, WOR power flow response to the N. Gila-Imperial Valley 500 kV line fault and clear event is shown in Figure 4-17. At 1 second, a 3-phase to ground fault was applied at N. Gila 500 kV bus, after 4 cycles the fault was cleared and the N. Gila-Imperial Valley 500 kV line was opened. The event stimulates power swings on the WOR interface. Shortly after the line opens, the magnitude of the swing is about 450 MW (7,959 MW at 2.0 seconds and 7,507 MW at 3.0 seconds). This swing is reduced to near 0 MW by about 8 seconds. These simulation results will act as a benchmark for determining the effect of dynamic transfers on small-signal stability.

Figure 4-18 shows the WOR power flow response to the three critical fault events. The blue line represents the response to the N. Gila-Imperial Valley 500 kV line fault and clear event, the red line represents the response to the Palo Verde-Colorado River 500 kV line fault and clear event, and the green line represents the response to the loss of two San Onofre units. While the Palo Verde-Colorado River 500 kV line fault has a larger initial swing amplitude, the response to the N. Gila-Imperial Valley 500 kV line fault has poorer damping. Therefore, the evaluation focused on the N. Gila-Imperial Valley 500 kV line fault.

An FFT analysis was then used to identify the frequency components of the resulting power oscillations across the WOR interface. Results of the FFTs for each of the three critical disturbances are shown in Figure 4-19 to Figure 4-21. The dominant swing modes are summarized in Table 4-7. These frequencies are consistent with those observed in the WECC grid. The swing modes associated with the line outages are more similar to each other, than to the swing modes associated with the generation outage.

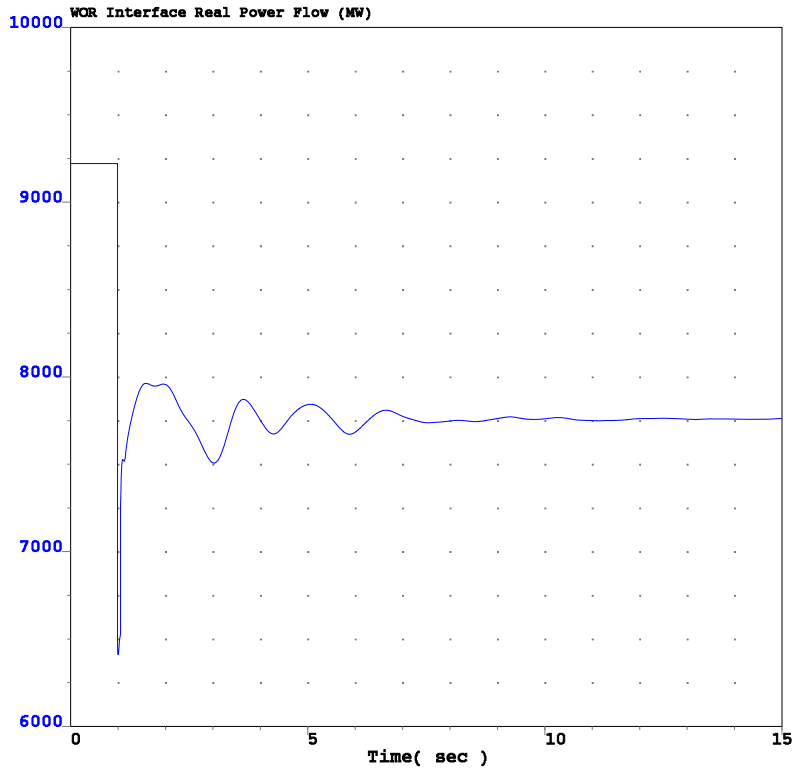


Figure 4-17. WOR Interface Flow Response to N. Gila-Imperial Valley 500 kV Line Event.

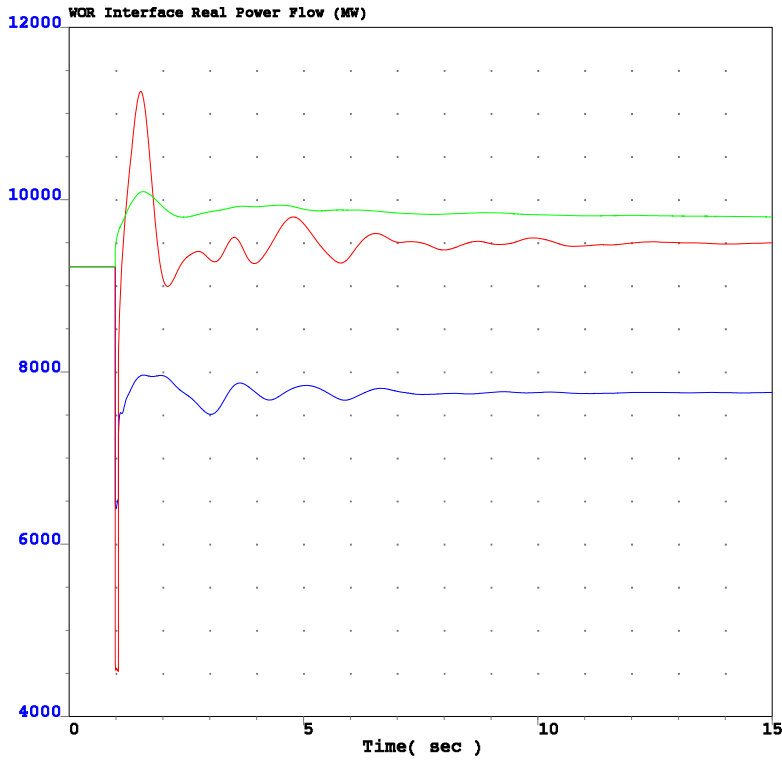


Figure 4-18. WOR Interface Flow Response to Critical Fault Events: N. Gila-Imperial Valley 500kV (blue), Palo Verde-Colorado River 500kV (red), 2 San Onofre Units (green).

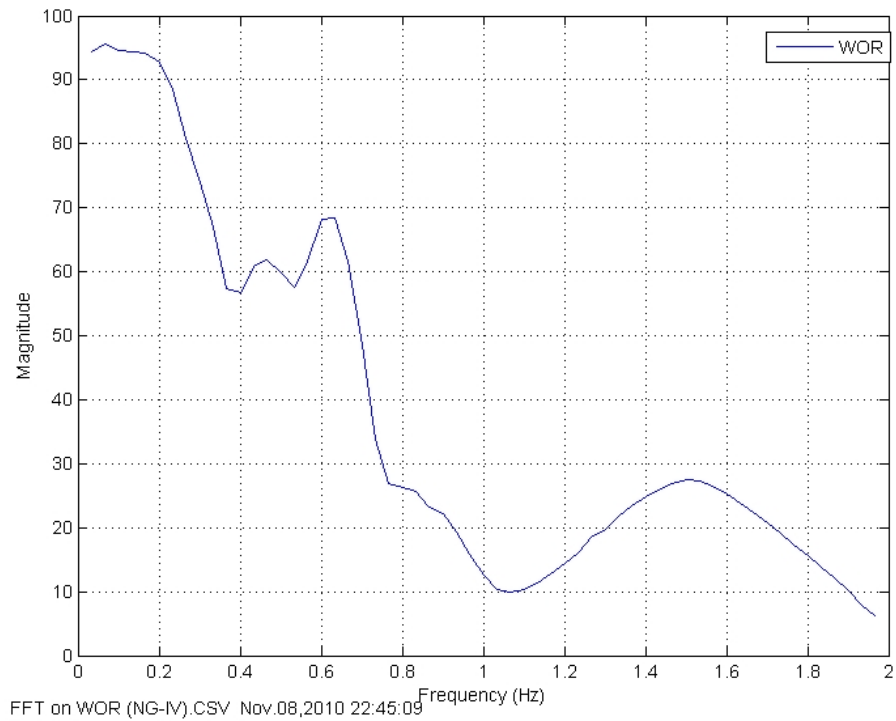


Figure 4-19. WOR Interface FFT Results for N. Gila-Imperial Valley 500 kV Line Event.

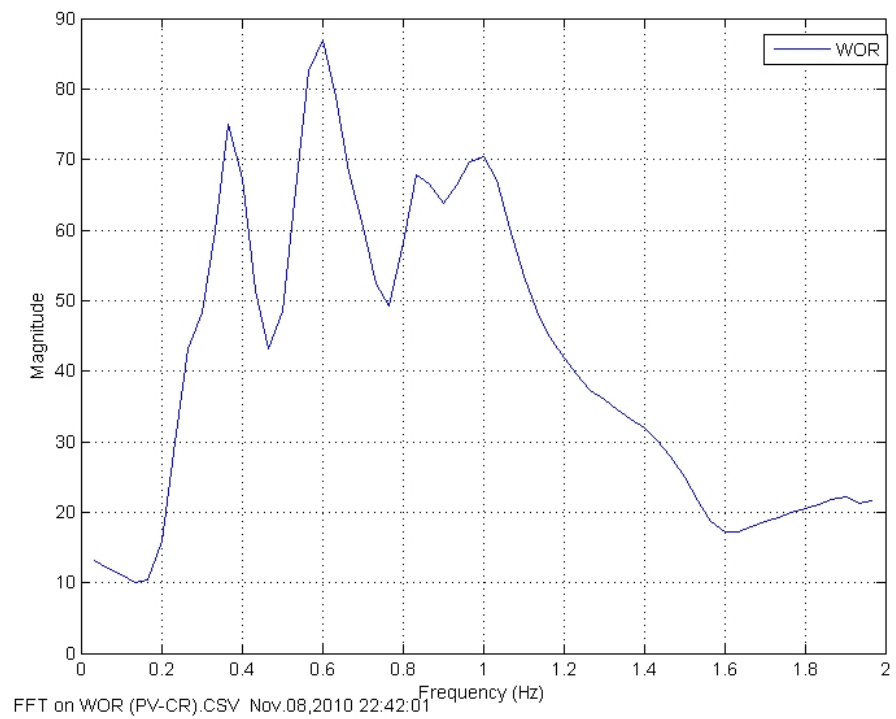


Figure 4-20. WOR Interface FFT Results for Palo Verde - Colorado River 500 kV Line Event.

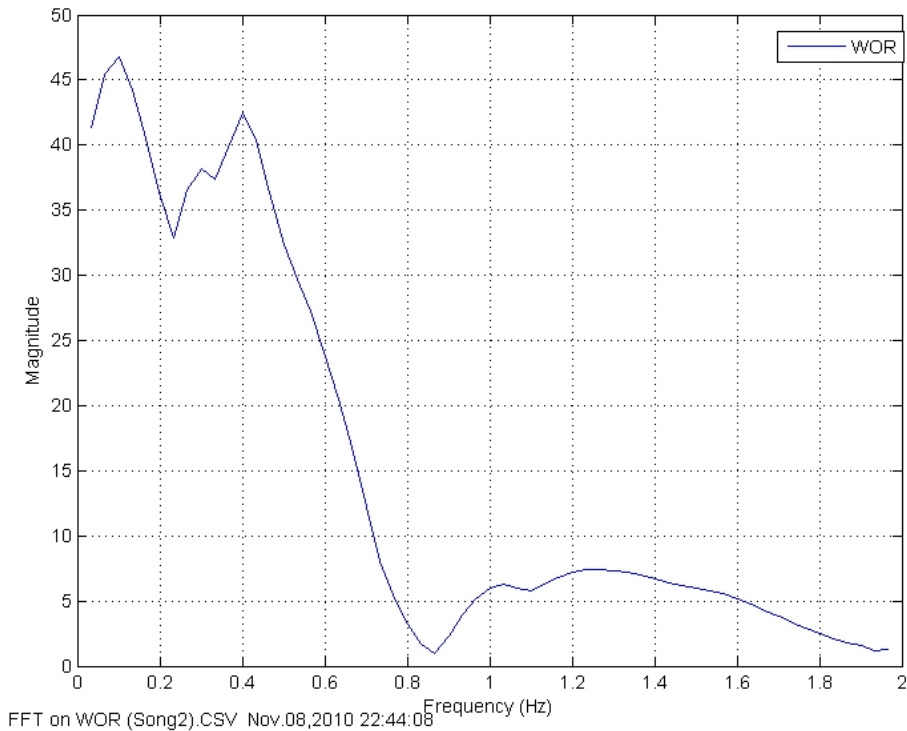


Figure 4-21. WOR Interface FFT Results for Loss of Two San Onofre Units.

Table 4-7. Dominant Swing Modes Across WOR Interface.

N. Gila-Imperial Valley 500 kV Line Event	Palo Verde - Colorado River 500 kV Line Event	Loss of Two San Onofre Units
0.47 Hz	0.37 Hz	0.10 Hz
0.60 Hz	0.60 Hz	0.30 Hz
1.50 Hz	1.00 Hz	0.40 Hz

4.2.2 Impact of Solar Variability on Small-Signal Stability

To test whether renewable generation could adversely affect power swing damping under challenging conditions, tests were devised in which all solar PV generation in the Southwest oscillated together at the Eldorado 500 kV bus near the WOR interface. This test, which has negligible risk of occurrence, provides maximum impact on grid oscillations. The assumption underlying this test is that common-mode oscillation of the solar generation will be worse than any variation that might occur in operation, and therefore provides a conservative upper bound. The variable renewable generation driving function was a sine wave at a selected frequency with a selected magnitude in increments of 1,000 MW.

The N. Gila-Imperial Valley 500 kV line fault and clear event was then simulated while the driving function was applied. The following figures and discussion will focus on that disturbance.

Figure 4-22 shows the WOR interface flow, N. Gila 500 kV bus voltage and N. Gila 500 kV bus frequency in response to the N. Gila-Imperial Valley 500 kV line fault and clear event. The blue line represents the benchmark system response, and the red line represents the system response with a 7,000 MW, 0.6 Hz stimulus.

As expected, the magnitude of the swings observed on the WOR interface are less than the magnitude of the stimulus, since about 1/3 of the stimulus flows on other paths. Also, the power swings sparked by the disturbance decay such that only the stimulus signal remains by the end of the simulation. This shows that the variable power injection stimulus will not destabilize, i.e., decrease damping or cause growing oscillations, an otherwise stable system. The next question is whether a stimulus can excite existing swing modes. Even with this extreme, coherent, and sustained excitation, the system meets the WECC voltage and frequency criteria for this stimulus, and no protective relays operate.

However, the system does not meet criteria with an 8,000 MW, 0.6 Hz stimulus. In that case, the amplitude of the driven system oscillations cause three UFLS relays at CFE 161 kV and 230 kV buses to operate at 2.5 seconds. Therefore, the oscillation magnitude limit for the WOR interface was 7,000 MW at 0.6 Hz.

A sensitivity analysis was performed with an 8,000 MW oscillation to investigate the impact of various stimulus frequencies. Figure 4-23 shows the system response to the N. Gila-Imperial Valley 500 kV line fault and clear event. The blue line represents the system response at 0.47 Hz, the red line represents the response at 0.6 Hz, and the green line represents 1.5 Hz.

The 0.47 Hz stimulus produces the largest variation in voltage and frequency. The 0.60 Hz stimulus causes the greatest change in WOR flow. This is due to the alignment of the stimulus with the dominant modes affecting voltage, angle and WOR flow. At 0.47 Hz, the Colstrip plant acceleration trend relay operated at about 2.4 seconds. At 0.6 Hz, one CFE UFLS relay operated at about 2.6 seconds. No relay operation occurred at 1.5 Hz.

The Marketplace SVC responses to the N. Gila-Imperial Valley 500 kV line fault for three different magnitudes of 0.6 Hz stimulus are shown in Figure 4-24. The blue line represents the benchmark response with no stimulus, the red line represents a 3,000 MW stimulus, and the green line represents a 6,000 MW stimulus. As the stimulus increases, the voltage and power swings increase and therefore, the SVC response. With a stimulus magnitude of 6,000 MW, equivalent to a 12,000 MW peak-to-peak swing, the SVC output is swinging from its minimum to maximum.

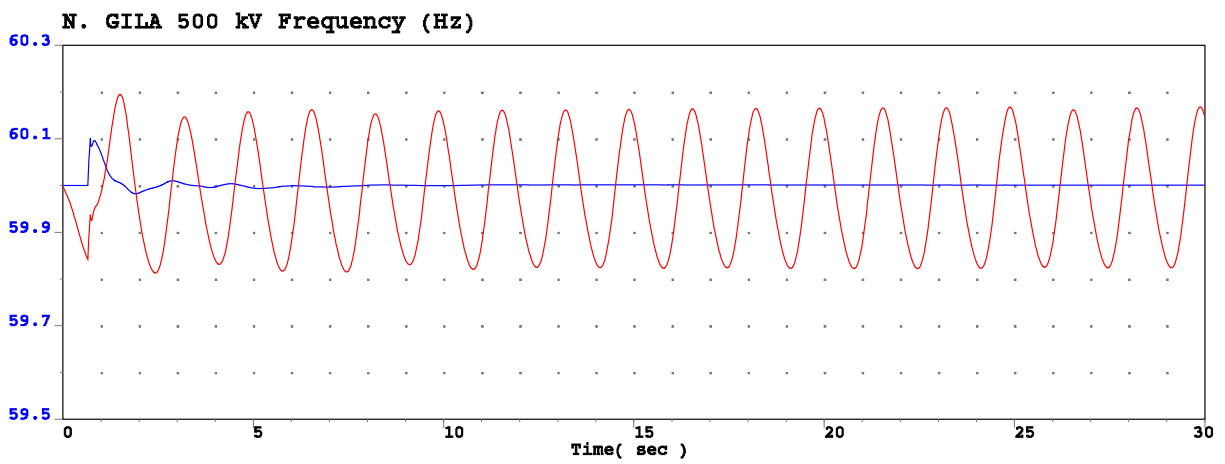
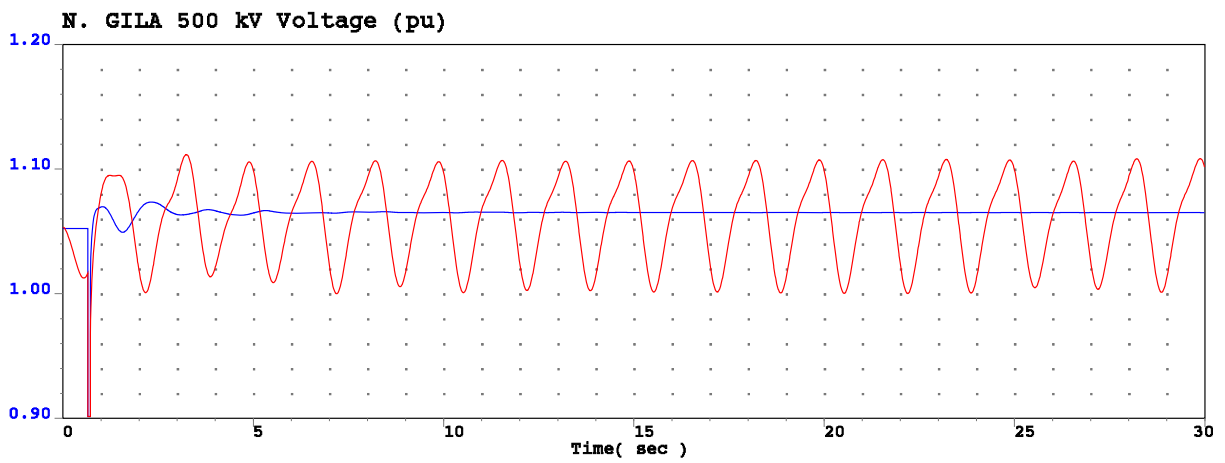
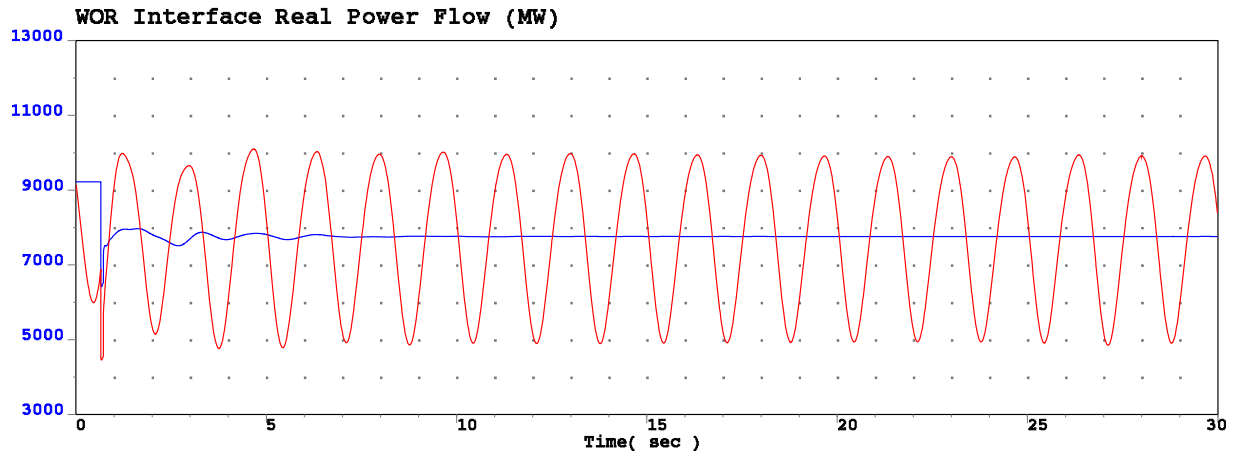


Figure 4-22. System Response to N. Gila-Imperial Valley 500 kV Line Event, with and without 7,000 MW, 0.6 Hz Stimulus.

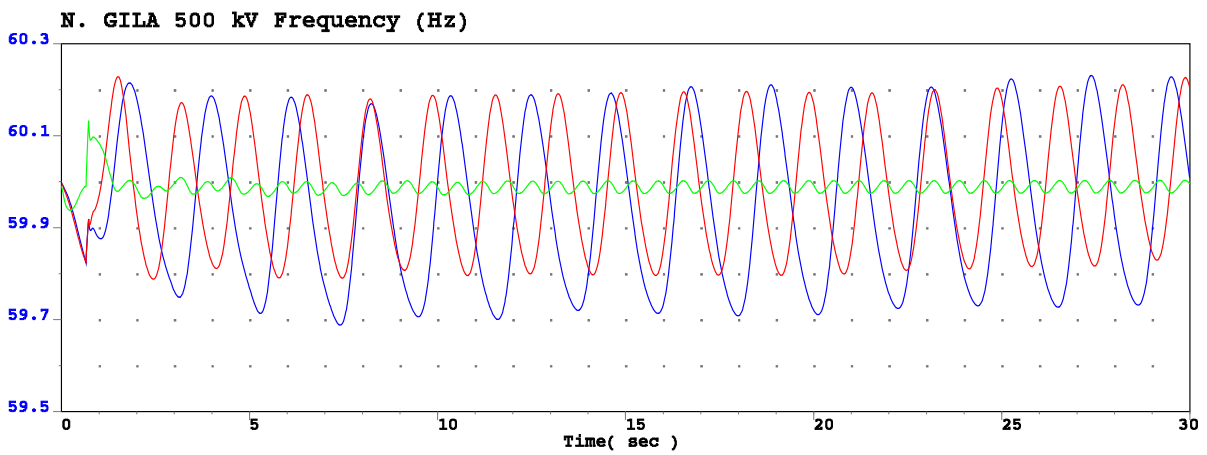
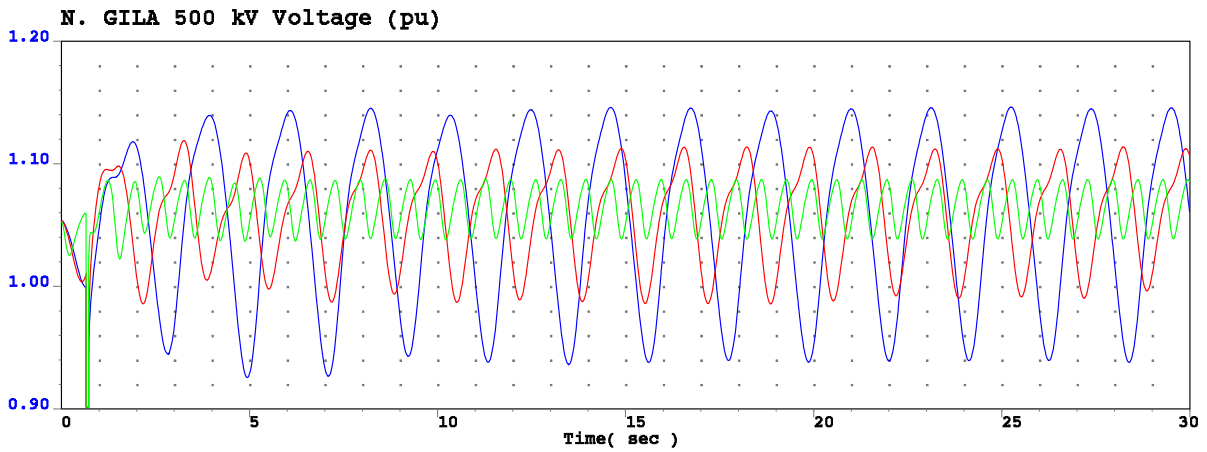
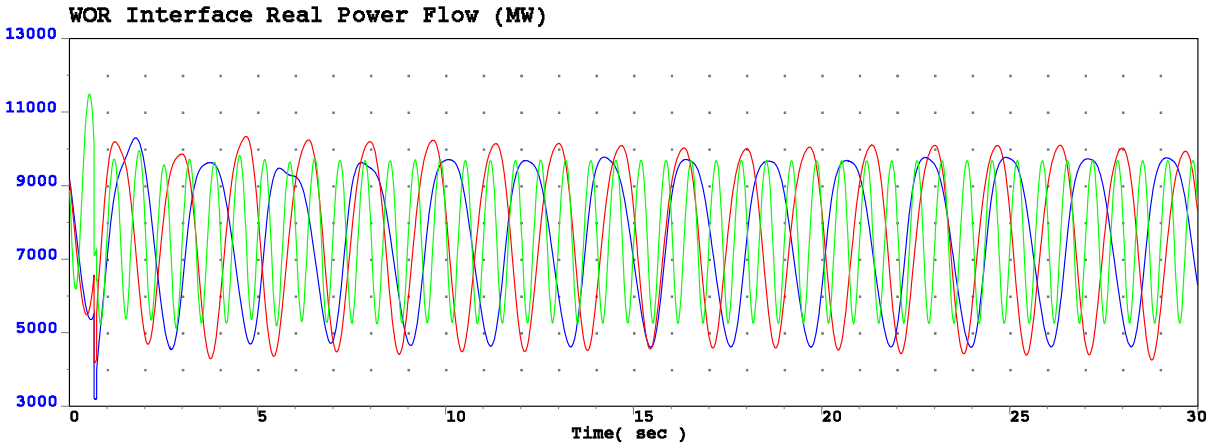


Figure 4-23. System Response to N. Gila-Imperial Valley 500 kV Line Event, with 8,000 MW Stimulus at 0.47 Hz (blue), 0.6 Hz (red) and 1.5 Hz (green).

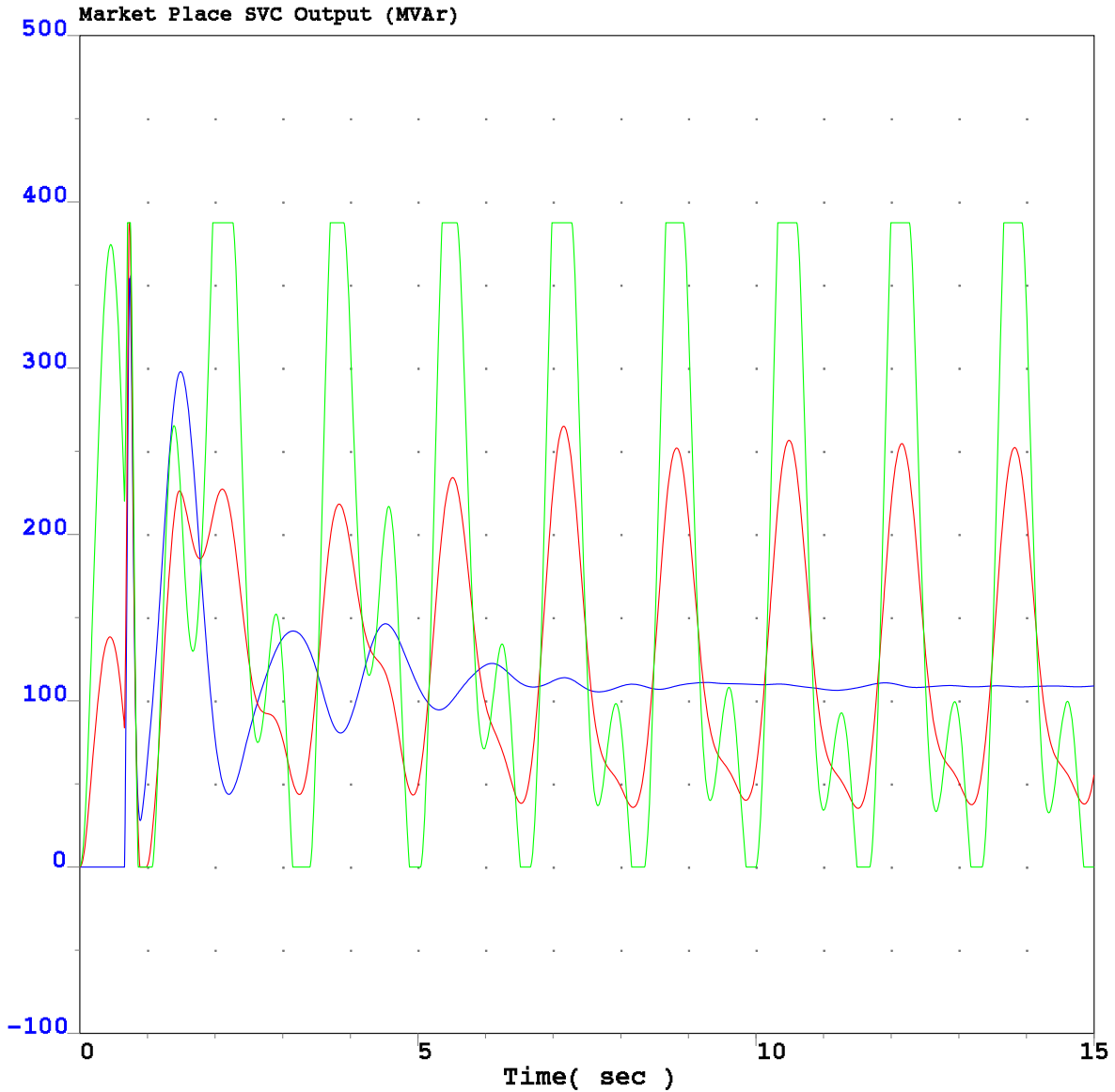


Figure 4-24. Marketplace SVC Response to N. Gila-Imperial Valley 500 kV Line Event, with 0 MW (blue), 3,000 MW (red), and 6,000 MW (green) Stimulus at 0.6 Hz.

The voltage changes of this dynamic analysis were compared to those observed in the steady-state analysis. Values of $\Delta V/\Delta P_{gen}$ are shown in Table 4-8 for the Pisgah 500 kV bus in response to the North Gila-Imperial Valley 500 kV line outage and a +/-8,000 MW stimulus. The values are shown for 0.47 Hz, 0.60 Hz and 1.5 Hz oscillation frequency. At 0.47 Hz oscillation frequency, $\Delta V/\Delta P_{gen}$ is similar to those calculated in the steady-state analysis. At the other frequencies, $\Delta V/\Delta P_{gen}$ is lower. The smaller change in voltage is likely due to regulation of the large SVCs along WOR for the dynamic analysis. They were not active in the steady-state analysis.

Table 4-8. $\Delta V/\Delta P$ at Pisgah 500 kV for North Gila-Imperial Valley 500 kV line Outage, +/-8,000 MW Stimulus. Values are Per Unit per 100 MW of Stimulus.

Oscillation Frequency	$\Delta V/\Delta P$ (pu/100MW)
0.47 Hz	0.0016
0.60 Hz	0.0009
1.50 Hz	0.0004

5 Summary and Conclusions

The objective of this study was to explore the impact of dynamic scheduling of renewable generation across interfaces into CAISO. Dynamic scheduling was narrowly defined to include only wind or solar PV variability. Other potential components of dynamic scheduling, such as hourly or sub-hourly schedule changes, were not considered. Two aspects of system performance (voltage changes and oscillatory response) were evaluated for two interfaces (California Oregon Interface (COI) and West of River (WOR)).

To begin, aggregate wind and solar PV profiles were analyzed to statistically characterize their expected variability. This statistical analysis evaluated the change in wind or PV solar generation from one 10-minute point to the next. These statistics provide a measure of how often relatively severe changes in power can be expected. For example, when 99% of changes in power (ΔP) per MW of dynamically scheduled wind or solar generation are within a given range, the statistical expectation is that more severe events will occur, on average, less than once per day. Daily tap motions and capacitor switching are presently expected during system operations. Wind and solar variations that result in normal switching or other control actions over a similar period were judged acceptable. The statistics of wind variation dictate that faster variations, i.e. on a period shorter than 10 minutes, will be of smaller amplitude.

From the power flow analysis, the change in voltage (ΔV) associated with such a change in power was calculated, as well as the potential impact of that ΔV on transformer LTC tap motion and shunt capacitor switching. Since the power flow analysis was performed with the COI and WOR interfaces near maximum, the focus was on the negative changes in power.

Finally, the impact of wind and solar PV variability on small signal oscillatory performance was examined. The dynamic performance evaluation incorporated extremely conservative assumptions. Specifically, all variable renewable generation in a given area (i.e., wind in the Northwest, solar PV in the Southwest) was oscillated at a single bus at one of the identified power swing frequencies. This test, which has negligible risk of occurrence, provided maximum impact on grid oscillations. The assumption underlying this test is that common-mode oscillation of the renewable generation will be worse than any variation that might occur in operation, and therefore provides a conservative upper bound.

The specific conclusions associated with each interface are discussed below.

COI Interface

The maximum power flow allowed across the COI interface is 4,800 MW. Therefore, the theoretical maximum dynamic schedule is also 4,800 MW. This maximum dynamic schedule was represented by a 5,000 MW aggregate wind profile in this study.

The statistical analysis showed that 99% of the time, the expected 10-minute drop in wind generation would be 301 MW or less (Table 3-5). The power flow analysis showed that this would result in at most a 0.012 pu change in voltage (Table 3-7) on the 500 kV system near

COI. Changes on the lower voltage system, i.e., closer to served loads, are considerably smaller - too small to result in additional transformer LTC tap motion or shunt capacitor switching. The maximum 10-minute drop was 1,672 MW, which occurred once in the year of data. The power flow analysis showed that this would result in up to a 0.065 pu ΔV , which would likely cause some LTC tap motion and shunt capacitor switching. The wind data shows that voltage changes of this magnitude will be rare, and will not occur in rapid succession. There is no significant risk of LTC tap hunting or rapid on/off cycling of shunt devices.

The dynamic analysis showed that an extreme test, driving all of the dynamically scheduled wind generation at a characteristic frequency with a peak-to-peak magnitude that exceeded the interface limit, still resulted in damped oscillations. At magnitudes greater than 3,000 MW peak-to-peak, some protective relays operated depending upon the system condition and fault event. There is no credible wind variation that can cause oscillatory destabilization of an otherwise stable system.

WOR Interface

The maximum power flow allowed across the WOR interface is 10,100 MW (WECC 2006 Path Rating Catalog). Therefore, the theoretical maximum dynamic schedule is also 10,100 MW. This maximum dynamic schedule was represented by a 15,000 MW DC/11,550 MW AC aggregate solar PV profile in this study.

The statistical analysis showed that 99% of the time, the expected 10-minute drop in solar PV generation would be 412 MW or less (Table 4-4). The power flow analysis showed that this would result in a 0.004 pu change in voltage (Table 4-6), which is too small to result in additional transformer LTC tap motion or shunt capacitor switching. The maximum 10-minute drop was 523 MW, which occurred once in the year of data. The power flow analysis showed that this would also result in relatively small (0.005 pu) change in voltage. Industry experience with large scale PV, including data measurement and development, is considerably less than that with wind power. As field and analytical experience grows, these results will likely benefit from refinement.

The dynamic analysis showed that the extreme test, driving all of the dynamically scheduled solar PV generation at a characteristic frequency with a peak-to-peak magnitude that exceeded the interface limit, still resulted in damped oscillations. At magnitudes greater than the 10,100 MW WOR limit, some protective relays operated and nearby SVC duty increased depending upon the system condition and fault event.

Conclusion

Under extreme conditions (e.g., combinations of 500 kV line or multiple generation unit outages, once-a-year changes in dynamically schedule renewable generation output, and unrealistically monolithic aggregate wind and/or solar PV behavior), it may be possible to trigger excessive shunt capacitor switching, transformer LTC motion, SVC response, and/or protective relay operation. However, the expected variability from the wind and solar PV generation when dynamically scheduled up to the overall maximum currently applied to each interface will not result in large changes in voltage nor excessive duty on voltage

regulating devices (e.g., LTC transformers and shunt capacitors). Therefore, this analysis shows that no additional limits are required on dynamically scheduled variable generation when the existing maxima are applied to each interface.

The expected change in voltage caused by dynamic scheduling is somewhat sensitivity to CAISO generation redispatch and to system operating condition (spring vs summer peak). However, the sensitivity is relatively low and does not change the conclusions of the study.

Note: The above conclusions are based on voltage and oscillatory performance of substation equipment within the ISO's footprint under high levels of import of intermittent resources during both normal and abnormal operating conditions. Neighboring Balancing Authorities may have limitations within their systems that could impact the level of import of renewable resources through dynamic transfers into the ISO.

6 References

- [1] Western Electricity Coordinating Council Reliability Criteria (Part I – NECR/WECC Planning Standards), "CriteriaMaster.pdf", April, 2005.
- [2] GE, "Western Wind and Solar Integration Study," NREL Subcontract Report NREL/SR-550-47434, May 2010.
- [3] 3TIER, "Development of Regional Wind Resource and Wind Plant Output Datasets," NREL Subcontract Report NREL/SR-550-47676, March 2010.
- [4] Wilcox, S., "National Solar Radiation Database, 1999-2005: User's Manual," NREL Report TP-581-41364, April 2007.